UNIVERSIDADE ESTADUAL PAULISTA
"JÚLIO DE MESQUITA FILHO"
Câmpus de Ilha Solteira

São Paulo State University – UNESP (Universidade Estadual Paulista – UNESP)
Faculty of Engineering of Ilha Solteira (Faculdade de Engenharia de Ilha Solteira – FEIS)
Department of Electrical Engineering (Departamento de Engenharia Elétrica – DEE)

LUIS GUSTAVO CORDERO BAUTISTA

OPTIMAL PROBABILISTIC FRAMEWORK FOR INTEGRATION OF HIGH PENETRATION OF DISTRIBUTED ENERGY RESOURCES IN ELECTRICAL DISTRIBUTION SYSTEMS OPERATION

Ilha Solteira – SP
2023

LUIS GUSTAVO CORDERO BAUTISTA

OPTIMAL PROBABILISTIC FRAMEWORK FOR INTEGRATION OF HIGH PENETRATION OF DISTRIBUTED ENERGY RESOURCES IN ELECTRICAL DISTRIBUTION SYSTEMS OPERATION

Ph.D. thesis presented to the Faculty of Engineering, Campus of Ilha Solteira – UNESP, as part of the requirements for obtaining the title of Ph.D. in Electrical Engineering. Field of knowledge: Automation

Prof. Dr. John Fredy Franco Baquero
Supervisor

Prof. Dr. João Soares
Co-Supervisor

Ilha Solteira – SP
2023

FICHA CATALOGRÁFICA
Desenvolvido pelo Serviço Técnico de Biblioteca e Documentação

C794o

Cordero Bautista, Luis Gustavo.
Optimal probabilistic framework for integration of high penetration of distributed energy resources in electrical distribution systems operation / Luis Gustavo Cordero Bautista. -- Ilha Solteira: [s.n.], 2023
105 f. : il.

Tese (doutorado) - Universidade Estadual Paulista. Faculdade de Engenharia de Ilha Solteira. Área de conhecimento: Automação, 2023

Orientador: John Fredy Franco Baquero
Co-orientador: João Soares
Inclui bibliografia

1. Central limit theorem. 2. Cumulant method. 3. Electric vehicle. 4. Edgeworth expansion. 5. Overvoltage probability constraint. 6. Probabilistic maximization of PV generation.

Amanda dos Santos
Amanda Sertori dos Santos
Bibliotecária - CRB/8-9061
Seção Técnica de Referência, Atendimento ao Usuário e Documentação
Diretoria Técnica de Biblioteca e Documentação

POTENTIAL IMPACT OF THIS RESEARCH

This research proposes a novel optimal probabilistic framework to probabilistically maximize photovoltaic power generation while mitigating the likelihood of overvoltage with a high degree of accuracy and efficient computational effort, with potential applications in electrical distribution networks with high penetration of photovoltaic systems and electric vehicles.

IMPACTO POTENCIAL DESTA PESQUISA

Esta pesquisa propõe uma nova abordagem probabilística ótima para maximizar probabilisticamente a geração de energia fotovoltaica e, ao mesmo tempo, mitigar a probabilidade de sobretensão com alto grau de precisão e esforço computacional eficiente, com aplicações potenciais em redes de distribuição elétrica com alta penetração de sistemas fotovoltaicos e veículos elétricos.

UNIVERSIDADE ESTADUAL PAULISTA

Câmpus de Ilha Solteira

CERTIFICADO DE APROVAÇÃO

TÍTULO DA TESE: OPTIMAL PROBABILISTIC FRAMEWORK FOR INTEGRATION OF HIGH PENETRATION OF DISTRIBUTED ENERGY RESOURCES IN ELECTRICAL DISTRIBUTION SYSTEMS OPERATION

AUTOR: LUIS GUSTAVO CORDERO BAUTISTA
ORIENTADOR: JOHN FREDY FRANCO BAQUERO
COORIENTADOR: JOÃO ANDRÉ PINTO SOARES

Aprovado como parte das exigências para obtenção do Título de Doutor em Engenharia Elétrica, área: Automação pela Comissão Examinadora:

John Fredy Franco B.

Prof. Dr. JOHN FREDY FRANCO BAQUERO (Participaçao Presencial)
Departamento de Engenharia Eletrica / Faculdade de Engenharia de Ilha Solteira - UNESP

Prof. Dr. LEONARDO HENRIQUE FARIA MACEDO POSSAGNOLO (Participaçao Presencial)
Departamento de Engenharia de Energia / Faculdade de Engenharia e Ciências - UNESP

Dr. DARWIN ALEXIS QUIJANO RODEZNO (Participaçao Presencial)
Departamento de Engenharia Elétrica / Faculdade de Engenharia de Ilha Solteira - UNESP

Prof. Dr. BRUNO CANIZES (Participaçao Virtual)
Departamento de Engenharia Eletrotécnica / Instituto Superior de Engenharia do Porto - ISEP

Prof. Dr. MARCOS JULIO RIDER FLORES (Participaçao Presencial)
Departamento de Sistemas e Energia / Universidade Estadual de Campinas - UNICAMP

Ilha Solteira, 28 de julho de 2023

‘A mi madre Teodora, por cada lucha de salir adelante y darme una vida, y enseñarme a confiar en Dios’

Acknowledgments

Foremost, I thank God for everything, and His faithfulness to carry me until here, and for helping me to contribute in some way to each person I meet in this journey of life, and the research field.

I want to thank to my supervisor Prof. Dr. John F. Franco, for the encouragement and support on my Ph.D. journey of research, for his dedicated and detailed observations to share his knowledge, for his patience and for his guidance along the research and writing of this thesis. I want to thank my co-supervisor Prof. Dr. João Soares, for his encouragement, guidance and supervision regarding this research journey, specially, the warm welcoming during the internship in GECAD Porto, Portugal. I would also like to express my gratitude to my Ph.D. thesis committee members: Prof. Dr. Leonardo H. Macedo, Prof. Dr. Darwin A. Quijano, Dr. Bruno Canizes, and Dr. Marcos J. Rider. Thank you for your time and effort reading my thesis and providing valuable insights and feedbacks that have greatly enriched the quality of my work.

I want to express my sincerest gratitude and thanks to Prof. Dr. Ruben Romero, for his friendship, his noble heart for helping me since my arrival to Ilha Solteira, and for his counselling at all times.

Thanks to all the colleagues and friends who are part of this great journey of being in Brazil, to the caring friends of church to support my mom, and I. Thanks to my colleagues Cleberton, and Tayenne for their friendship and time we spent in Portugal. Thanks to Jaimis and Raul for being good friends and their willingness to always help with ideas of research and opportunities since I came to Ilha Solteira.

I want to thank all my friends that I made during these years, Douglas, Mariane, Brauna, Julino, Brian, Richard, Wilson, Angel, Farhad, Rafael, Paula, Prof. Jaime, the family of Valdeci and Esther, the family of Jorge Oliveira and Raquel.

I also want to joyfully express my deepest gratitude to God for bringing Kailey Anna Ryan into my life, my best friend, wife-to-be and purest love for wholeheartedly trusting God everything, for being so faithful, gracious, committed, patient, supportive, hopeful, and the most beautiful heart and blessing to me, and to our loved son Sohayl, and her wonderful family, Jeanne, George Terry, Sean, Natalia to trust, believe, support and love my mom and I with the sincerest and kindest heart. To my family, Dula, Angel, Juan, Isa, Fer, and Lito for supporting my mom; and me. Also, I totally want to thank my mother Teodora Bautista Cabrera, for her relentless heart to be patient, supportive, and to be a healing and wise mother in counselling and for always reminding me to trust in God for everything.

And finally, with thankful heart to all my colleagues in the department of Electrical Engineering, and the LaPSEE laboratory for the last four years. This research was supported by the Brazilian institution of Coordination for the Improvement of Higher Education Personnel (CAPES) – Finance Code 001".

God bless you all. Thank you.

‘In the beginning was the Word, and the Word was with God, and the Word was God’ John 1:1

ABSTRACT

Worldwide clean energy policies are accelerating the deployment of distributed energy resources (DERs) integration into the distribution networks aiming to zero-emission targets, system support benefits and cost-effective grid services. Although clean DERs brings opportunities to customers and utilities, they can be unpredictable due to their stochastic nature leading to an increase of the probability of thermal overloading, overvoltage and reverse power flow. Therefore, traditional distribution network operation becomes more complex due to the increasing in variability and uncertainty of high penetration of DERs. It becomes imperative then take into account its stochastic nature to optimize the use and potential value of the DERs to provide crucial statistical information and evaluate their impacts without compromising the grid operation. In this pathway, this thesis explores and develops a novel optimal probabilistic framework to cater for the uncertainties of PV generation, aggregated demand and EVs with the goal to probabilistically maximize PV generation while evaluating and reducing the probability of technical challenges such as overvoltage using confidence interval constraint. Different probabilistic techniques are implemented through this thesis such as the Monte Carlo simulation, the Point Estimate Method, the Cumulant method with probability distribution reconstruction techniques of the Central Limit Theorem and Edgeworth expansion whose statistical information is employed within the optimization process. The efficiency and accuracy of the Cumulant method with Central Limit Theorem and Edgeworth expansion, 2m+1 PEM with Central Limit Theorem and Edgeworth expansion are presented with a detailed comparison in their performances with the Monte Carlo simulation. The validation of the proposed model is carried out using the IEEE 33 bus system, IEEE 69 bus system and a real electrical distribution system 202 bus system with high penetration of PV generation and EVs. Moreover, the application of the novel optimal probabilistic framework is tested in each test system to probabilistically maximize PV generation while effectively reducing overvoltage probability. The proposed method yielded satisfactory results to probabilistically maximize PV generation in terms of higher fitting accuracy of statistical information and optimal probability distribution for voltage, current, power flow through lines, PV generation with an efficient computational processing with promising application to industries.

Keywords: central limit theorem; cumulant method; electric vehicle; Edgeworth expansion; overvoltage probability constraint; point estimate method; probabilistic maximization of PV generation; probabilistic power flow; probabilistic optimization framework.

RESUMO

As políticas energéticas mundiais estão acelerando a integração dos recursos energéticos distribuídos (REDs) nas redes de distribuição visando metas de zero emissões de carbono, suporte e serviços na operação da rede de maneira accessível e econômica. Embora os REDs tragam oportunidades para clientes e concessionárias, sua natureza estocástica aumenta a probabilidade de sobretensão, sobrecarga, e fluxo reverso de potência. Portanto, a operação ótima da rede de distribuição com a alta penetração dos REDs torna-se mais complexa. Por esse motivo torna-se imperativo ter em conta a natureza estocástica dos REDs para otimizar o uso e o potencial dos REDs, assim como também utilizar as informações estatísticas para avaliar seus impactos sem comprometer a operação da rede. Nesse contexto, esta tese explora e desenvolve uma nova abordagem ótima probabilística para atender às incertezas da geração fotovoltaica (FV), demanda agregada e carregamento de veículos elétricos (VEs) com o objetivo de probabilisticamente maximizar a geração FV enquanto se reduz a probabilidade da sobretensão usando uma restrição de intervalo de confiança. Diferentes técnicas probabilísticas são implementadas ao longo desta tese, como o método de Simulação de Monte Carlo, o Método de Estimação de Pontos, o Método dos Cumulantes, e técnicas de reconstrução da distribuição de probabilidade como o Teorema do Limite Central e a expansão de Edgeworth, são empregadas na análise probabilística cujas informações são usadas no processo de otimização. A eficiência e precisão dos métodos probabilísticos com as curvas aproximadas de probabilidade são comparadas e avaliadas nos sistemas de IEEE 33 barras, IEEE 69 barras e um sistema elétrico de distribuição real 202 barras com alta geração FV e carregamento de VEs para maximizar a geração FV. Além disso, a aplicação do algoritmo ótimo probabilístico é avaliada em cada sistema teste com o intuito de probabilisticamente maximizar a geração FV enquanto se reduz efetivamente a probabilidade de sobretensão. O método proposto apresentou resultados satisfatórios na optimização probabilística da geração FV, precisão das informações estatísticas e distribuição de probabilidade ótima para tensão, corrente, fluxo de potência nas linhas e geração FV, sob um tempo computacional eficiente com potencial de aplicação na indústria.

Palavras-chaves: algoritmo ótimo probabilístico; expansão de Edgeworth; fluxo de potência probabilístico; método dos cumulantes; método de estimação de pontos; otimização probabilística da geração fotovoltaica; restrição de probabilidade de sobretensão; teorema do limite central; veículos elétricos.

LIST OF FIGURES

LIST OF TABLES

LIST OF ABBREVIATION AND ACRONYMS

CDF	Cumulative density function.
CI	Confidence interval.
CLT	Central limit theorem.
CM	Cumulant method.
DER	Distributed energy resources
EDS	Electrical distribution system.
EE	Edgeworth expansion.
EVs	Electric Vehicles.
MCS	Monte Carlo simulation.
OPF	Optimal power flow.
PV	Photovoltaic system.
PDF	Probability density function.
PEM	Point estimate method.
PPF	Probabilistic power flow.
POPF	Probabilistic optimal power flow
PRE	Percentage relative error.
PRMSE	Percentage relative mean square error.

LIST OF SYMBOLS

Sets and Indices

F	Set of phases {A, B, C}.
L	Set of circuits.
N	Set of nodes.
s	Index of substation

Parameters

$\mu_{n,f}^{load}$	Expected value of the aggregated demand at node n for phase f.
$\mu_{n,f}^{EV}$	Expected value of the aggregated EVs charging demand at node n for phase f.
μ_r	Expected value of a random variable r.
μ_{Gen}	Expected value generation.
σ_r	Standard deviation of a random variable r.
σ_{Gen}	Standard deviation of generation.
$\lambda_{r,3}$	Skewness value of a random variable r.
$\lambda_{r,4}$	Kurtosis value of a random variable r.
$\delta_{\boldsymbol{\mu}_{\boldsymbol{Gen}}}$	Relative error of the expected value of generation.
$\delta_{\boldsymbol{\sigma}_{\boldsymbol{Gen}}}$	Relative error of the standard deviation of generation.
ΔS	Power injection variation.
$B_{nm,f,h}^{shunt}$	Shunt susceptance of circuit mn between phases f and h.
C_0	Current matrix evaluated at the operating point.
L_s	Load shape.
J_0	Jacobian matrix evaluated at the operating point.
L_0	Line matrix at the operating point.
L_s	Load shape.
$P_{n,f}^D$	Active power demand at node n for phase f.
$\bar{P}_n^G$	Maximum active power of the PV generator at node n.
$Q_{n,f}^D$	Reactive power demand at node n for phase f.
$R_{mn,f,r}$	Resistance of circuit mn between phases f and r.
$\underline{V_n}, \overline{V_n}$	Minimum and maximum voltage magnitude limits.
$X_{mn,f,r}$	Reactance of circuit mn between phases f and r.

Variables:

$E\left[v^j\right]$	Raw moment of *i-th* order of voltages.
ϵ_T^y	Percentage relative error of variable *y* of the statistical *T* value.
δ_y	Percentage relative mean square error of variable *y*.
ΔV	Voltage variation.
μ_n^{PV}	Expected value of PV power injection at node *n*.
k_m^V	Cumulant of *m-th* order of voltages.
k_m^{PQ}	Cumulant of *m-th* order of power flow through lines.
k_m^I	Cumulant of *m-th* order of currents.
$I_{n,f}^{Dim}$	Imaginary part of the current demanded by a conventional load at node *n* for phase *f*.
$I_{n,f}^{Dre}$	Real part of the current demanded by a conventional load at node *n* for phase *f*.
$I_{n,f}^{Gim}$	Imaginary part of the current generated at node *n* for phase *f*.
$I_{n,f}^{Gre}$	Real part of the current generated at node *n* for phase *f*.
$I_{se,f}^{im}$	Imaginary part of the substation current at node *se* for phase *f*.
$I_{se,f}^{re}$	Real part of the substation current at node *se* for phase *f*.
$I_{mn,f}^{im}$	Imaginary part of the current in circuit *mn* for phase *f*.
$I_{mn,f}^{re}$	Real part of the current in circuit *mn* for phase *f*.
P_n^G	Active power generated at node *n*.
Q_n^G	Reactive power generated at node *n*.
$V_{n,f}^{re}$	Real part of the voltage at node *n* for phase *f*.
$V_{n,f}^{im}$	Imaginary part of the voltage at node *n* for phase *f*.
$\overline{V_{CI}^n}$	Upper value of confidence interval of voltage at bus *n*.
P_{se}^s	Substation active power supply at node *se*.

CONTENT

1 INTRODUCTION

Worldwide clean energy policies are accelerating the deployment of distributed energy resources (DERs) including non-variable and variable resources aiming to counteract climate change, balancing and restoring sustainable economic growth, and bringing system support benefits and cost-effective grid services in the modern electricity sector (IRENA, 2022). Particularly, the traditional distribution network is transitioning with the advent of smart grid technologies, clean energy development goals, supporting policies and the rapid adoption of DERs (DILEEP, 2020; SUN et al., 2020).

Among DERs such as wind power, photovoltaic units, energy storage devices, dynamic load like plug-in electric vehicles (EV), photovoltaic (PV) systems have been increasingly deployed due to its competitive investment cost, continuing increased production efficiency and attractive financial incentives. This technology not only brought benefits for the system but also energy bill reduction and increase of the independence from traditional fossil fuels from dedicated commercial and residential sized to distributed generation power plants (CARSTENS; DA CUNHA, 2018). For instance, PV centralized installed capacity operation in Brazil has grown from 0.93 GW in 2017 to 7.18 GW in 2022 as shown in Fig. 2, now including distributed generation and centralized generation; with a PV generation growth forecasts of an additional 60 GW for the next five years (ANEEL, 2023).

Another low-carbon technology is the electric vehicle (EV) that has shown a rapid globally uptake in the roadmap for electrified transportation that is also taking place in the electrical distribution network in many countries (IEA, 2022). This is due to the significant energy policy intervention to reduce carbon emissions looking forward to an efficient and sustainable transport sector in many countries (DE LIMA et al., 2022). For example, the Brazilian government enacted electric vehicles policies and bills such as the normative act nº 1.000/2021 and the 'Rota 30' program to promote the transition to sustainable mobility. This action in the transport sector leads to an increase in transport electrification and higher EVs deployment in the Brazilian mobility sector which reached a total of 107,770 EVs in 2022 as shown in Fig. 1 (ANEEL, 2021; BRAZIL FI GROUP, 2018; NEOCHARGE, 2023).

Although these technologies bring new opportunities for customers and utilities, traditional electrical distribution systems (EDS) were not designed to operate with a growing variability and intermittency of high penetration of PV systems and EVs, which also increased the likelihood of new technical challenges in operation and planning.

Fig. 2 Photovoltaic installed capacity growth in Brazil, ANEEL 2023.

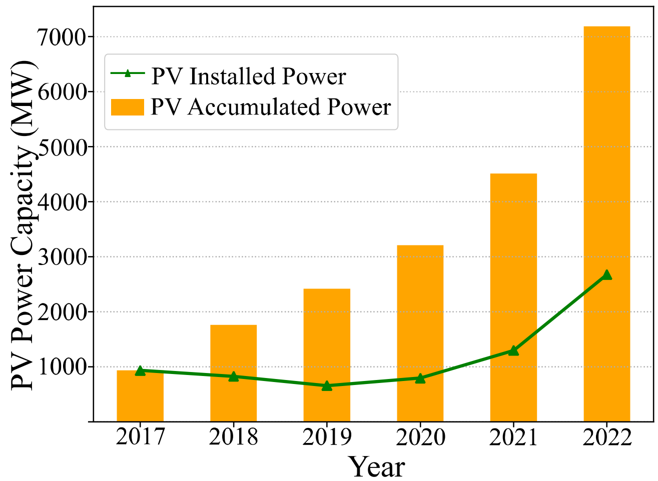

Source: Adapted ANEEL 2023.

Fig. 1 Total EV growth including hybrid and plug-in electric vehicles.

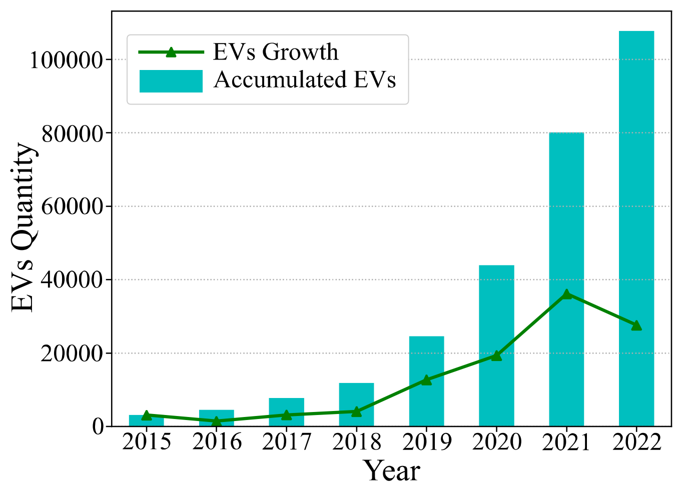

Source: Adapted NeoCharge 223.

For instance, reverse power flow, overvoltage, undervoltage and thermal overloading, overload risk of distribution transformers, especially during periods when stochastic generation and variable demand have a low coincidence (STREZOSKI et al., 2022).

Therefore, this increases the complexity and arises new technical challenges for a secure and optimal grid operation, and investment decision analysis of evolving EDS with the rapid integration of DERs.

Some solutions for the technical challenges brought by the high penetration of DERs, such as overvoltage include grid reinforcement, generation curtailment schemes, on-load tap changers, usage of reactive power capability of PV inverters, battery energy systems, and demand response programs (HASHEMI; ØSTERGAARD, 2017). However, these approaches may reduce potential energy generated, neglect stochastic behavior and loses relevant statistical information of the EDS state variables and the intermittency associated with the PV generation, aggregated load demand, and EV charging demand. Moreover, providing statistical information of the system state variables is vital and of great interest to capture a more realistic behavior of the EDS and assist distribution system operators in evaluating the corresponding impacts of the stochastic energy resources that might be accepted without compromising the EDS operation and planning (NAVARRO-ESPINOSA; OCHOA, 2016).

1.1 OBJECTIVES

The main goal of this thesis is to develop an optimal probabilistic tool combining the statistical information from the PPF analysis and use the statistical information of the EDS within an optimization model to maximize PV generation while probabilistically satisfy the operational voltage constraint. To accomplish this study, uncertain variables modeling and the implementation of different probabilistic techniques with their respective probability distribution approximation for the PPF is carried out. The optimization process considers a non-linear model to represent the optimal operation of the EDS with the aim to maximize PV generation.

The proposed method is developed within the Python environment, while the analysis of PPF requires the execution of an algorithm that interact with the Open source for Distribution System Simulator (OpenDSS). The optimization process for the maximization of PV generation is implemented using the AMPL software with a commercial solver KNITRO. The test systems of IEEE 33 bus, IEEE 69 bus and a real radial EDS 202 bus are employed for the performance and assessment of the electrical power system with high penetration of PV generation and EV.

The development of this thesis to meet the goals presented above can be summarized as follows.

1) The uncertain variable modeling of demand, PV generation and EVs in terms of their probability distribution function.
2) The implementation of the probabilistic techniques of Monte Carlo Simulation (MCS), Point Estimate Method (PEM), Cumulant Method (CM) for the PPF analysis and their respective probability distribution approximation functions.
3) The development of the optimal probabilistic framework that aims to maximize PV generation while reducing overvoltage likelihood with a probabilistic restriction

that considers confidence interval levels in the presence of high penetration of PV generation and EVs.

4) A comparison of the probabilistic techniques and the optimization method performance and accuracy to probabilistically maximize PV generation applied within the proposed model using the test cases of IEEE 33 bus system, IEEE 69 bus system and a real EDS 202 bus system.

1.2 THESIS STRUCTURE

The remainder of the manuscript is organized as follows. Chapter 2 presents a literature review of the probabilistic power flow and optimal probabilistic power flow applications to study the EDS operation under uncertainty. Chapter 3 describes the concept of moments and cumulants, develops the probability distribution functions for the uncertain variables of demand, PV generation and EVs. Chapter 4 presents the implementation of five probabilistic techniques applied to the PPF problem with their respective probability curve approximations using the Central Limit Theorem (CLT) and Edgeworth expansion. Chapter 5 presents the mathematical formulation for the optimal operation of an EDS with the aim of maximizing PV generation and it is also presented the proposed probabilistic optimization framework that employ the statistical information from the PPF evaluation within the optimization process while complying with the confidence interval voltage restriction. Chapter 5 also presents the algorithm to probabilistically reduce the overvoltage likelihood within the optimization process and also it is discussed some metrics to be used for performance comparison with the MCS. Chapter 6 discusses the different probabilistic techniques performances using the IEEE 33 bus system, IEEE 69 bus system and a real EDS 202 bus system. First, the evaluation of the PV generation and technical challenges of overvoltage likelihood analysis. Second, the results of the proposed probabilistic optimization framework by probabilistically optimizing the PV power injection while reducing the overvoltage likelihood in the EDS. Additionally, more results are described in terms of the optimal probability density functions of variable of interest, the confidence interval of operation for the PV generation, daily voltage operation and grid power operation with their respective statistical analysis for each test system. Finally, conclusions on the advantages for the evaluation of the proposed method in the EDSs test systems and future research pathways for the application of the optimal probabilistic framework in the EDS operation are drawn in Chapter 7.

2 LITERATURE REVIEW

Traditional tools such as the deterministic power flow (DPF) have often been used to analyze and assess the operation and planning of EDSs. This traditional practice of the system operation and planning analysis works well when sources are predictable and fixed. However, these practices are ill-suited to cater and analyze stochastic power grids; furthermore, the actual EDS is becoming more complex and dynamically changing with the emerging trend of high penetration of DERs such as wind power, photovoltaic units, energy storage devices, dynamic load like plug-in electric vehicles (EV), automated metering devices (e.g., smart meters), real-time energy pricing signals, and local energy markets (STREZOSKI et al., 2022; ULLAH et al., 2022). Hence, the conservative approach of traditional tools is insufficient and inaccurate to capture the EDS stochastic operation since this approach ignores the uncertainties present in the power system. This may lead to increased congestion problems, conservative grid operation limits, voltage unbalance and instability, and excessive or insufficient operating reserves. Thus, the growing stochastic variables in the power system requires a novel modeling of suitable probabilistic tools for the analysis to quantify, evaluate, and mitigate the impact of resource variability to aid planners and operator for informed-decisions to ensure safe and optimal grid operation. (RAMADHANI et al., 2020).

There are several approaches to model the power system performance subject to uncertainty and variability of grid components. For instance, probabilistic, possibilistic, information gap decision theory, robust optimization, and interval analysis (RAMADHANI et al., 2020). Among these approaches, probabilistic tools are able to incorporate uncertainties within their formulation using probability density functions (PDFs) that can be easily modelled since their historical data is usually available. For instance, aggregated demand can be modelled using the normal distribution to represent their stochastic behavior, while PV generation that is highly related to solar irradiation can be modeled by the Beta distribution (FERNANDES et al., 2019; PRUSTY; JENA, 2017). Regarding the probabilistic distribution modeling of aggregated EV charging demand, this work proposes a PDF-built simulation based on an algorithm for EV charging demand considering uncertainties in drivers' behavior, EV type, energy requirements, and state of charge.

In general, probabilistic techniques can be classified into sampling such as Monte Carlo simulation (MCS), approximate such as Point Estimate Method (PEM), and analytical methods such as Cumulant Method (CM). Generally, a variable probability distribution approximation can be assumed to follow a Normal distribution based on the Central Limit Theorem (CLT) approximation (GIRALDO et al., 2019). Although this approximation may estimate the mean and standard deviation values, it is not necessarily sufficient and accurate when there are dissimilar input probability distributions. Approximations such as the Gram-Charlier and Edgeworth expansions overcome this issue by considering moments or cumulants information of these dissimilar distributions (BLINNIKOV; MOESSNER, 1998).

These probabilistic techniques have been applied to the problem of EDS operation and optimization analysis leading to the probabilistic power flow (PPF) and the probabilistic optimal power flow (POPF). Among the probabilistic techniques that handle the uncertainty of power flow analysis is the MCS which is commonly used for benchmark purposes. For instance, a POPF based on a Quasi-MCS is used to minimize fuel cost considering the correlation of wind farms in a transmission system (XIE et al., 2018). In another work, a PPF based on MCS studied the effect of reverse power flow due to PV and Wind random allocation with different levels of penetration in the EDS (CONSTANTE-FLORES; ILLINDALA, 2019). Although the MCS is relatively easier to implement and commonly utilized in engineering areas for comparison and validation purposes, its disadvantage is that it requires a significant number of thousands of deterministic analyses leading to a large computational burden.

Regarding approximate methods, the PEM calculates representative scenarios and associated weights for the uncertain variables, this approximate technique is efficient and capable of achieving acceptable results of expected value and standard deviation with a reasonable and faster execution time compared with the MCS. For instance, a work proposed an OPF based on *2m* PEM for a market model that considers uncertainties in demand and supply-side bidding in order to deal with local marginal prices behavior in a transmission system (VERBIC; CANIZARES, 2006). A POPF with probability constraints based on a *2m+1* PEM with Central Limit Theorem (CLT) scenario generating for optimal generation dispatch in the presence of wind and PV units is proposed in (GIRALDO et al., 2019). Another work, a PPF based on *2m+1* PEM combined Edgeworth expansion studied the effects of different levels of PV penetration in terms of overvoltage and reverse power flow (CORDERO; FRANCO, 2020). Other researchers developed a POPF to minimize power losses using a linearization of the branch flow equations, and the *2m+1* PEM is used to cater to demand, PV generation, and Wind generation scenarios that are applied in the optimization input parameters (GALLEGO; FRANCO; CORDERO, 2021). Aiming to employ the statistical information of the PPF, an optimal probabilistic framework based on *2m+1* PEM Edgeworth is proposed to probabilistically maximize PV generation considering overvoltage confidence levels restrictions (CORDERO et al., 2022). Although these approximate techniques are faster for computational process and yield acceptable results, it decreases accuracy for other than normal distribution inputs, and their execution time is linearly dependent on the number of uncertain variables.

Another probabilistic technique is the Cumulant method (CM) which requires a mathematical calculation to obtain a linear mapping of input stochastic variables and the output of the stochastic variable of interest. For instance, a PPF is proposed using combined cumulants with Gram-Charlier expansion to calculate possible ranges of power flow and the probability of overloaded line occurrence in transmission systems (ZHANG; LEE, 2004).

In another work, a PPF based on a cumulant algorithm with curve approximation using Gram-Charlier, Edgeworth and Cornish-Fisher expansion was proposed to assess the impact of PV generation in terms of overvoltage and overloading for transmission systems (FAN et al., 2012). The use of a cluster-based cumulant probabilistic assessment tool was also proposed to study the impact of high penetration of wind farms on grid operation for distribution systems (ZHOU et al., 2020). A reliability-based probabilistic network pricing with demand uncertainty using the PPF based on CM with Gram-Charlier expansion was examined to assess the impact of demand uncertainties on the investment cost of distribution systems (YANG et al., 2020). One of the major advantages of the power flow analysis based on CM is that it requires only one power flow calculation, thus, obtaining an efficient computational time and it also provides a sufficient accuracy to obtain the probability density function of variables of interest.

Even though the aforementioned different probabilistic methods have been applied for the PPF and OPPF problem in previous works as shown in Table 1, to capture and assess the impacts of DERs integration on the EDS, some challenges remain to be addressed. First, control and mitigation of the increasing likelihood of technical challenges of grid operation. Second, to probabilistically maximize the PV generation in an uncertain environment with high penetration of PV generation and EV charging demand, while reducing the likelihood of technical challenges such as overvoltage, overloaded lines, power flow reverse by considering confidence interval restrictions. Furthermore, a probabilistic framework has the potential to provide critical operating points and reconstruct relevant statistical information of the EDS state variables.

In this pathway, the proposed work motivation is to provide an optimal probabilistic assessment framework to identify, quantify, and reduce the likelihood of uncertainties impact of high penetration of DERs promoting an economical and sustainable green energy-based integration in the EDS for operation and planning.

The main contribution of this thesis are: 1) The development of the optimal probabilistic framework that aims to maximize PV generation while reducing overvoltage likelihood with a

Table 1. Literature review of probabilistic assessment tools comparing with the proposed model

Reference	Probabilistic technique	DERs PDF modeling	Optimization variable	PDF Maximization. PV Generation	Overvoltage probability restriction
(XIE et al., 2018)	Quasi-MCS	Wind	Fuel cost	×	×
(CONSTANTE-FLORES; ILLINDALA, 2019)	MCS	Load, PV and Wind	×	×	×
(VERBIC; CANIZARES, 2006)	*2m* PEM	Demand and supply biding	Local marginal prices	×	×
(GIRALDO et al., 2019)	*2m+1* PEM	Wind, PV generation and demand	Generation dispatch	×	×
(CORDERO; FRANCO, 2020)	*2m+1* PEM Edgeworth	Demand and PV generation	×	×	×
(GALLEGO; FRANCO; CORDERO, 2021)	*2m+1* PEM	Load, PV and Wind	Power losses	×	×
(CORDERO et al., 2022)	*2m+1* PEM Edgeworth	Load, PV and Wind	PV Generation	✓	✓
(ZHANG; LEE, 2004)	CM Gram-Charlier	Load and generation	×	×	×
(FAN et al., 2012)	CM Gram-Charlier, Edgeworth and Cornish-Fisher	Load and PV generation	×	×	×
(ZHOU et al., 2020)	Adaptive cluster-based CM	Load and wind generation	×	×	×
(YANG et al., 2020)	CM Gram-Charlier	Load	×	×	×
Proposed Optimal Probabilistic Framework	2m+1 PEM CLT, 2m+1 PEM Edgeworth, CM CLT, CM Edgeworth	Load, PV and EVs	PV generation	✓	✓

MCS: Monte Carlo simulation; PEM: Point Estimate Method; CM: Cumulant method; PV: Photovoltaic; EV: Electric vehicles; ×: Not considered, ✓: considered.

Source: Created by the author.

probabilistic restriction that considers confidence interval levels in the presence of high penetration of PV generation and EVs; 2) An algorithm that uses the statistical information from the probabilistic analysis of the likelihood of technical issues as input parameters in the optimization process; 3) The implementation of a probabilistic algorithm based on different probabilistic techniques such as the MCS, *2m+1* PEM with CLT, *2m+1* PEM with Edgeworth expansion, CM with CLT, CM with Edgeworth expansion with the goal to identify and quantify the likelihood of technical challenges such as overvoltage likelihood.

Among these techniques, the proposed method explores their accuracy regarding the stochastic state variables statistical information such as expected values, standard deviation, skewness, kurtosis and probability distribution functions. Second, the proposed method investigates the efficiency in computational effort of each probabilistic technique with their respective advantages and disadvantages regarding grid size and the number of uncertain variables involved in the grid operation analysis. Third, the proposed method probabilistically optimizes the PV generation of electrical distribution systems with high penetration of PV units and EVs obtaining their operation in terms of confidence interval bounds, probability distribution functions, statistical information of the energy production and loss.

2.1 CHAPTER CONCLUSION

In conclusion, this literature review has provided a comprehensive overview of the existing research on probabilistic techniques applied to the PPF and OPF in electrical distribution networks, through an analysis of the various studies, the need to use specialized probabilistic tools to unleash its potential for the optimal integration of DERs in the modern EDS operation was identified.

The increasing integration of DERs due to globally concern and energy policies to carbon reduction bring challenges to the traditional passive distribution network, which is evolving towards a more complex and dynamic changing system. Therefore, specialized tools are needed to enable system operators and planners to overcome the challenges caused by DERs and to maximize the benefits of the presence of high penetration of PV generation.

This research serves to operators and planners to define acceptable levels of technical challenges likelihood, to handle uncertainties and risk tolerance, to quantify their risk for status-quo operation and at what point an intervention to probabilistically optimize the PV generation in an uncertain environment with high penetration of PV generation and EVs is required to maintain grid reliability and safe

Future research may benefit to apply these findings and to build from this other research path such as hosting capacity of DERs, cost minimization and grid reconfiguration. Overall, the literature reviewed here highlights the significance of probabilistic tools. This knowledge serves as a foundation for the subsequent chapters of this thesis, where statistical concepts will be defined, the implementation of probabilistic techniques of PPF based on the MCS, *2m+1* PEM, CM and curves approximation of probability distribution using the CLT and Edgeworth expansion will be explored and described, and the novel optimal probabilistic framework that is developed to probabilistically maximize PV generation complying with overvoltage likelihood restriction in an uncertain environment will be presented and discussed.

.

3 UNCERTAIN VARIABLE PROBABILITY DENSITY MODELING

The presence of DERs is becoming more ubiquitous in the EDS. Therefore, this increases the complexity for an optimal operation and planning decision analysis of the evolving EDS subject to increasing uncertainty and variability of DERs. Therefore, modeling the behavior of DERs through PDFs (e.g., using available historical data from aggregated demand, solar irradiation, and EV charging demand) provides crucial statistical information that can be easily incorporated into probabilistic assessment tools. In this chapter, the definition of moments and cumulants in statistics are presented, along with the uncertain variables, PDFs modeling for aggregated demand, PV power generation, and aggregated EV charging demand.

3.1 DEFINITION OF MOMENTS AND CUMULANTS

3.1.1 Moments

Moments in statistics describe the characteristic of a distribution by measures of central tendency (raw moments), dispersion (central moments), and higher moments such as skewness for asymmetry and kurtosis for outliers (standardized moments) (ZHANG; LEE, 2004). Moments around zero of a discrete random variable X also known as raw moments can be computed using (1). If $k = 1,$ the formulae yields the expected value $\mu = E[X]$ as its first raw moment.

$$\alpha_k = \mathrm{E}[X^k] = \left(\sum_{i=1}^{n} (X_i)^k / n\right) \tag{1}$$

Moments around the mean of a discrete random variable X also known as central moments, can also be computed in a similar way using (2). If $k = 2$, the variance of variable X is obtained $\beta_2 = Var(X) = \mathrm{E}[(X - \mu)^2]$ and also the standard deviation is obtained using $\sigma = \sqrt{Var(X)}$.

$$\beta_k = \mathrm{E}[(X - \mu)^k] = \left(\sum_{i=1}^{n} (X_i - \mu_X)^k / n\right) \tag{2}$$

A standardized moment of a probability distribution is a moment whose central moment is normalized (generally moments of higher degree) as shown in (3).

$$\tilde{\mu}_k = \mathrm{E}\left[(\frac{X - \mu}{\sigma})^k\right] = \frac{(\sum_{i=1}^{n} (X_i - \mu_X)^k / n)}{(\sum_{i=1}^{n} (X_i - \mu_X)^2 / n)^{k/2}} \tag{3}$$

These metrics are commonly used to describe statistical properties of a variable distribution in terms of expected value, standard deviation, skewness and kurtosis as depicted in Fig. 3. For instance, the measure of asymmetry or skewness ($\tilde{\mu}_3$) is a real-value that characterizes the mass concentration of the distribution and its value for a normal distribution is usually zero or around small values around zero; it can be positive (left-leaning curve) or negative(right-leaning curve). Another feature is the measure of the thickness of the tail of the distribution or kurtosis ($\tilde{\mu}_4$) whose value is 3 for a normal distribution, less than 3 for a light tail, and greater than 3 for higher tails.

Fig. 3 Expected value, standard deviation, skewness and kurtosis metrics

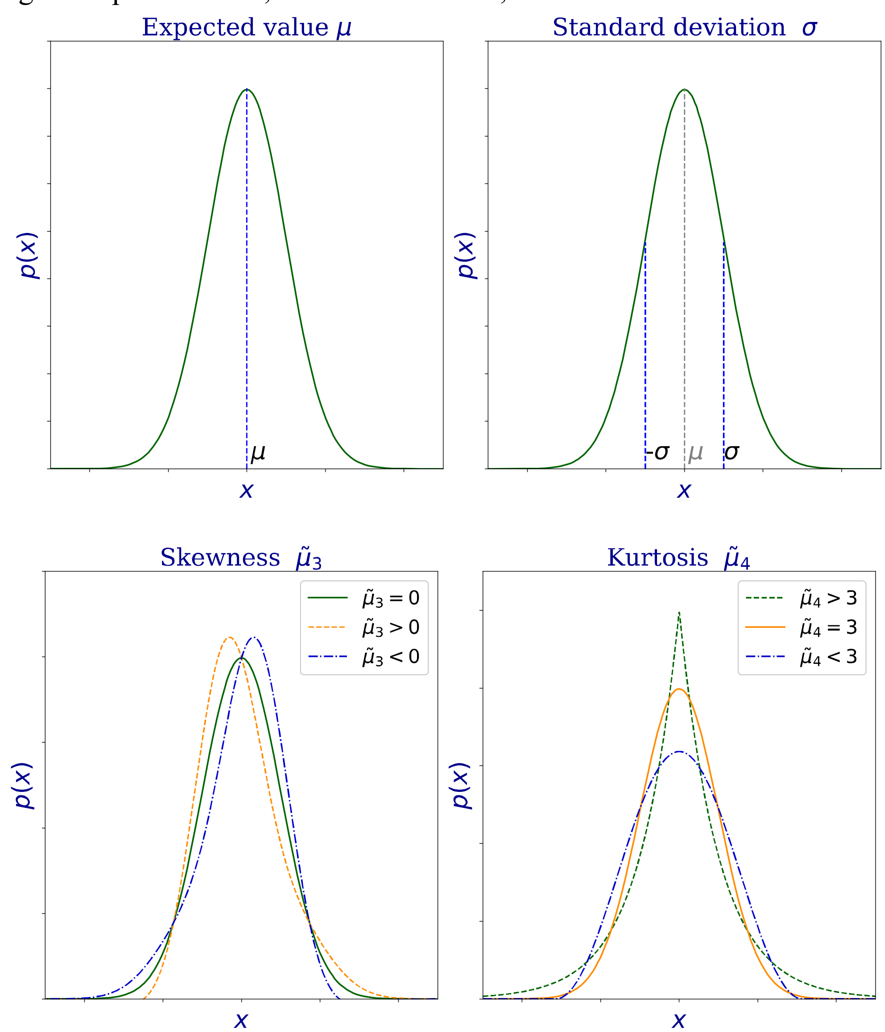

Source: Created by the author

3.1.2 Cumulants

Cumulants in statistics are important since they can represent the properties of a random variable with certain simplicity and efficiency. This reason resides in two special properties of cumulants which are invariance and additivity to deal with random variables (YANG et al., 2020). Let *R* be a random variable; then its *m-th* order cumulant is $k_m(R)$. Let $aR + b$ a random variable in which a and b are real parameters; then its *m-th* order cumulant is expressed in (4), according to the invariance and equivariance property of cumulants:

$$k_m(aR + b) = \begin{Bmatrix} ak_1(R) + b & m = 1 \\ a^m k_m(R) & m \geq 2 \end{Bmatrix} \quad (4)$$

Now, according to the additivity property, let denote *R* and *S* to be uncorrelated random variables; then their *m-th* order cumulants are $k_m(R)$ and $k_m(S)$, respectively. Let *R*+*S be* a random variable, then its *m-th* order cumulant is calculated according to (5).

$$k_m(R + S) = k_m(R) + k_m(S) \quad (5)$$

Furthermore, the cumulant of a random variable can be easily calculated using its raw moments. For instance, the υ^th cumulant κ_υ is calculated in terms of the raw moments α_j using (6)–(8) (FAN et al., 2012).

$$\kappa_\upsilon = \alpha_\upsilon - \sum_{i=1}^{\upsilon-1} \binom{\upsilon - 1}{i - 1} \kappa_i \alpha_{\upsilon-i} \quad (6)$$

$$\alpha_j = E\left[x^{\mathrm{j}}\right] \quad (7)$$

$$\binom{n}{i} = \frac{n!}{i!\,(n - i)!} \quad (8)$$

3.2 PROBABILITY DENSITY OF AGGREGATED DEMAND

The uncertainty of aggregated demand can be represented using the normal distribution function. This is applied to the active and reactive power demand (ZHOU et al., 2020). Let D represent active or reactive power for the aggregated demand, then its probability density function $f(D)$ is written in (9), in which μ_D is the expected value, and σ_D is the standard deviation of the variable D.

$$f(D) = \frac{1}{\sqrt{2\pi\sigma_D^2}} \mathrm{e}^{\left(-\frac{\mathrm{D}-\mu_D}{2\sigma_D^2}\right)} \quad (9)$$

3.3 PROBABILITY DENSITY OF PHOTOVOLTAIC GENERATION

This non-dispatchable form of generation can be modeled with a unitary power factor. The PV active power injection is variable due to the stochastic nature of solar irradiation s. The irradiation is modelled using the Beta distribution as expressed in (10) (FERNANDES et al., 2019; NOR et al., 2018).

$$f_\beta(s) = \frac{\Gamma(\alpha+\beta)}{\Gamma(\alpha)\Gamma(\beta)} s^{(\alpha-1)}(1-s)^{\beta-1} \tag{10}$$

in which, $f_\beta(s)$ represents the PDF of s, $\Gamma(\cdot)$ represents the gamma function, and the parameters α and β are determined in terms of the mean and standard deviation of s using (11) and (12).

$$\alpha = \mu^2(1-\mu)/\sigma^2 - \mu \tag{11}$$

$$\beta = \alpha(1-\mu)/\mu \tag{12}$$

For instance, the PDF and CDF of a specific value of irradiance with an expected solar irradiation $\mu = 0.663\ (kW/m^2)$ and a standard deviation $\sigma = 0.162\ (kW/m^2)$ is computed as shown in Fig. 4. Then, the PV power injection P^{PV} that is highly related to the irradiation can be calculated using (13) (GALLEGO; FRANCO; CORDERO, 2021).

$$P^{PV} = P^{Inst} f_\beta(s) \tag{13}$$

Fig. 4 PDF and CDF of irradiance approximation with Beta function.

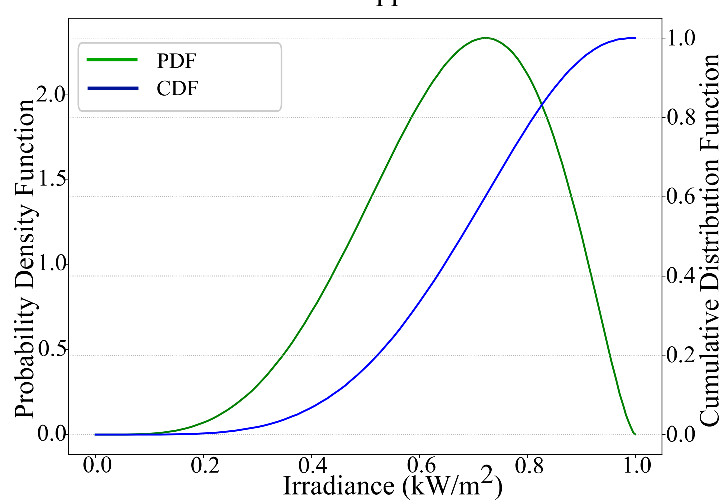

Source: Created by the author.

3.4 PROBABILITY DENSITY OF EV CHARGING DEMAND

An aggregated EV charging demand algorithm was proposed by De Lima et al., (2022). This modeling considers the stochastic behavior of EV charging demand, the EV battery and two fast charging power types of 50 kW and 150 kW, a random state of charge (SOC) with a minimum of 20 % SOC, a total daily travel distance in terms of their probability which is modeled using a normal distribution between 10 km and a maximum of 200 km, and the number of total EVs. This work modifies and adapts the previous algorithm to obtain the hourly PDF of the aggregated EV charging demand.

The hourly stochastic EV charging demand is repeated thousands of times (e.g., N=10000) over each hour in a specific day of analysis. With this high number of samples characterizing the stochastic pattern of EV charging demand, their PDF is obtained as described in Fig. 5. In this figure, the process being with the variable initialization, starting with first hour, within an algorithm to calculation the stochastic EVs charging demand and the process ends when all 24 periods are calculated obtaining the hourly PDF of the aggregated EVs charging demand.

Fig. 5 Algorithm to obtain the PDF of the aggregated EVs charging demand.

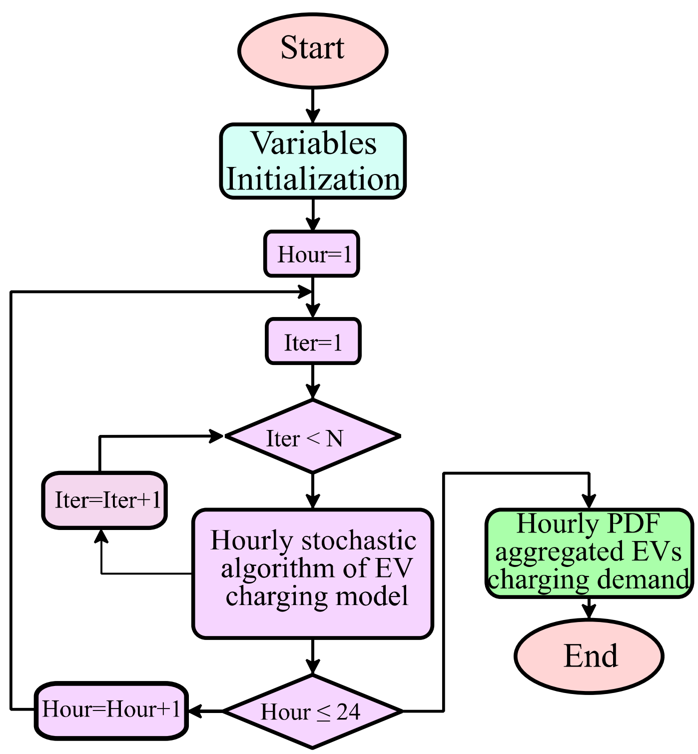

Source: Created by the author.

The probability of charging is obtained from data source in De Lima et al., (2022) that describes the characteristics of EV patterns for charging during the day. The algorithm 1 describes the hourly stochastic algorithm of EV charging demand.

Algorithm 1 Pseudocode of the hourly stochastic algorithm of EV charging demand.

1. Define probability of EV charging for the 24-hour period.
2. Create total number of EV battery type.
3. Define the charger power types.
4. For each EV, random calculation of SOC with minimum of 20%.
5. For a selected day, a normal distribution of distance travel and its energy calculation.
6. If there is enough energy to travel, there is no charging demand.
7. Else, charge the EV to meet the distance travel
8. Calculate randomly a specific hour and day for the EV charging.
9. Finally, calculate the total EVs charging demand for the previous calculated hour.

3.5 CHAPTER CONCLUSION

In this chapter, the concepts of moments, cumulants and uncertain variable probability distribution modeling is examined and described. Uncertainty is an inherent aspect of the real EDS operation and planning situations, and understanding how to model and work with uncertain variables is crucial for making informed decisions to assist the power system operator.

Firstly, the concept of moments and cumulants to describe the characteristics of uncertain variables is presented. The probability distribution modeling of aggregated demand, PV generation and EVs charging demand is discussed, recognizing that modeling can be obtained using available real measurement. The uncertainty quantification of these variables can lead to a more robust and reliable operation for the optimal integration of DERs into the EDS.

It can be concluded in this chapter that uncertain variables modeling by means of the probability distribution functions is a valuable information that can be used within probabilistic tools to address the complex and uncertain nature of the real EDS.

4 PROBABILISTIC POWER FLOW TECHNIQUES

The increasing deployment of DERs poses new challenges for operation and planning in the electrical power system. Therefore, the PPF was developed to cater to the stochastic nature associated with the DERs and the electrical power system aiming to provide an adequate and more realistic assessment tool for the state system variables in terms of their statistical information, which provides a better understanding in operation and management of the power system (PRUSTY; JENA, 2017; RAMADHANI et al., 2020). Among PPF using probabilistic techniques, this thesis adopts and implements the PFF based on MCS, *2m+1* PEM with CLT, *2m+1* PEM with Edgeworth expansion, CM with CLT, and CM with Edgeworth expansion approximations applied to the analysis of EDS with the integration of PV and EVs to obtain statistical characteristics of a system state variable.

4.1 PPF BASED ON MONTE CARLO SIMULATION

The MCS technique is commonly used as a benchmark model that provides accurate statistical results when it comes to assessing complex systems.

The PPF based on MCS approach for the EDS operation analysis have the advantages of a random selection of samples from the PDF of uncertain variables to obtain the scenarios for the deterministic power flow calculation and a relatively simple representation of complex systems.

However, the disadvantages for the PPF based on MCS evaluation is that the technique usually requires high computation processing due to thousands of deterministic power flow calculations needed to reach acceptable values of convergence, becoming unattractive for practical applications in real-time operation (CONSTANTE-FLORES; ILLINDALA, 2019; XIE et al., 2018).

The PPF based on MCS is describe in Fig. 6. In this figure, the stochastic input variables and variable initialization get started, a random selection of scenarios for the PPF beings and the deterministic power flow calculation runs N times, which N represents the total number of iterations (e.g., N=10000). Finally, all executions yield a value to reconstruct the true distribution of the variable of interest and their statistical information.

Fig. 6 PPF based on MCS.

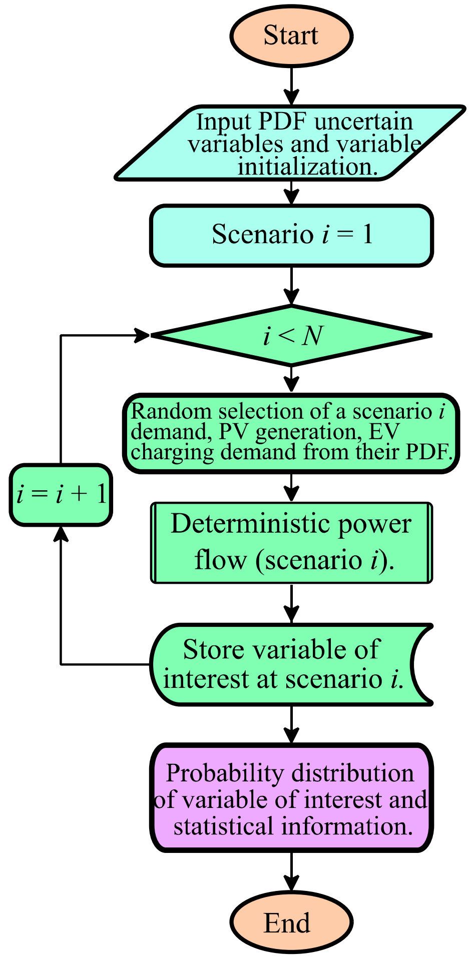

Source: Created by the author.

A general implementation of the PFF based on MCS is also described using the pseudocode of Algorithm 2.

Algorithm 2 Pseudocode of the PPF based on MCS

1. Input uncertain variables probability distribution.
2. Random selection of a scenario (e.g., demand and generation values from the probability distribution).
3. Compute a deterministic power flow.
4. Store state variable of interest (e.g., voltage, current) at each deterministic evaluation.
5. Repeat steps 2 to 4 until a stopping criterion (e.g., the maximum number of iterations or the tolerance convergence of a variable of interest) is satisfied.
6. Once all evaluations are completed, the probability distribution of the variable of interest (e.g., voltage, current, generation, power flow, cost) is available to calculate statistical information (e.g., expected value, standard deviation, confidence interval).

4.2 PPF BASED ON *2M+1* POINT ESTIMATE METHOD

The PPF based on the *2m+1* PEM is an approximate technique that requires *2m+1* times deterministic power flow calculations. This technique's computational burden is linearly dependent on the total number of uncertain variables *m*. A scenario for the power flow calculation is calculated using a simple arithmetic approach to obtain weight and representative values based on the information of mean $\mu_{\boldsymbol{r}}$, standard deviation $\sigma_{\boldsymbol{r}}$, skewness $\lambda_{r,3}$ and kurtosis $\lambda_{r,4}$ at each uncertain variable r which is employed for the execution of a DPF (GALLEGO; FRANCO; CORDERO, 2021; GIRALDO et al., 2019; VERBIC; CANIZARES, 2006). This specific technique computes two constant values $\xi_{\boldsymbol{r},\boldsymbol{i}}$ associated to random variable r, two weighting factors $\omega_{r,i}$, and two representative values $y_{\boldsymbol{r},\boldsymbol{i}}$ as expressed in (14)–(16), let $i \in \{1, 2\}$ for each uncertain variable and its respective scenario i.

$$\xi_{\boldsymbol{r},\boldsymbol{i}} = \lambda_{\boldsymbol{r},\boldsymbol{3}}/2 + (-1)^{3-\boldsymbol{i}} \sqrt{\lambda_{\boldsymbol{r},\boldsymbol{4}} + 3(\lambda_{\boldsymbol{r},\boldsymbol{3}})^2/4} \tag{14}$$

$$\omega_{r,i} = (-1)^{3-i} \left(\xi_{r,i} (\xi_{r,1} - \xi_{r,2}) \right)^{-1} \tag{15}$$

$$y_{\boldsymbol{r},\boldsymbol{i}} = \mu_{\boldsymbol{r}} + \xi_{\boldsymbol{r},\boldsymbol{i}} \sigma_{\boldsymbol{r}} \tag{16}$$

Once the *2m* DPF is computed, an additional DPF is executed with a scenario that considers the expected values of each uncertain variable as representative values, and then its weighting factor is calculated using (17).

$$\omega_0 = 1 - \sum_{r=1}^{m} \sum_{i=1}^{2} \omega_{r,i} \tag{17}$$

Now, for the calculation of state variables of the PPF, let define $W_v = \{\omega_{r,i} \cup \omega_0\}$ as the weighting factors and $Y_v = \{v_{r,i} \cup v_0\}$ group-specific state variable of interest such as voltages *v*. Then the *j-th* statistical raw moment $E[v^j]$ is calculated using (18).

$$E[v^j] = E[v^j] = \sum_{r=1}^{m} \sum_{i=1}^{2} \left(\omega_{\boldsymbol{r},\boldsymbol{i}} (v_{r,,i})^{\boldsymbol{j}} \right) + \omega_0 (v_0)^{\boldsymbol{j}} \tag{18}$$

In a similar fashion, the statistical characteristics of any other state variables (e.g., current, power flow, power generation, supply energy, cost) can be expressed in terms of expected value μ_v, standard deviation σ_v, skewness $\lambda_{v,3}$, and kurtosis $\lambda_{v,4}$ using (19)–(22).

$$\mu_v = E[v^1] = \sum_{r=1}^{m} \sum_{i=1}^{2} \left(\omega_{\boldsymbol{r},\boldsymbol{i}} (v_{r,,i})^{\boldsymbol{j}} \right) + \omega_0 (v_0)^{\boldsymbol{j}} \tag{19}$$

$$\sigma_v = \sqrt{E[v^2] - (E[v^1])^2} \tag{20}$$

$$\lambda_{v,3} = \frac{E[v^3] - 3E[v^1]E[v^2] + 2(E[v^1])^3}{{\sigma_v}^3} \tag{21}$$

$$\lambda_{v,4} = \frac{E[v^4] - 4E[v^3]E[v^1] + 6E[v^2](E[v^1])^2 - 3(E[v^1])^4}{{\sigma_v}^4} \tag{22}$$

The PPF based on *2m+1* PEM is described in Fig. 7. In this figure, the stochastic input variables and variable initialization get started, the total number of scenarios are *2m+1* which *m* represents the total number of uncertain variables. The PEM method calculates the scenario *i-th* for the deterministic power flow calculation. Finally, all *2m+1* executions yield the raw moments information of the variable of interest.

Fig. 7 PPF based on *2m+1* PEM.

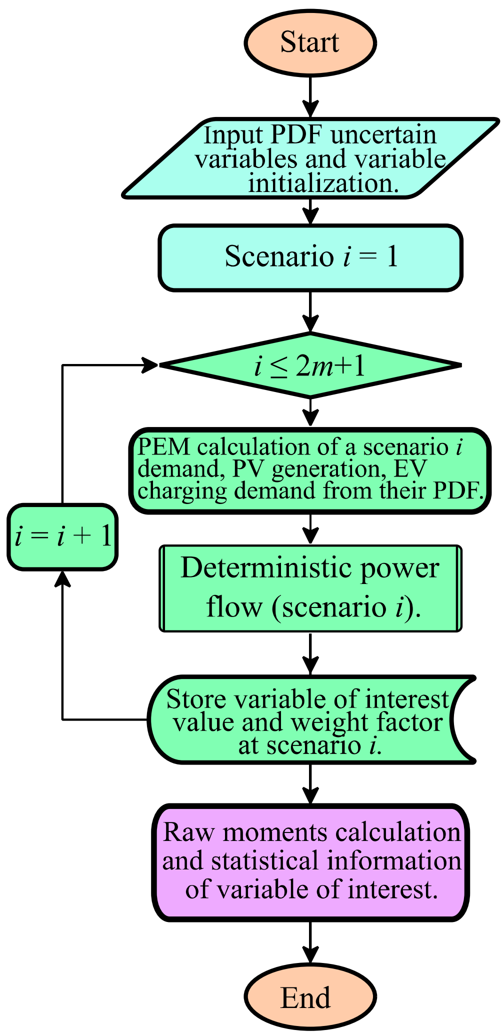

Source: Created by the author.

The probability density function of a variable of interest can be reconstructed based on its statistical information using probability curves approximation such as the CLT or the Edgeworth expansion for raw moments. A general implementation of the PFF based on *2m+1* PEM is described using the following pseudocode of Algorithm 3.

Algorithm 3 Pseudocode of the PPF based on *2m+1* PEM

1. Input uncertain variables probability distribution.
2. Define a scenario calculation based on the *2m+1* PEM probabilistic technique (e.g., weighting factors and representative values for demand and generation).
3. Compute a deterministic power flow.
4. Store state variable of interest (e.g., voltage, current) and its weighting factors at each deterministic evaluation.
5. Calculate the next scenario using step 2, and repeat the process of step 3 and 4 until the completion of *2m+1* deterministic power flows.
6. Once all evaluations are completed, the raw moments of the variable of interest (e.g., voltage, current, generation, power flow, cost) are available.
7. The probability distribution of a variable of interest can be reconstructed based on the statistical information of step 6 using CLT or Edgeworth expansion for raw moments to calculate more statistical information such as confidence intervals.

4.3 PPF FLOW BASED ON CUMULANT METHOD

The PPF based on the CM is an analytical technique that requires the identification of a linear relation with the stochastic input variables and output variables of interest to obtain their statistical information in terms of cumulants (FAN et al., 2012; YANG et al., 2020; ZHANG; LEE, 2004). In this sense, the application of this analytical technique allows to obtain a linear relation between input and output variables for the non-linear power flow equation that is represented in (23).

$$S = F(V, Y) \tag{23}$$

in which S represents the bus power injection (net generation minus net demand of active and reactive power calculated at each bus); V and Y represent voltage phasor and network admittance matrix, respectively. This linear relation is calculated using the Taylor series expansion around an operating point $\{S_0, V_0, Y_0\}$ and taking into account the first order of the series expansion. In (24), the voltage variation ΔV causes a power injection variation ΔS. Then, the function $F(V_0 + \Delta V, Y_0)$ is written in its Taylor series expansion in (25).

$$S = S_0 + \Delta S = F(V_0 + \Delta V, Y_0) \tag{24}$$

$$S = F(V_0, Y_0) + \frac{\partial F(V, Y)}{\partial V} |(V_0, Y_0) \Delta V \tag{25}$$

Subsequently, the power injection variation can be expressed in terms of the first derivative of the function $F(*)$ evaluated around the operating point (V_0, Y_0) multiplied by the voltage variation in (26).

$$\Delta S = \frac{\partial F(V,Y)}{\partial V}|(V_0, Y_0)\Delta V = J_0 \Delta V \tag{26}$$

in which J_0 is the Jacobian matrix in (27) evaluated at (V_0, Y_0). Then, the voltage variation is obtained in terms of the inverse of the Jacobian and the variation of power injection in (28).

$$J_0 = \begin{bmatrix} \frac{dP}{d\theta} & \frac{dP}{dv} \\ \frac{dQ}{d\theta} & \frac{dQ}{dv} \end{bmatrix} \tag{27}$$

$$\Delta V = {J_0}^{-1} \Delta S \tag{28}$$

Afterward, the cumulant properties are applied to the linear combination of voltage variation and power injection variation. Generally, the active and reactive power injection can be considered as stochastic input variables (e.g., demand and generation).

Equation (28) is modified by replacing $\Delta V = V - V_0$ to obtain $\Delta S = S - S_0$, leading to (29) which represents the linear relation of voltage phasor and power injection. Now, using cumulant properties in this equation, the cumulants of voltage phasor k_m^V that contains the angle θ and voltage magnitude v are obtained in terms of the Jacobian inverse and power injection cumulants k_m^S. For instance, k_1^V is obtained for $m = 1$ in (30). Then, cumulants of voltage phasor of *2-nd* order or more for $m \geq 2$ in (31).

$$V = V_0 + {J_0}^{-1}(S - S_0) \tag{29}$$

$$k_1^V = V_0 + {J_0}^{-1}(k_1^S - S_0); m = 1 \tag{30}$$

$$k_m^V = [{J_0}^{-1}]^m k_m^S \,; m \geq 2 \tag{31}$$

The power injection cumulants contains the active and reactive power injection of the stochastic information of demand and generation. Since the PDF of power injection is a known distribution that can be obtained by real measurements probability function modeling, their cumulants k_m^S of order *m-th* can be calculated using their raw moments α_m^S information. For instance, the calculation of the *4-th* order of cumulants, k_m^S is expressed in (32)–(35).

$$k_1^S = \alpha_1^S \tag{32}$$

$$k_2^S = \alpha_2^S - (k_1^S)^2 \tag{33}$$

$$k_3^S = \alpha_3^S - 2\alpha_1^S k_2^S - \alpha_2^S k_1^S \tag{34}$$

$$k_4^S = \alpha_4^S - 3\alpha_1^S k_3^S - 3\alpha_2^S k_2^S - \alpha_3^S k_1^S \tag{35}$$

Therefore, after calculating the cumulants of power injections, the cumulants of voltage (e.g., k_1^V, k_2^V, k_3^V, and k_4^V) can be obtained. Furthermore, the expected value μ_V and standard deviation σ_V of the voltage phasor can be easily calculated by $\mu_V = k_1^V$ and $\sigma_V = \sqrt{k_2^V}$, respectively.

Similarly, the linear mapping for active and reactive power flow through lines *j* to *k* can be expressed in terms of their cumulants in (36) and (37).

$$k_1^{PQ} = PQ_{jk_0} + L_0 {J_0}^{-1}(k_1^S - S_0); m = 1 \tag{36}$$

$$k_m^{PQ} = [L_0 {J_0}^{-1}]^m k_m^S \, ; m \geq 2 \tag{37}$$

$$L_0 = \begin{bmatrix} \frac{dP_{jk}}{d\theta_j} & \frac{dP_{jk}}{d\theta_k} & \frac{dP_{jk}}{dv_j} & \frac{dP_{jk}}{dv_k} \\ \frac{dQ_{jk}}{d\theta_j} & \frac{dQ_{jk}}{d\theta_k} & \frac{dQ_{jk}}{dv_j} & \frac{dQ_{jk}}{dv_k} \end{bmatrix} \tag{38}$$

in which the matrix L_0 represents the derivatives of active and reactive power flow through lines with respect to the angle and magnitude of voltages in (38). The process is similar for the linear mapping of line current in (39)–(41), where C_0 represents the derivative of line current with respect to the angle and magnitude of voltages. This process of linear mapping and cumulants can be extended to other variables, such as power losses.

$$k_1^I = I_{km_0} + C_0 {J_0}^{-1}(k_1^S - S_0); m = 1 \tag{39}$$

$$k_m^I = [C_0 {J_0}^{-1}]^m k_m^S \, ; m \geq 2 \tag{40}$$

$$C_0 = \begin{bmatrix} \frac{dI_{jk}}{d\theta_j} & \frac{dI_{jk}}{d\theta_k} & \frac{dI_{jk}}{dv_j} & \frac{dI_{jk}}{dv_k} \end{bmatrix} \tag{41}$$

The PPF based on CM is describe in Fig. 8. In this figure, the stochastic input variables and variable initialization get started, the method executes one deterministic power flow with a scenario of expected values for all uncertain variables. The cumulants properties applied to the power flow equations presented above are calculated to obtain the *n-th* cumulant of the variable of interest. Finally, the statistical characteristics of the variable of interest are obtained.

Then, the probability density function of a variable of interest (e.g., voltages, power flows, and currents through lines) can be reconstructed based on their statistical information of cumulants using probability curves approximation such as the CLT or the Edgeworth expansion for cumulants. A general implementation of the PFF based on CM is described using the pseudocode of Algorithm 4.

Fig. 8 PPF based on CM.

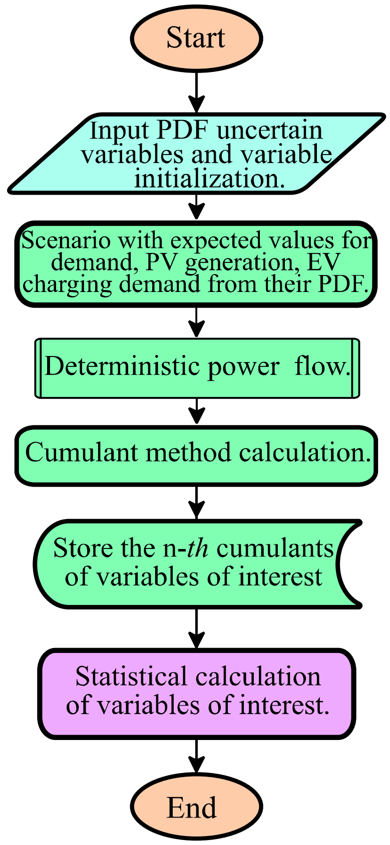

Source: Created by the author.

Algorithm 4 Pseudocode of the PPF based on CM

1. Input uncertain variables probability distribution.
2. Compute a deterministic power flow with a scenario of expected values of the uncertain variables (e.g., demand and generation).
3. Calculate the linear relation of variables of interest (e.g., the Jacobian matrix J_0 for voltage and power injection obtained in Step 2) and the initial point of operation (e.g., voltages V_0 and calculated injected power S_0 obtain in Step 2)
4. Calculate the cumulants of order *m-th* for the active and reactive power injection probability distribution k_m^S.
5. Compute cumulants of order *m-th* for the variable of interest (e.g., k_1^V, k_2^V, k_3^V, and k_4^V for voltage phasor).
6. The probability distribution of a variable of interest can be reconstructed based on their cumulant's information of Step 5 using CLT or Edgeworth expansion for cumulants, to calculate more statistical information such as skewness, kurtosis and confidence intervals.

4.4 CENTRAL LIMIT THEOREM

The central limit theorem (CLT) states that the larger the sample of a random variable distribution the more it approximates to a Gaussian or Normal distribution (GIRALDO et al., 2019). This can be applied to the PPF output variables probability distribution. For instance, it can be assumed that a probability distribution of voltages can be approximated by a Normal distribution. Then, a control parameter α^V can be calculated to limit a specific interval of voltage possibilities ($[\mu_V + \alpha^V\sigma_V, \mu_V - \alpha^V\sigma_V]$) with a maximum voltage value v_m as depicted in Fig. 9 and using the error function, expressed in (42) and (43).

$$P^V = \Pr[\mu_V - \alpha^V\sigma_V < \mathrm{V} < \mu_V + \alpha^V\sigma_V] = \mathrm{erf}(\frac{\alpha^V}{\sqrt{2}}) \tag{42}$$

$$\alpha^V = \mathrm{erf}^{-1}(P^V)\sqrt{2} \tag{43}$$

in which, $\mathrm{erf}(*)$ signifies the error function, $\mathrm{erf}^{-1}(*)$ means the inverse of the error function, and P^V represents the probability value. For instance, a 95% of possibilities for voltage realizations to fall somewhere between $[\mu_V + \alpha^V\sigma_V, \mu_V - \alpha^V\sigma_V]$ requires a value of 1.96 for α^V.

The application of the CLT to approximate PDF of variables of interest obtained from the PPF can be particularly powerful when the expected value and standard deviation are the only statistical parameters to be known from the variable of interest.

4.5 EDGEWORTH EXPANSION APPROXIMATION

The Edgeworth expansion is a powerful PDF approximation curve due to its asymptotic properties that only require the information of moments or cumulants (BLINNIKOV; MOESSNER, 1998). This function utilizes the Normal distribution as a reference function $\varphi(x)$ of a variable of interest x, with an expected value μ_x and standard deviation σ_x in (44), and $\phi(x)$ represent its CDF in (45).

$$\varphi(x) = \frac{1}{\sqrt{2\pi{\sigma_x}^2}}e^{\left(-\frac{x-\mu_x}{2{\sigma_x}^2}\right)} \tag{44}$$

$$\phi(x) = \int_{-\infty}^{z}\varphi(x)dx \tag{45}$$

The Edgeworth expansion with cumulants information satisfies the asymptotic property with the first four cumulants (e.g., k_1^x, k_2^x, k_3^x, and k_4^x) of the uncertain variable x under

Fig. 9 Confidence interval calculation for a Normal distribution.

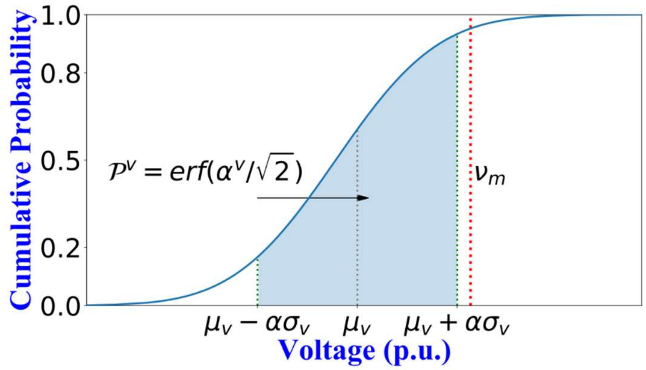

Source: Created by the author.

analysis. Now, let be a normalized value $z = \frac{x-\mu_x}{\sigma_x}$ that is used for the calculation of the Chebyshev-Hermite polynomial in (46) which is then used in the Edgeworth expansion in (47).

$$He_n(z) = n! \sum_{k=0}^{n/2} \frac{(-1)^z z^{n-2k}}{k!\,(n-2k)!\,2^k} \tag{46}$$

$$f(x) = \varphi(x) \left\{ 1 + \frac{k_3^x He_3(z)}{3!\,k_2^{x1.5}} + \frac{k_4^x He_4(z)}{4!\,k_2^{x2}} + \frac{10 k_3^{x2} He_3(z))}{6!\,k_2^{x3}} \right\} \tag{47}$$

Similarly, a formulation of the Edgeworth expansion with the moments information that satisfy the asymptotic property considers the first four moments (e.g., raw moments obtained from the evaluation of PPF based on the *2m+1* PEM) of the variable of interest x. Since the raw moments are known, the expected μ_x, standard deviation σ_x, skewness $\lambda_{x,3}$ and kurtosis $\lambda_{x,4}$ values of x can be calculated, then the Edgeworth expansion can be expressed in (48).

$$f(x) = \varphi(x) \left\{ 1 + \frac{\lambda_{x,3} He_3(z)}{3!} + \frac{(\lambda_{x,4} - 3) He_4(z)}{4!} + \frac{\lambda_{x,3}^2 He_6(z)}{6!} \right\} \tag{48}$$

After computing the Edgeworth expansion, the PDF function is obtained. This function is transformed to obtain an approximation of their data distribution. Then, using this reconstructed data distribution and applying a Kernel estimator, the probability distribution and statistical analysis for quantiles or confidence intervals for a variable of interest such as voltage, current and power flow through lines, can be calculated.

4.6 CHAPTER CONCLUSION

This chapter has explored into the essential concepts of probabilistic power flow techniques with their respective implementation algorithms. First, the Monte Carlo simulation (MCS), the 2m+1 Point Estimate Method (PEM), the Cumulant Method (CM), and curve approximations of Central Limit Theorem (CLT) and Edgeworth expansion and their potential in handling uncertainties were presented.

Throughout this chapter, the PPF based on MCS is a technique that requires a great number of deterministic calculations, the PPF based on $2m+1$ PEM improves computational efficiency though highly related to the number of uncertain variables, PPF based on CM stands among the other techniques due to its only single deterministic calculation to solve the probabilistic approach. This chapter also presents curve approximations of CLT for Normal distribution and the Edgeworth expansion to reconstruct the true distribution. These algorithms have been described for their implementation of probabilistic power flows and curve approximations that offer an important probabilistic tool for assessing the impact of uncertainties on power system operations.

These probabilistic techniques applied to the PPF problem allow us to quantify the likelihood of different variables of interest such as voltages, current, power flow through lines. Moreover, as power systems become more complex and subject to increasing uncertainties due to renewable energy integration and changing operational conditions, probabilistic power flow techniques emerge as indispensable tools to realistically address the stochastic nature of the EDS planning and operation. By providing a probabilistic perspective, these methods have the potential to assist system operators, planners and researchers to make informed decisions for the optimal integration of DERs into the EDS in the face of uncertainty.

In the next chapter, the proposed optimal probabilistic framework will be presented. It employs the statistical information obtained from the probabilistic power flow techniques to probabilistically optimize PV generation by means of using statistical information within a mathematical model for grid optimization while addressing the technical challenges of overvoltage likelihood.

5 PROBABILISTIC FRAMEWORK FOR THE OPTIMAL GRID OPERATION

This chapter introduces the proposed probabilistic framework with the goal to maximize PV energy production; while mitigating the likelihood of overvoltage considering confidence interval restrictions. In this sense, an optimization process is required to keep a suitable operation of the system operation in the presence of high penetration of PV generation and EVs, which is developed in the following subsections. First, it is presented the algorithm for the optimal probabilistic framework that employs the statistical information from the analysis of PPF based on different probabilistic techniques which is used within an optimal power flow model that iteratively calculates the optimal probability distribution of PV generation. Second, the mathematical model to represent the maximization of PV generation is presented, as well as the algorithm that iteratively set the operational limits for voltage based on the statistical information of expected value, standard deviation and confidence interval of voltage units, as along with the statistical information of expected values from demand, PV generation and EVs charging demand.

5.1 PROBABILISTIC FRAMEWORK

The proposed framework to probabilistically maximize PV power generation units, while mitigating the probability of overvoltage considering a certain confidence interval restriction for a suitable grid operation in the presence of high penetration of PV generation and EVs, is described in Fig. 10.

In Fig. 10, the variable initialization is started, then the strategy to solve this problem begins with the probability distribution modeling of the stochastic variables, and this probability modeling is based on historical data from solar irradiation for the PV power generation, stochastic charging behavior algorithm for the aggregated EV charging demand PDF, and load profiles for the aggregated demand modeled using the normal distribution.

Then, a probabilistic evaluation of the EDS is carried out by the PPF which executes the probabilistic power flow calculation to obtain the statistical information of voltages with a specific confidence interval level and their probability of overvoltage. This work implemented different probabilistic techniques such as the PPF based on Monte Carlo simulation, $2m+1$ PEM with CLT, 2m+1 PEM with Edgeworth expansion, CM with CLT and CM with Edgeworth expansion with the goal of studying their performance on the proposed model to solve probabilistically the maximization of PV generation in an uncertain environment.

After the PPF evaluation and PDF approximations, the confidence interval of voltages is evaluated using the CLT or the Edgeworth expansion approximations. The CLT uses the Normal distribution; and the Edgeworth expansion calculates the PDF and CDF of a variable based on their moments or cumulants information enabling the calculation of quantiles and confidence intervals.

Then, as previously mentioned, the PV power generation is a stochastic variable that particularly increases its power injection during periods of high solar irradiation which may coincide with low load demand, thus, causing an increase in the likelihood of overvoltage. The voltage statistical information provided from the PPF evaluation that do not comply with the

Fig. 10 Proposed model to probabilistically maximize PV power generation.

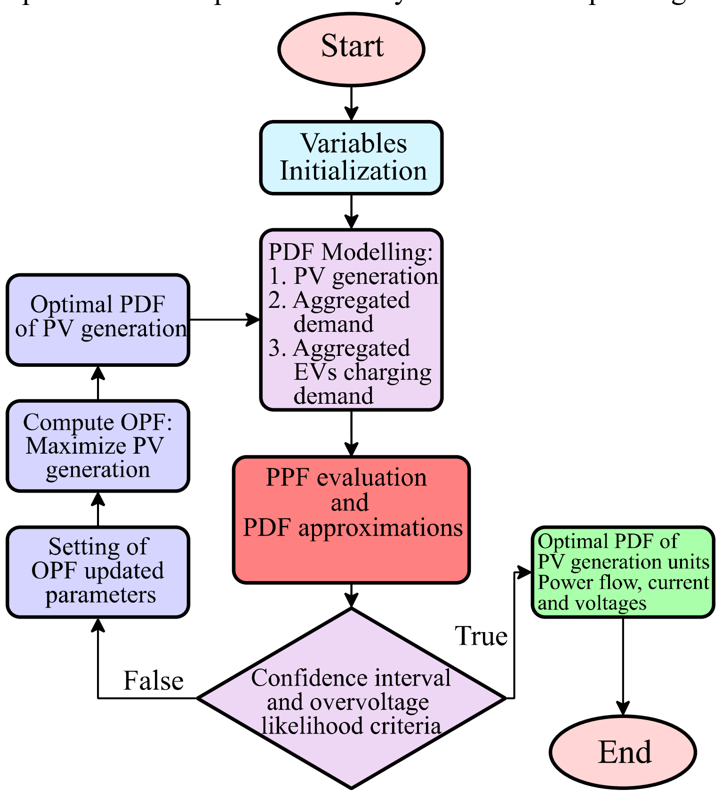

Source: Created by the author.

probabilistic restriction enters within the optimization process. Within the optimization process, an algorithm is developed to compute the statistical information regarding the confidence interval of all voltages, expected value, standard deviation and bus identification with a higher probability of overvoltage occurrence greater than a maximum allowable voltage (e.g., 1.05 p.u.).

This statistical voltage information plus the expected values from the current probability distribution of the PV generation units, the aggregated EV charging, and load demand drawn from the PPF evaluation serves as input information within the iterative optimization process. This optimization process consists of the mathematical formulation to probabilistically maximize PV generation and within the optimization model, the statistical information obtained from the PPF is set to update the parameters model.

Then, the optimization problem is solved under this new setting of parameters to obtain the expected values for the optimal generation of each PV unit. The probability distribution of each PV generation is calculated using this new set of optimal values of expected power injections. A PPF evaluation is carried out to verify that the new settings of PV generation satisfy the voltage confidence interval restriction, and this iterative process continues until the probability of overvoltage occurrence of all voltages is less than the allowable maximum voltage (1.05 p.u.). Once the criterion of the probability of overvoltage is satisfied to be less than an established or desired setting for maximum voltage, it is obtained the optimal probability functions for the PV generation units, power supply, power flow through lines, current and voltages which is a crucial statistical information for the optimal integration of DERs into the EDS operation and planning.

5.2 OPTIMAL POWER FLOW FORMULATION

The optimal power flow problem is formulated as a non-linear optimization problem whose controllable variable is the power injection from PV units, and the technical constraints considers the current injection balance, voltage drop, current injection of load, generators, operating limits for generators, and voltage limits. This work uses the three-phase representation of the EDS based on real and imaginary parts of voltages and currents (SABILLON ANTUNEZ et al., 2016). The mathematical formulation of the OPF objective function aims to maximize the power injection of PV units in (49).

$$maximize \sum_{n} P_n^G \quad \forall\, n \in G \tag{49}$$

The operational constraints considered for the EDS optimal operation are: 1) the balance of the real and imaginary parts of the circuit currents at each node in (50) and (51); 2) the real and imaginary parts for Kirchhoff’s voltage law of each circuit loop in (52) and (53); 3) the real and imaginary parts of a relation between current, power and voltage for load demand in (54) and (55); 4) the real and imaginary parts of a relation between current, power and voltage for PV power units under the assumption that each PV equally inject power at each phase in (56) and (57); 5) the operation limits of the PV power injection units in (58) and (59), and the operation limit for voltage magnitude at each circuit loop in (60).

$$\begin{aligned} -\sum_{nm \in L} I^{re}_{nm,f} + \sum_{mn \in L} I^{re}_{mn,f} \\ + \sum_{h \in F} \left\{ \frac{\left(\sum_{nm \in L} B^{shunt}_{nm,f,h} + \sum_{mn \in L} B^{shun}_{nm,f,h}\right) V^{im}_{n,h}}{2} \right\} \\ = I^{Dre}_{n,f} - I^{Gre}_{n,f} - I^{re}_{se,f} \quad \forall\, n \in N, f \in F \end{aligned} \tag{50}$$

$$\begin{aligned} -\sum_{nm \in L} I^{im}_{nm,f} + \sum_{mn \in L} I^{im}_{mn,f} \\ - \sum_{h \in F} \left\{ \frac{\left(\sum_{nm \in L} B^{shunt}_{nm,f,h} + \sum_{mn \in L} B^{shunt}_{nm,f,h}\right) V^{re}_{n,h}}{2} \right\} \\ = I^{Dim}_{n,f} - I^{Gim}_{n,f} - I^{im}_{se,f} \quad \forall\, n \in N, f \in F \end{aligned} \tag{51}$$

$$V^{re}_{m,f} - V^{re}_{n,f} = \sum_{r \in F} \left\{ R_{mn,f,r} I^{re}_{mn,r} - X_{mn,f,r} I^{im}_{mn,r} \right\} \quad \forall\, m,n \in L, f \in F \tag{52}$$

$$V^{im}_{m,f} - V^{im}_{n,f} = \sum_{r \in F} \left\{ X_{mn,f,r} I^{re}_{mn,r} + R_{mn,f,r} I^{im}_{mn,r} \right\} \quad \forall\, m,n \in L, f \in F \tag{53}$$

$$I^{Dre}_{n,f} = L_s * \left\{ \frac{P^D_{n,f} V^{re}_{n,f} + Q^D_{n,f} V^{im}_{n,f}}{{V^{re}_{n,f}}^2 + {V^{im}_{n,f}}^2} \right\} \quad \forall\, n \in N, f \in F \tag{54}$$

$$I^{Dim}_{n,f} = L_s * \left\{ \frac{-Q^D_{n,f} V^{re}_{n,f} + P^D_{n,f} V^{im}_{n,f}}{{V^{re}_{n,f}}^2 + {V^{im}_{n,f}}^2} \right\} \quad \forall\, n \in N, f \in F \tag{55}$$

$$I^{Gre}_{n,f} = \frac{1}{3} \left\{ \frac{P^G_n V^{re}_{n,f} + Q^G_n V^{im}_{n,f}}{{V^{re}_{n,f}}^2 + {V^{im}_{n,f}}^2} \right\} \quad \forall\, n \in G, f \in F \tag{56}$$

$$I^{Gim}_{n,f} = \frac{1}{3} \left\{ \frac{-Q^G_n V^{re}_{n,f} + P^G_n V^{im}_{n,f}}{{V^{re}_{n,f}}^2 + {V^{im}_{n,f}}^2} \right\} \quad \forall\, n \in G, f \in F \tag{57}$$

$$0 \le P^G_n \le \bar{P}^G_n \quad \forall\, n \in G \tag{58}$$

$$Q^G_n = 0 \quad \forall\, n \in G \tag{59}$$

$$\left(\underline{V_n}\right)^2 \leq V_{n,f}^{re\,2} + V_{n,f}^{im\,2} \leq \left(\overline{V_n}\right)^2 \quad \forall\, n \in N, f \; in \; F \tag{60}$$

The load $P_{n,f}^{D}$ is calculated in terms of the expected value $\mu_{n,f}^{load}$ and $\mu_{n,f}^{EVs}$ from the probability distribution of load and the aggregated EVs charging demand in (61), and the maximum value of PV power injection units in terms of their respective expected value μ_n^{gen} in (62).

$$P_{n,f}^{D} = \mu_{n,f}^{load} + \mu_{n,f}^{EVs} \tag{61}$$

$$\overline{P}_n^{G} = \mu_n^{gen} \tag{62}$$

$$\overline{V_n} = F(\mu_{V,n}, \sigma_{V,n}, \overline{V_{CI}^{n}}, t) \tag{63}$$

Finally, the maximum voltage limit $\overline{V_n}$ expressed in (63) is calculated in terms of $\mu_{V,n}$ and $\sigma_{V,n}$ which are expected and standard deviation voltage of the *n-th* bus, $\overline{V_{CI}^{n}}$ represents the upper bound of the *n-th* voltage confidence interval, and t is an iteration parameter.

$$F\left(\overline{V_{CI}^{n}}, t\right) = \begin{cases} \dfrac{v_m\left(1 + \dfrac{(2-0.04\text{t})\sigma_{V,n}}{\mu_{V,n}}\right)}{\left(1 + \dfrac{2\sigma_{V,n}}{\mu_{V,n}}\right)}; \; t = 0 \\ v_m(1 - a \cdot t)\,; t > 0 \; and \; \mu_{V,n} > v_m \\ \mu_{V,n}(1 - b \cdot t)\,; t > 0 \; and \; \mu_{V,n} < v_m \\ \mu_{V,n}(1 - c \cdot t)\,; t > 0 \; and \left\lfloor \overline{V_{CI}^{n}} \right\rfloor = v_m \end{cases} \tag{64}$$

in which, v_m is the maximum allowable voltage (e.g., 1.05 p.u.), while a, b, and c represent parameters that proportionally reduce the voltage limits based on the voltage statistical information. Since the stochastic input variables have uncertainty and variability in the EDS, the output variables (e.g., voltage) may present lower or higher variations depending on the

Fig. 11 Iterative optimization process of the voltage confidence interval.

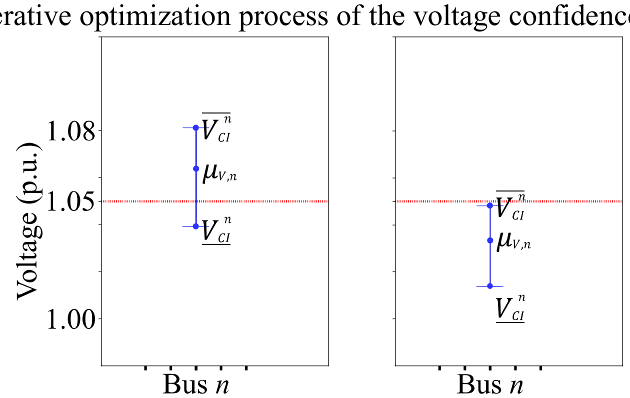

Source: Created by the author.

input variables uncertainty. With this in mind, the initial voltage variation is approximated to a normal variation whose upper bound value becomes closer to the maximum allowable voltage of 1.05 p.u. as depicted in Fig. 11. In this figure, the iterative optimization process of reducing the voltage variation is obtained using (64).

5.3 ACCURACY METRIC INDEX

This work uses the percentage relative error (PRE) in (65) and the relative mean square error (PRMSE) in (66) as accuracy indices ϵ_T^y and δ_y of a variable y to evaluate the performance of the PPF and the proposed probabilistic optimization framework with different probabilistic techniques compared to the MCS. For instance, the statistical information of voltage, current and power flow through a line, and PV power injection will be assessed in terms of their expected values, standard deviation, skewness, kurtosis, and upper and lower bound of confidence interval values.

$$\epsilon_T^y = \frac{\left|T_{MCS}^y - T_{METHOD}^y\right|}{T_{MCS}^y} \cdot 100\% \tag{65}$$

$$\delta_y = \sqrt{\frac{1}{m}\frac{\sum_{i=1}^{m}(y_{MCS,i} - y_{METHOD,i})^2}{\sum_{i=1}^{m} {y_{METHOD,i}}^2}} \cdot 100\% \tag{66}$$

in which T represents a statistical evaluation (e.g., mean, expected deviation, skewness, and kurtosis), m represents sample number, $y_{MCS,i}$ represents the value for a variable of interest obtained with the MCS, while $y_{METHOD,i}$ corresponds to the proposed method value.

5.4 CHAPTER CONCLUSION

This chapter has presented a novel probabilistic optimal framework designed to probabilistically maximize PV generation while satisfying voltage confidence interval constraint. By leveraging probabilistic techniques, mathematical model of the EDS optimal operation and an iterative algorithm for the voltage confidence optimization were formulated. With this probabilistic optimization tool, a more robust and accurate solution can be obtained to better represent and make informed-decision regarding the EDS optimal operation. The subsequent chapters will assess the implementation of the proposed method using test system, discussion of the results, providing a comprehensive view of the potential impact of this framework in the optimal integration of DERs into the EDS operation and planning.

6 RESULTS AND DISCUSSIONS

This chapter presents the results that involves the process of the proposed optimal probabilistic framework. First, the hourly probability distribution modeling of uncertain variables. Second, the assessment of computational efficiency when executed the implemented PPF with different probabilistic techniques. Third, the evaluation of IEEE 33 bus system, IEEE 69 bus system and a real test system EDS 202 bus operation with high penetration of PV generation and EV applying the PPF and the proposed optimal probabilistic framework.

This proposed method was implemented within the Python environment due to its potential and flexibility to manage various applications (VAN ROSSUM; DRAKE, 2012). This work employs the Python package *py_dss_interface* that provides an interface for the open distribution system simulator (OpenDSS) (DUGAN; MCDERMOTT, 2011). This application interface is used for the modeling of grid parameters and access to the results obtained for the power flow calculations. The PPF algorithm based on the *2m+1* PEM with CLT, *2m+1* PEM with Edgeworth expansion, the CM with CLT, CM with Edgeworth expansion, and MCS are written in the python environment using the Python package *py_pss_interface* that executes the OpenDSS application to perform the power flow calculations. Another Python package is the *amplpy* for the interaction with the mathematical programming language (AMPL) to write over the mathematical formulation, and update its parameters (BRANDAO et al., 2021; FOURER; GAY; KERNIGHAN, 2003). The optimization model is solved using the KNITRO solver (BYRD; NOCEDAL; WALTZ, 2006). The assessment and implementation of the proposed method is carried out on a computer featured with Intel Core i5 2.4 GHz processor and 6 GB of RAM.

6.1 PROBABILITY DISTRIBUTION OF UNCERTAIN VARIABLES

The hourly probability distribution modeling of each uncertain variable, namely aggregated demand, PV generation and aggregated EV charging demand considers 10,000 samples to build their probability distribution. This high number of sampling values aims to guarantee convergence for an acceptable PDF representation. The active and reactive power of the aggregated demand is considered with a standard deviation of 10%. For instance, the probability distribution of the active power of the aggregated load demand at specific 15h is depicted in Fig. 12. It is worth noting that data is symmetrically distributed around the expected value of 90 kW following a Normal distribution.

Fig. 12 Histogram of aggregated load demand.

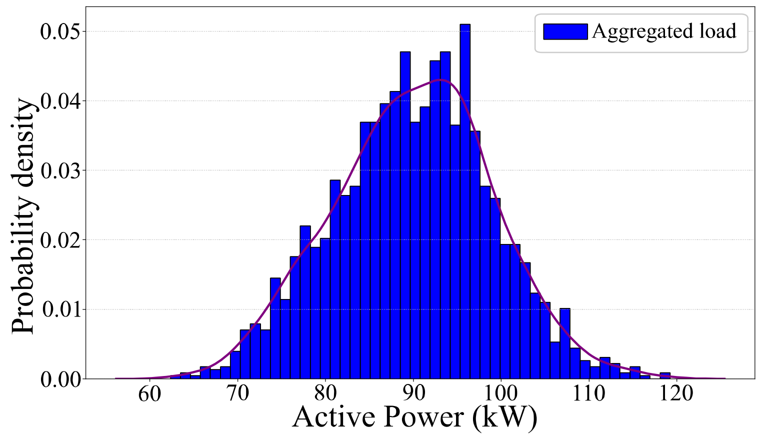

Source: Created by the author.

Another example, the injection of power from the PV systems of 2.5 MWp that takes place at the highest power injection that occurs at 15h with an expected irradiation of 0.78 and standard deviation of 0.13 kW/m2, in terms of active power injection, the value is about 1952 kW with a standard deviation of 323.22 kW. For instance, the probability distribution of PV power injection at specific 15h is shown in Fig. 13. It is worth noting that its skewness value is negative which means a large number of data is right-hand side at this specific time.

Fig. 13 Histogram of PV power injection.

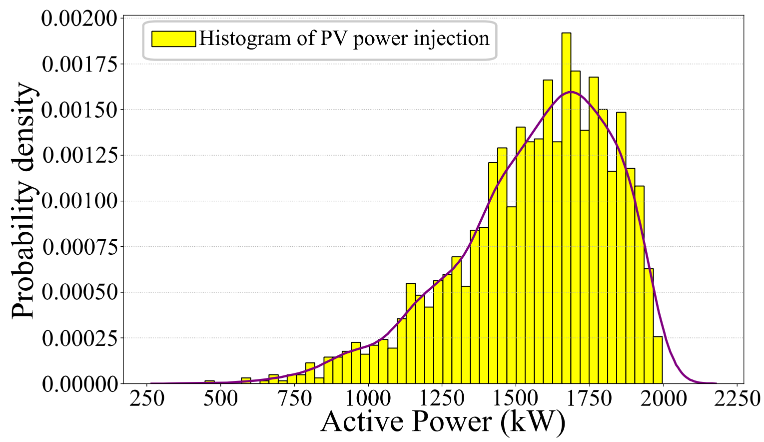

Source: Created by the author.

Regarding the PDF modeling for the aggregated EV charging demand, it is considered for each EV a daily trip from 10 km to 200 km. Two types of EV are adopted, a 40 kWh (Nissan Leaf) and a 60 kWh (Chevrolet Bolt); two fast charging power types of 50 kW and 150 kW, and their batteries have a state of charge (SOC) with a minimum value of 20%.

For instance, the probability distribution of aggregated 200 EV charging demand at specific 15h is described in Fig. 14. It is worth noting that its skewness value is positive which means a large number of data is left-hand side at this specific time.

Fig. 14 Histogram of Aggregated EVs charging demand

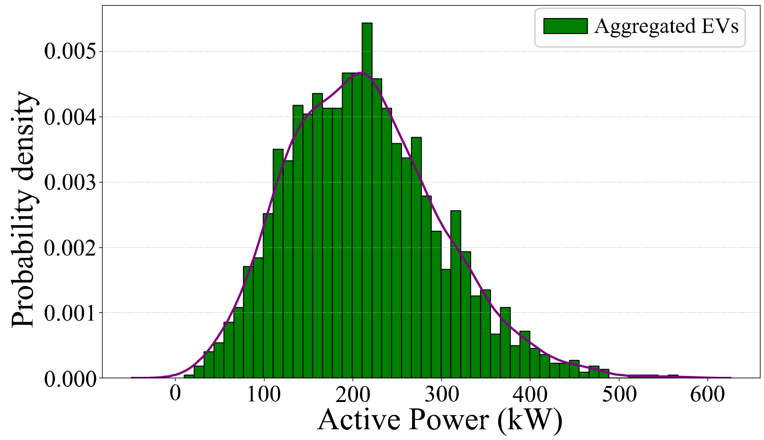

Source: Created by the author.

Now, an hourly boxplot is used to depict the statistical behavior of these uncertain variables over a day. For instance, it is observed that the behavior of active load demand of 3.7 MW increases from afternoon until evening with a maximum demand variation from 18h to 20h, as shown in Fig. 15. Similarly, a daily boxplot for the total PV generation installed of 4 MWp is depicted in Fig. 16; it can be observed that the maximum PV power variation occurs during 12h until 17h, and its highest power injection takes place around 15h. Finally, the daily boxplot for the total of 800 EV charging demand shows an increasing demand in the afternoon around 14h and evening around 20h, and it can also be observed its different variations of skewness per hour along the day as appreciated in Fig. 17.

Fig. 15 Boxplot of the total aggregated demand of 3.7 MW.

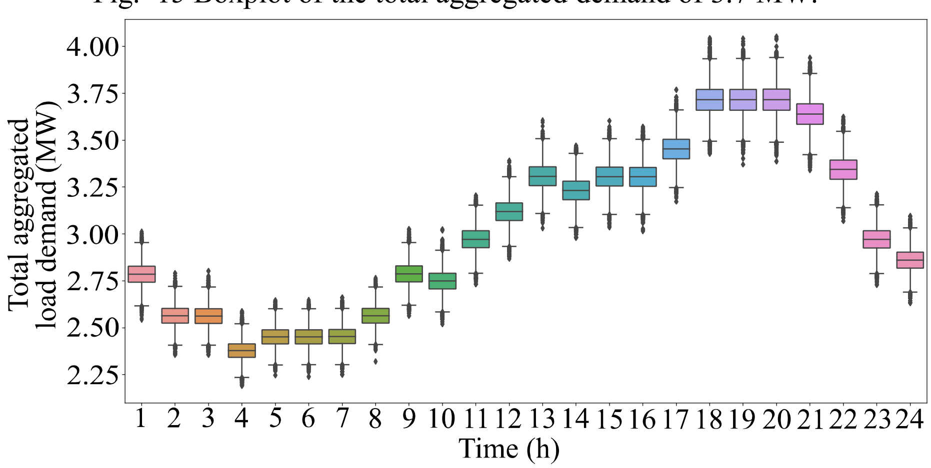

Source: Created by the author.

Fig. 16 Boxplot of the total PV generation installed of 4 MWp.

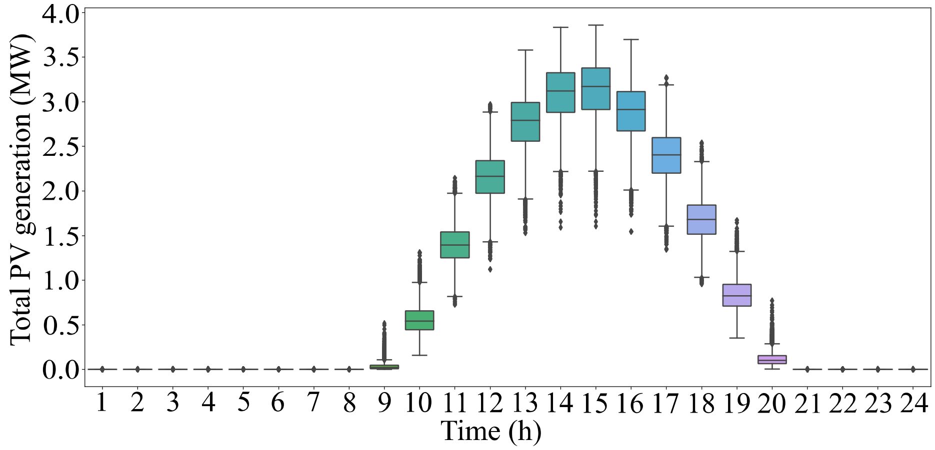

Source: Created by the author.

Fig. 17 Boxplot of 800 aggregated EVs charging demand.

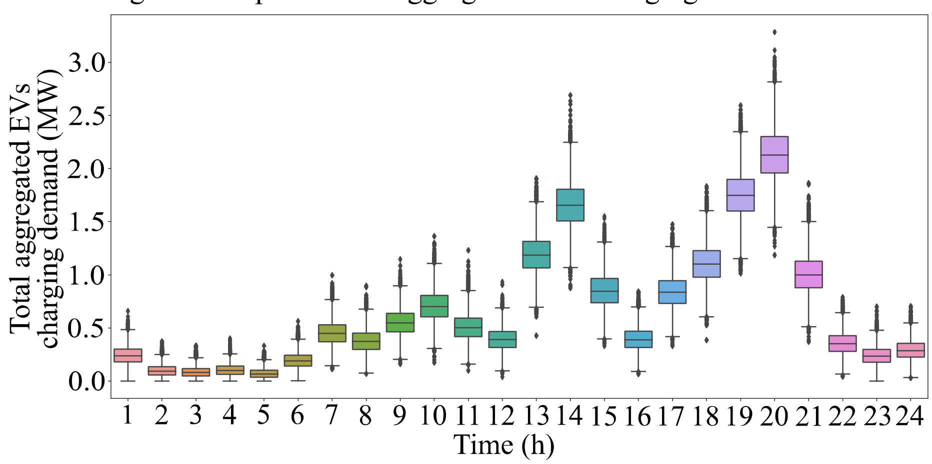

Source: Created by the author.

6.2 PPF COMPUTATIONAL PERFORMANCE AND ACCURACY

The accuracy and computational performance of the PPF based on the different probabilistic techniques employed in this work such as the CM with CLT, the CM with Edgeworth expansion, *2m+1* PEM with CLT, *2m+1* PEM with Edgeworth expansion and MCS are assessed using the three different radial electrical distribution systems. The probabilistic data of demand, PV generation, EVs charging demand for a specific 15h and the electrical network data of each test system can be found and accessed in a cloud-based service (LUIS G. CORDERO, 2023).

Now, the characteristic of these test EDS are presented. First, the IEEE 33-bus system with 4 PV units and 800 Evs is shown in Fig. 18; its voltage level is 12.66 kV with a total base power supply of 3.9 MW and 2.4 MVAr without the installation of PV units and EV operation. This EDS is integrated with one PV unit of 2.5 MWp and 200 Evs connected at bus 18, along with three PV systems each of 0.5 MWp and 200 Evs connected to buses 22, 25, and 33. This test system including the PV units and Evs considers a total of 72 input stochastic variables that consists of 32 active and 32 reactive demand, 4 active power injections for PV units and 4 points of aggregated EV charging demand. Moreover, the system also considers a capacitor bank of 0.5 MVAr connected to bus 18 that helps prevent voltage drop during high demand of Evs during periods when solar irradiation is low.

The IEEE 69 bus system has a nominal voltage of 12.66 kV with a base power supply of 4.02 MW and 2.79 MVAr without PV units and EV operation. This system is integrated with a total of 8 PV units and 800 Evs as shown in Fig. 28. A PV unit of 2.5 MWp and 100 Evs are connected to bus 28, along with seven PV systems each of 0.5 MWp and each group of 100 Evs connected to buses 36, 47, 51, 53, 66, 68, and 70. This system considers a total of 112 input stochastic variables that consists of 48 active and 48 reactive demand, 8 active power injection for PV units and 8 points of aggregated Evs charging demand.

The real EDS 202-bus system with a nominal voltage of 13.8 kV and must supply a total load of 28.18 MW and 18.39 MVAr without PV units and EV operation. This system has a total of 6 PV units and 3000 Evs as shown in Fig. 36. A PV unit of 50 MWp and 500 Evs are connected to bus 57, along with five PV systems each of 5 MWp and 500 Evs connected to buses 50, 116, 128, 187, and 194. This system considers a total of 262 input stochastic variables that consists of 125 active and 125 reactive demand, 6 active power injections for PV units and 6 points of aggregated Evs charging demand.

The proposed probabilistic optimization framework employs the MCS as a benchmark model to verify the accuracy of the *2m+1* PEM CLT, *2m+1* PEM Edgeworth expansion, CM CLT and CM Edgeworth expansion in terms of the statistical characteristics, probability distribution fitting and confidence interval levels for voltage, current, active and reactive power flow. The modeling of probability distribution considered 10,000 samples for each uncertain variable, namely aggregated load demand, PV generation and aggregated EV charging demand. This high number of sampling values is used to guarantee a converge of the MCS state variables to obtain an acceptable accuracy for the purpose of benchmark model comparison with PEM and CM probabilistic techniques.

The average execution time performance for the PPF assessment using the different probabilistic techniques and the three electrical distribution systems is presented in Table 2. Among these techniques, the CM with CLT presents the fastest computational time with 0.4, 0.6 and 0.9 in seconds for the systems of IEEE 33 bus, IEEE 69 bus, and EDS 202 bus, respectively. It can be noted that the CM with Edgeworth expansion also presents a faster execution time compared to PEM and MCS with a stable execution of cumulants calculation effort of about 18.13 seconds on average; this processing time is mainly due to the complexity to better approximate the PDF with Edgeworth expansion. The CM with Edgeworth expansion also depends on the system size for the single power flow calculation of computational burden leading to a total of 9.05 seconds for IEEE 33 bus system, 19.26 seconds for IEEE 69 bus system and 26.08 seconds for the EDS 202 bus system.

On the other hand, the *2m+1* PEM CLT and *2m+1* PEM Edgeworth present a higher computational burden compared to the CM; furthermore, its computational time increases the larger the systems become reaching up to 67.98 and 82.78 seconds for the EDS 202 bus assessed by the *2m+1* PEM CLT and *2m+1* PEM Edgeworth, respectively. It is also observed that the PEM presents a faster computational efficiency when compared to the MCS for the IEEE 33 bus system and IEEE 69 bus system. The execution time demonstrates that the PEM computational processing efficiency is highly related to the number of uncertain variables, thus, the PEM reduces increases its computational burden for the EDS 202 bus system.

The PFF based on the MCS execution time presents an 56ncreaseng computational burden the larger the system becomes, and this is also due to higher number of deterministic power flow calculations (e.g., 10 000 power flow computations) reaching up to 74.62 seconds for the EDS 202 bus system, 35.6 seconds for the IEEE 69 bus system and 22.95 seconds for the IEEE 33 bus system to obtain an acceptable representation of the true probability distribution for the variables of interest.

Table 2. Computational performance of the PPF based on different probabilistic techniques

System	**Total random variables**	**CPU Time (s)**				
		MCS	***2m+1* PEM CLT**	***2m+1* PEM EE**	**CM CLT**	**CM EE**
IEEE 33 Bus	72	22.95	4.99	13.88	0.4	9.05
IEEE 69 Bus	102	35.6	13.89	25.62	0.6	19.26
EDS 202 Bus	262	74.62	67.98	82.78	0.9	26.08

Source: Created by the author.

Table 3 presents the relative error percentage of voltage, current, power flow through line assessment of PPF based on *2m+1* PEM CLT and CM CLT. The metric of relative error percentage is used to measure the accuracy of the PPF based on the different probabilistic techniques respect to the benchmark MCS in terms of expected value, standard deviation, skewness, and kurtosis of voltage, current, active and reactive power flow through lines for the IEEE 33 bus, IEEE 69 bus and the EDS 202 bus.

Table 3 shows that the *2m+1* PEM CLT and CM CLT well approximates the expected value for all the EDS test systems with a relative error percentage about less than 0.05% and 0.7% on average.

The CM CLT approximates the standard deviation for all the EDS test systems with a relative error percentage about less than 0.98% on average. However, the *2m+1* PEM CLT presents a higher error of about 14.49%, 30.57% and 44.32% for voltage and current standard deviation regarding the IEEE 33 bus, IEEE 69 bus and the EDS 202 bus, respectively. Regarding the skewness and kurtosis, both methods present about 3.29% and 1.2% of relative error on average for all variables in the tests systems.

Second, Table 4 shows the *2m+1* PEM Edgeworth and CM Edgeworth well approximates the expected value for all the EDS test systems with a relative error percentage about less than 0.03% and 0.7% on average.

The CM Edgeworth approximates the standard deviation for all the EDS test systems with a relative error percentage about less than 0.98% on average. However, the *2m+1* PEM Edgeworth presents a higher error of about 14.49%, 30.57% and 48.36% for voltage and current standard deviation regarding the IEEE 33-bus, IEEE 69-bus and the EDS-202 bus, respectively. Regarding the skewness and kurtosis, both methods present about 4.8% and 4.3% of relative error on average for all variables in the tests systems. Therefore, among the probabilistic techniques, the CM presents the lower relative errors for the state variables of voltage, current and power flow through lines.

One common characteristic of the PPF based on CM CLT and CM EE for the three test EDSs is that the average relative error percentage of expected value about ϵ_{μ}^{z} is lower than 1% and for the standard deviation, skewness and kurtosis are about $\epsilon_{\sigma}^{z}, \epsilon_{S}^{z}, \epsilon_{K}^{z} \leq 5\%$. On the other hand, the PPF based on *2m+1* PEM CLT and *2m+1* EE for the three test EDSs have an average relative error of expected value $\epsilon_{\mu}^{z} \leq 0.5\%$, voltage standard deviation about $\epsilon_{\sigma}^{z} \leq 33\%$, current standard deviation about $\epsilon_{\sigma}^{z} \leq 26\%$ and for skewness and kurtosis values about $\epsilon_{S}^{z}, \epsilon_{K}^{z} \leq 5\%$.

Table 3. Relative average error percentage of voltage, current, and power flow through line assessment of PPF based on *2m+1* PEM CLT and CM CLT.

	Random Variables Output (p.u.)	Method							
		2m+1 PEM CLT				CM CLT			
		ϵ_{μ}^{z}	ϵ_{σ}^{z}	ϵ_{S}^{z}	ϵ_{K}^{z}	ϵ_{μ}^{z}	ϵ_{σ}^{z}	ϵ_{S}^{z}	ϵ_{K}^{z}
IEEE 33 Bus	V_n	0.002	14.980	6.497	2.044	0.008	1.758	6.506	2.076
	I_{km}	0.213	14.003	11.150	5.316	1.829	3.929	11.200	5.331
	P_{km}	0.058	0.439	8.446	2..741	0.445	1.182	8.507	2.751
	Q_{km}	0.050	38.08	1.578	0.931	0.516	1.267	1.605	0.900
IEEE 69 Bus	V_n	0.0002	25.492	2.840	0.945	0.001	0.451	2.881	0.942
	I_{km}	0.085	35.652	3.383	1.668	0.857	0.864	3.402	1.683
	P_{km}	0.004	0.919	2.337	0.865	1.346	0.273	2.284	0.867
	Q_{km}	0.003	3.667	0.734	0.476	1.900	0.323	0.722	0.481
EDS 202 Bus	V_n	0.001	58.010	0.469	0.286	0.0001	0.579	0.467	0.284
	I_{km}	0.103	30.636	0.997	0.530	0.216	0.534	1.001	0.529
	P_{km}	0.049	0.367	0.686	0.291	0.535	0.324	0.687	0.287
	Q_{km}	0.051	4.002	0.414	0.280	0.735	0.354	0.418	0.283

Source: Created by the author.

Table 4. Relative error percentage of voltage, current, and power flow through line assessment of PPF based on *2m+1* PEM Edgeworth and CM Edgeworth.

	Random Variables Output (p.u.)	Method							
		2m+1 PEM EE				CM EE			
		ϵ_{μ}^{z}	ϵ_{σ}^{z}	ϵ_{S}^{z}	ϵ_{K}^{z}	ϵ_{μ}^{z}	ϵ_{σ}^{z}	ϵ_{S}^{z}	ϵ_{K}^{z}
IEEE 33 Bus	V_n	0.002	14.980	3.824	4.737	0.008	1.758	3.205	2.921
	I_{km}	0.213	14.003	9.434	10.421	1.829	3.929	9.631	9.101
	P_{km}	0.058	0.439	6.170	7.996	0.445	1.182	6.720	7.445
	Q_{km}	0.050	38.084	3.079	3.496	0.517	1.267	8.813	3.431
IEEE 69 Bus	V_n	0.0002	25.492	11.870	11.623	0.001	0.447	11.227	11.410
	I_{km}	0.085	35.652	6.708	3.564	0.855	0.864	5.264	3.071
	P_{km}	0.004	0.918	5.640	2.894	1.345	0.275	5.783	2.453
	Q_{km}	0.003	3.667	2.862	1.991	1.914	0.323	7.511	3.341
IEEE 202 Bus	V_n	0.0001	62.974	0.470	2.340	0.0001	0.579	0.324	0.476
	I_{km}	0.0460	33.757	3.237	2.748	0.216	0.534	0.768	0.929
	P_{km}	0.0005	0.325	1.697	2.329	0.535	0.324	0.256	0.734
	Q_{km}	0.0005	3.208	0.902	1.878	0.735	0.354	1.349	1.500

Source: Created by the author.

6.3 PPF EVALUATION OF THE IEEE 33 BUS TEST SYSTEM

The assessment of the PPF based on different probabilistic techniques are applied to the test system IEEE 33 bus with 4 PV units and 800 EVs, as shown in Fig. 18. The installation of each distributed PV units of 0.5 MWp and each group of 200 Evs connected to buses 22, 25 and 33 aiming to support the grid voltage profile. These buses represent the end points of the radial EDS from the feeder location. The major distributed PV unit power installation is 2.5 MWp at bus 18 with the goal to study the impact of PV generation in terms of likelihood of overvoltage greater than 1.05 p.u., current variation and power reverse through lines.

Fig. 18 IEEE 33 test system with 4 PV units and 800 EVs.

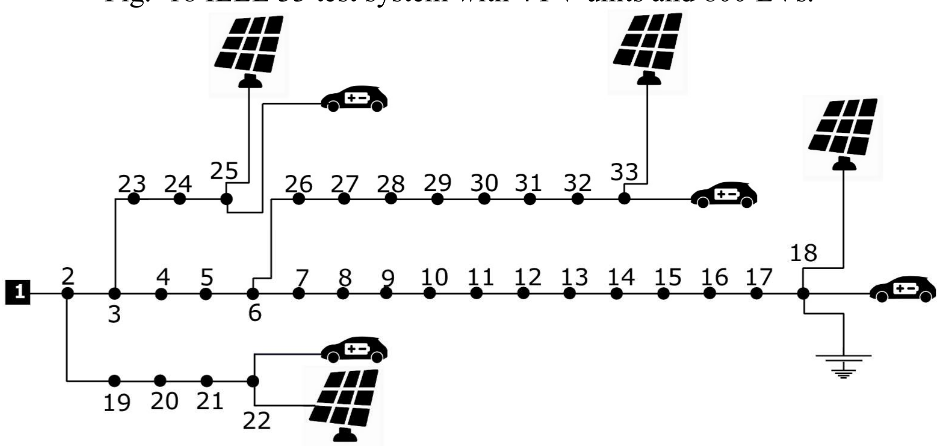

Source: Adapted from (BARAN; WU, 1989)

The PPF based on different probabilistic techniques yields the probability distribution function of voltage, current and power flow. They are compared to the true probability distribution obtained from PPF based on MCS. In this particular case, the maximum point of irradiation occurs at 15h when overvoltage likelihood becomes notorious at bus 18, increasing line overloading and the effects of power flow reverse take place through line 17-18.

First, the probability distribution of voltage at bus 18 for each probabilistic technique is depicted in Fig. 19. The histogram represents the true distribution of voltage obtained with the MCS, it is observed that the *2m+1* PEM Edgeworth (green dashed-line) and the CM Edgeworth (blue solid-line) well shape and contours the histogram with a negatively skewed shape. This particular characteristic is associated to the influence of the PV power generation behavior, thus, leading to an increase in the likelihood of overvoltage with more data right-hand side above 1.05 p.u. (red vertical dotted-line as depicted in Fig. 19). On the other hand, the probability distribution approximations with the *2m+1* PEM CLT (orange dotted-line) and CM

CLT (purple dashed-line) tends to approximate closer to a Normal distribution whose representation departs from the true probability distribution of MCS.

Fig. 19. Probability distribution approximation for voltage bus 18 of IEEE 33 bus system.

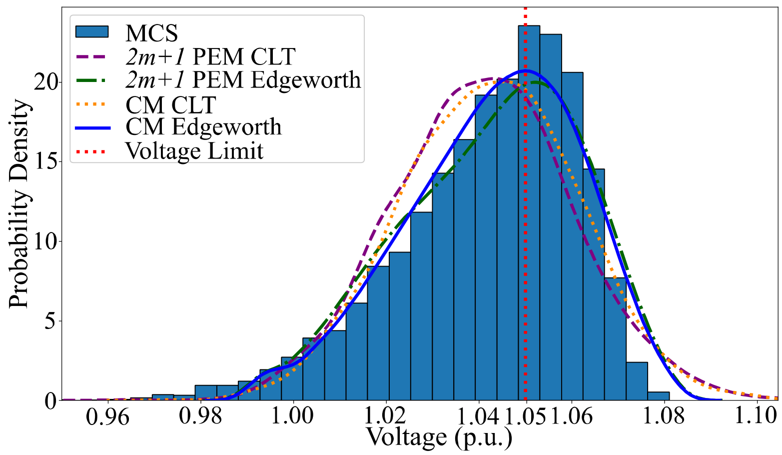

Source: Created by the author.

Second, the probability distribution of current through line 17-18 for each probabilistic technique is depicted in Fig. 20. The histogram represents the true probability distribution of current obtained with the MCS, and it is observed that the *2m+1* PEM Edgeworth (green dashed-line) and the CM Edgeworth (blue solid-line) well shape and contours the histogram with a negatively skewed shape. Similarly, this particular characteristic is also associated to the influence of the PV power injection, thus, leading to an increase in the likelihood of overload lines (e.g., there is 70% of probability current greater than 200 A through line 17-18).

Fig. 20. Probability distribution approximation for line current 17-18 of IEEE 33 bus system.

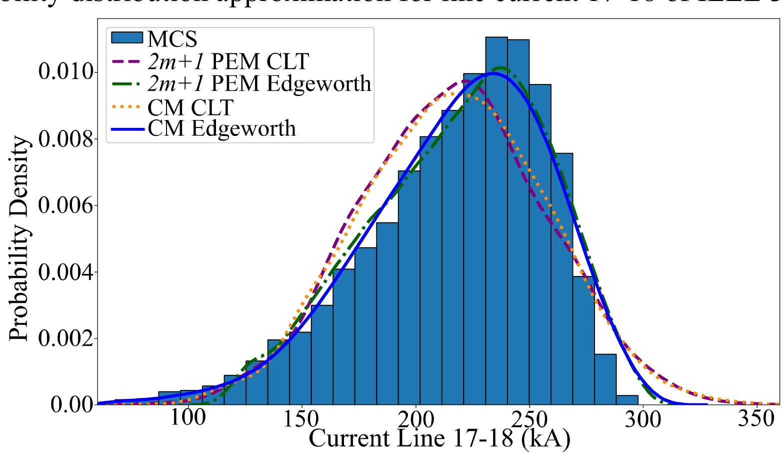

Source: Created by the author.

On the other hand, the probability distribution approximations with the *2m+1* PEM CLT (orange dotted-line) and CM CLT (purple dashed-line) represent an approximation for a Normal distribution though this departs from the behavior of the MCS distribution.

Third, the probability distribution of active power flow through line 17-18 for each probabilistic technique is depicted in Fig. 21. The histogram represents the true distribution of line power flow obtained with the MCS, and it is observed that the *2m+1* PEM Edgeworth (green dashed-line) and the CM Edgeworth (blue solid-line) well shape and contours the histogram with a positively skewed shape. Interestingly, this particular characteristic proves reverse power behavior that is associated with the influence of the PV power injection, thus, leading to an expected value of 1644 kW of reverse power in lines 17-18. On the other hand, the probability distribution approximations with the *2m+1* PEM CLT (orange dotted-line) and CM CLT (purple dashed-line) represent an approximation to Normal distribution which departs from the true distribution of MCS.

Fig. 21. Probability distribution for active power flow through line 17-18 of IEEE 33 bus system.

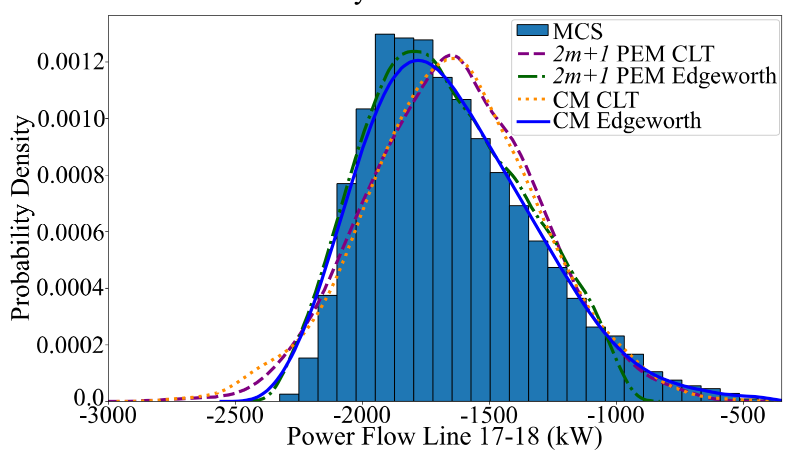

Source: Created by the author.

Now, to evaluate the value of overvoltage probability, a PPF computation is carried out based on MCS, *2m+1* PEM, *2m+1* PEM Edgeworth approximation, CM, and CM Edgeworth approximation for the analysis of the IEEE 33 bus with 4 PV units and 800 Evs. This evaluation is considered at 15h due to higher solar irradiation during this time of the day. Table 5 shows results for the voltage confidence interval (CI) V_{CI} of 95% as well as the probability of occurring overvoltages. It can be observed a higher value for overvoltage probability occurrence $P(V < v_m)$ with 39.29% of chance at bus 18 due to the higher penetration of PV generation. Moreover, this PV power injection impacts on the neighbouring buses 16 and 17 with a probability of overvoltage with 20.36% and 0.48%, respectively.

Although the analysis of PPF based on different probabilistic techniques presents acceptable values for all V_{CI} and $P(V < v_m)$, the CM with Edgeworth expansion presents the lowest relative error when compared to MCS in terms of the voltage confidence interval and probability of overvoltage values less than about 0.28% and 3.57% on average, respectively.

Table 5. Overvoltage probability with confidence interval of 95% of the IEEE 33 bus system at 15h

	MCS		*2m+1* PEM CLT		*2m+1* PEM Edgeworth		CM CLT		CM Edgeworth	
Bus	V_{CI} (p.u.)	$P(V < v_m)$ (%)	V_{CI} (p.u.)	$P(V < v_m)$ (%)	V_{CI} (p.u.)	$P(V < v_m)$ (%)	V_{CI} (p.u.)	$P(V < v_m)$ (%)	V_{CI} (p.u.)	$P(V < v_m)$ (%)
16	1.045	0.48	1.045	2.65	1.054	3.3	1.054	4.7	1.048	1.2
17	1.060	20.36	1.065	23.8	1.070	20.3	1.070	21.3	1.063	21.81
18	1.069	39.29	1.074	40	1.080	33.2	1.079	32.7	1.072	38.27

Source: Created by the author.

Fig. 22. Confidence Intervals of 95% for all voltages using PPF based CM with Edgeworth expansion applied to the IEEE 33 bus system.

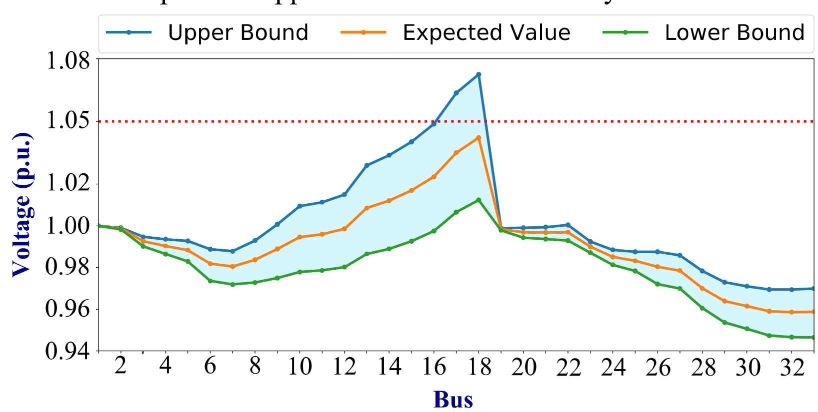

Source: Created by the author.

A PPF based on CM with Edgeworth expansion is computed to obtain 95% confidence intervals for all voltages, as depicted in Fig. 22. This figure describes the confidence interval of 95% for all voltages within the blue area between the blue line (upper bound) and the green line (lower bound), and the average voltage is presented with the orange line, and a maximum allowable voltage (1.05 p.u.) is represented with a red dotted-line.

6.4 OPTIMAL PROBABILISTIC FRAMEWORK APPLIED TO THE IEEE 33 BUS TEST SYSTEM

The test system of IEEE 33 bus with 4 PV units and 800 Evs depicted in Fig. 18 is considered for the assessment of the optimal probabilistic framework and the following parameters $a = 0.005$, $b = 0.002$ and $c = 0.0005$ are set for the iterative calculation of voltage limits in the equation (64) within the optimization process. The average execution time of the proposed optimal probabilistic framework to optimize PV generation and guarantee a likelihood of voltage to be within a range above a maximum allowable value (e.g., 1.05 p.u.) is shown in Table 6. It can be observed that the proposed method based on CM CLT requires only 4.31 seconds to solve the problem, and with a better probability distribution approximation of the CM Edgeworth with 44.13 seconds. The proposed method based on *2m+1* PEM CLT with 36.81 seconds and CM Edgeworth with 44.13 seconds. These methods are 5 to 50 times faster than the MCS which requires 273.27 seconds. One of the advantages of the CM CLT and CM Edgeworth method is that its execution time depends on a single deterministic power flow evaluation.

Table 6. Execution time and iterations of the proposed method for the IEEE 33 bus system.

	Probabilistic Optimization Framework				
	MCS	***2m+1* PEM CLT**	***2m+1* PEM Edgeworth**	**CM CLT**	**CM Edgeworth**
Execution Time (s)	237.27	36.81	45.12	4.31	44.13
Iterations	5	5	5	5	5

Source: Created by the author.

The assessment of the proposed method is carried out using the CM Edgeworth expansion to optimize the PV power injection while satisfying the restriction of overvoltage likelihood with 95% of a confidence interval.

The voltage variation with 95% confidence intervals for all buses is depicted in Fig. 23. This figure describes the confidence interval of 95% for all voltages within the blue area between the blue line (upper bound) and the green line (lower bound), and the expected voltage is presented with the orange line, and all values within this range set below the maximum allowable voltage of 1.05 p.u. with a red dotted-line. The higher variation of voltage remained at bus 18 with an upper bound value of confidence interval of about 1.049 p.u. complying with the operational limits.

Fig. 23. Voltage optimization with 95% CI applying the proposed method based CM with Edgeworth expansion for the IEEE 33 bus system.

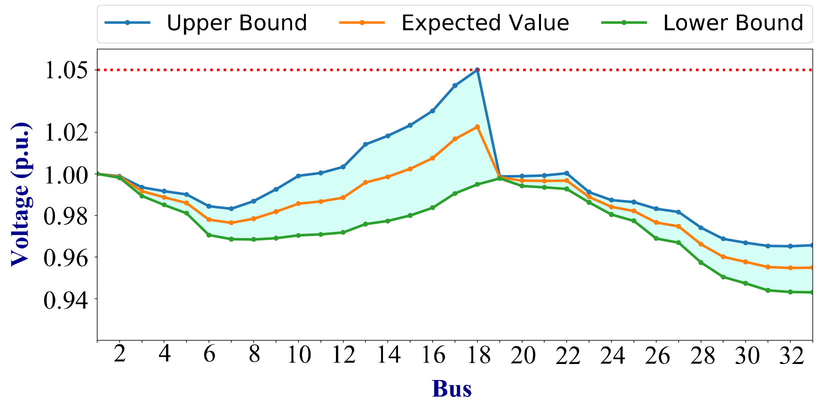

Source: Created by the author.

The optimal cumulative probability of voltage at bus 18 is depicted in Fig. 24 using the MCS, the *2m+1* PEM CLT, *2m+1* PEM Edgeworth, CM CLT and CM Edgeworth. Among the different probabilistic techniques, the proposed model based on the CM with Edgeworth expansion presents the higher fitting accuracy for the cumulative probability distribution of variables. Fig. 24 shows that the proposed probabilistc optimization framework effectively reduce the overvoltage probability ocurrence with a set of 95% of chances that a voltage value will fall below 1.05 p.u.

Fig. 24. Optimal cumulative probability of voltage using the proposed method based CM with Edgeworth expansion.

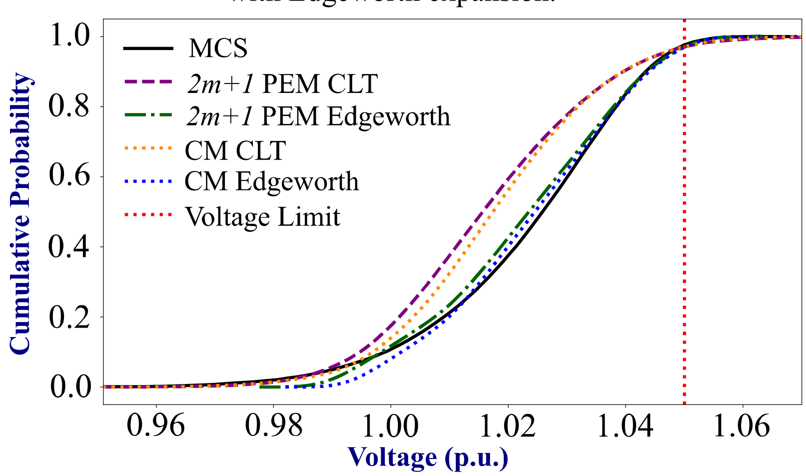

Source: Created by the author.

It is worth to note that the CLT simplifies the complexity of probability curves approximations, thus, leading to a CDF of *2m+1* PEM CLT (purple dashed-line) and CM CLT (orange dotted-line) though they depart from the true distribtion of MCS (solid black-line). On the other hand, the application of the Edgeworth expansion to the *2m+1* PEM Edgeworth (green dashed- line) and CM Edgeworth (blue dotted-line) results in better shapping and accuracy of the cumulative probability function.

The cumulative probability for the optimal PV generation is depicted in Fig. 25 where it shows curve approximations of the various probabilistic techniques. Among these techniques, it can be observed the CLT approximation losses accuracy to reconstruct the true distribution. On the other hand, it is worth to note that the *2m+1* PEM Edgeworth (green dashed-line) and CM Edgeworth (blue dotted-line) expansion approximation presents a high fitting accuracy in comparison to those with CLT approximation.

Fig. 25. Optimal probabilistic cumulative distribution of PV unit connected to bus 18 at 15h.

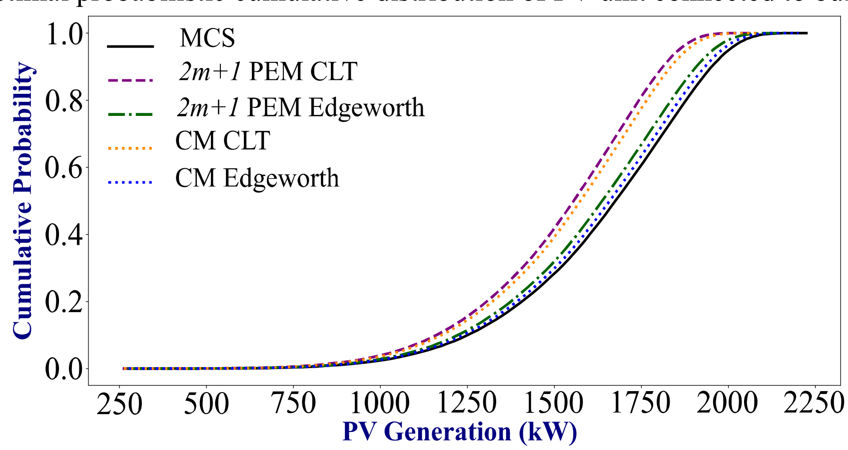

Source: Created by the author.

The optimal PV power injection values in terms of expected and standar deviation as well their respective relative errors are shown in Table 7. Initially, the available capacity of PV generation connected to bus 18 at 15h is 2.42 MW, with an expected value of 1952 kW and standard deviation of 323.22 kW which leads to an overvoltage probability of 39.29% at bus 18 and their neighbouring buses. The application of the proposed method probabilistically optimizes the PV power generation to 1.99 MW, with an expected value of 1617.12 kW and standard deviation of 267.77 kW thus a reduction about 16% considering a 95% CI while also mitigating the chances of likelihood of overvoltage. Furthermore, the CM Edgeworth presents a PRMSE less than about 1% for the expected and standard deviation values of optimal PV generation.

Table 7. Optimal statistical values for PV Generation connected to bus 18 at 15h

	μ_{Gen} (kW)	σ_{Gen} (kW)	$\delta_{\mu_{Gen}}$(%)	$\delta_{\sigma_{Gen}}$(%)
MCS	1633.49	270.48	-	-
***2m+1* PEM CLT**	1516.09	251.04	7.74	7.74
***2m+1* PEM Edgeworth**	1596.42	264.34	2.32	2.32
CM CLT	1535.27	254.27	6.39	6.39
CM Edgeworth	1617.12	267.77	1.01	1.01

Source: Created by the author.

Regarding the evolution of the probabilistically optimal PV generation with 95% of confidence interval is shown in Fig. 26. It can be observed that the optimization of PV generation occurs during 14h until 16h with a maximum of 17.44% of PV curtailment at 15h.

Finally, the optimal probabilistic evolution of power supply from the grid, PV generation units, Aggregated EVs charging demand and load with 95% of confidence interval is depicted in Fig. 27.

The total optimal energy production is calculated with a 95% of confidence interval for the energy supply with 71.22 ± 4.97 MWh, the energy from PV units with 20.27 ± 2.65 MWh, and its energy loss of 3.54 ± 0.38 MWh with an expected reduction about 2.5% respect to the case without optimization.

Fig. 26. Optimal PV Generation bus 18 with 95% CI 24h period for the IEEE 33 bus system.

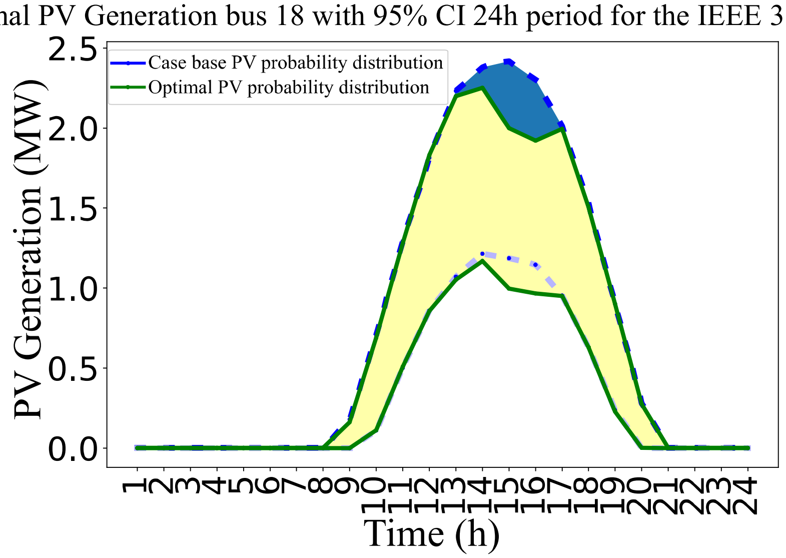

Source: Created by the author.

Table 8. Optimal PV Generation with 95% CI for the PV unit at bus 28 of the IEEE 33 bus system.

	PV Generation with 95% CI (MW)		
Time (h)	**Case base**	**Optimal**	**Curtailment(%)**
13	2.24	2.19	1.99
14	2.36	2.25	4.94
15	2.42	1.99	17.44
16	2.29	1.92	16.37
17	2.00	1.99	0.31

Source: Created by the author.

Fig. 27. Optimal probabilistic evolution of grid power for the IEEE 33 bus system.

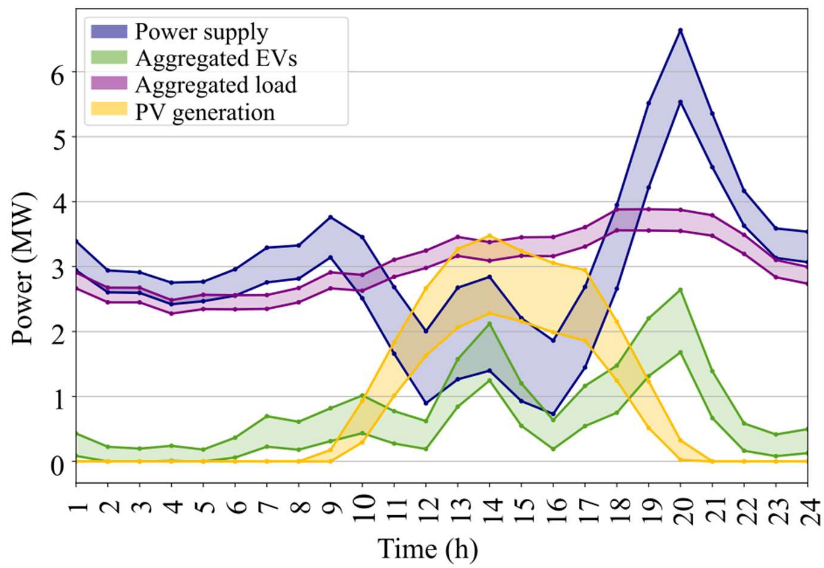

Source: Created by the author.

6.5 PPF EVALUATION OF THE IEEE 69 BUS TEST SYSTEM

The application of the PPF based on probabilistic techniques are also applied to the IEEE 69 bus system, as shown in Fig. 28. A total of 8 PV units and 800 EVs were considered. The installation of each distributed PV units of 0.5 MWp and each group of 100 EVs connected to buses 36, 47, 51, 53, 66, 68 and 70 aiming to support the grid voltage profile. These buses represent the end points of the radial EDS from the feeder location. The major distributed PV unit power injection is 2.5 MWp at bus 28 with the goal to study the impact of PV generation in terms of likelihood of overvoltage greater than 1.05 p.u., current flow variation and power reverse through lines.

Fig. 28 IEEE 69 test system with 8 PV units and 800 EVs.

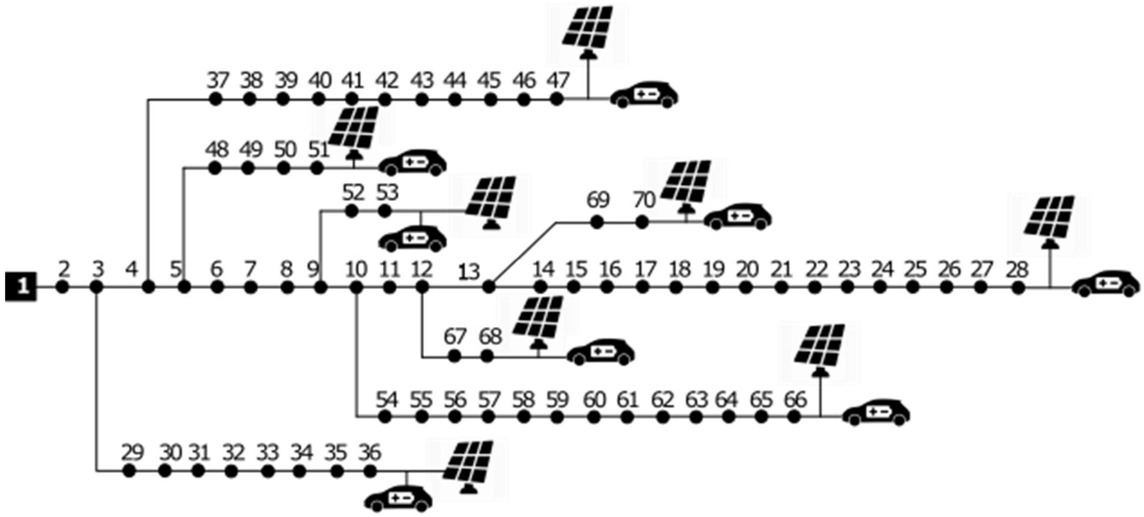

Source: Adapted from (GALLEGO; FRANCO; CORDERO, 2021).

This test system under the analysis of the PPF based on CM with Edgeworth expansion presents the technical challenges of high penetration of PV generation. Specifically, during the hours when the overvoltage probability increases from 12 h to 17 h. In this particular case, the maximum point of irradiation occurs at 15h when overvoltage likelihood becomes notorious at bus 18, increasing line overloading and the effects of power flow reverse through line 27-28.

First, the confidence interval of 95% for all bus voltages at 15 h is depicted in Fig. 30. It is observed that the PV power injection increases the overvoltages likelihood from bus 28 to bus 16 along the radial line connections. This figure also demonstrates that high variation of PV generation at bus 28 causes high variation of the voltage values thus a higher standard deviation of voltage is observed along buses 16 to 28. It can be observed that the penetration of PV generation at buses 47, 51 and 53 also causes voltage variation though within their operation limits.

Fig. 30 depicts the upper bound of voltages with 95% of confidence in blue-line, the expected value voltages in orange-line and the lower bound of voltages in green-line along the buses.

Fig. 30. Confidence Intervals of 95% for all voltages using PPF based CM with Edgeworth expansion applied to the IEEE 69 bus system.

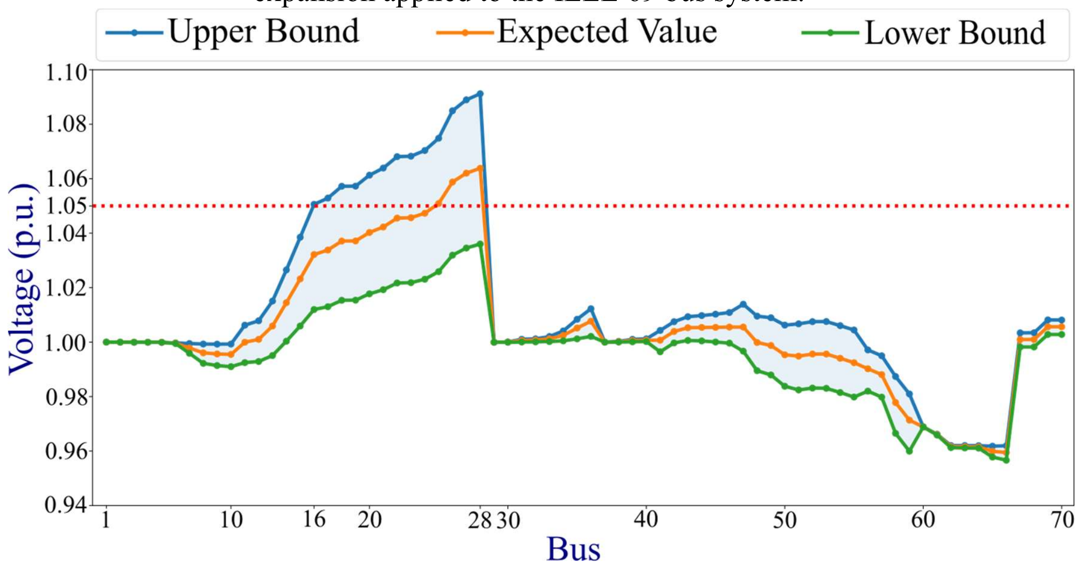

Source: Created by the author.

Second, the evaluation of the PPF based on the Edgeworth expansion of the voltage behavior with 95% of confidence interval for all voltages along the day is shown in Fig. 29. The voltage analysis of Fig. 29 points out the higher variation of voltage takes place around 12 h to 17 h when the probability of overvoltage value for voltage limits is greater than 1.05 p.u. (red-dotted line). Despite the fact that EVs is operating during these particular hours, they do not reduce the value of overvoltage likelihood since the major voltage issue happens at bus 28 where only 100 EVs are operating.

Fig. 29. Confidence interval of 95% for all voltages 24h period of the IEEE 69 bus system.

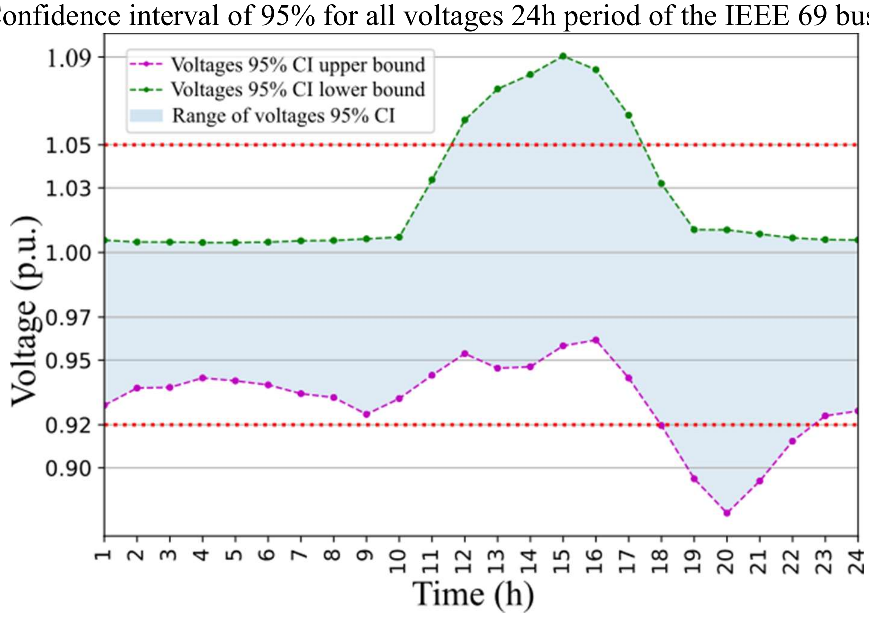

Source: Created by the author.

Another particular features in this figure is at 20 h where the voltage drops below 0.92 p.u. due to the high penetration of EVs and the lack of solar irradiation to support the system.

Third, the evaluation of the probability of overvoltage with 95% of confidence interval is computed along the buses as depicted in Fig. 31. This figure shows the overvoltage probability is described in green-line from a minimum value of 3.12% at bus 16 to a maximum value of 82.35% at bus 28. This statistical information is of great importance since the system operator can make decision with a tolerance of PV power injection up to some degree of overvoltage likelihood to maximize the PV generation.

In this particular case, Fig. 31 points out the PV power injection at bus 28 is creating a high likelihood of overvoltages with almost 13 buses impacted due to the high penetration of PV generation. The next analysis tackles the reduction of overvoltage likelihood to comply voltage operational limits using confidence interval knowledge with the challenge to optimally maximizes the PV power injection of each unit

Fig. 31. Voltage upper bound with 95% CI with their respective overvoltage probability of the IEEE 69 bus system at 15h.

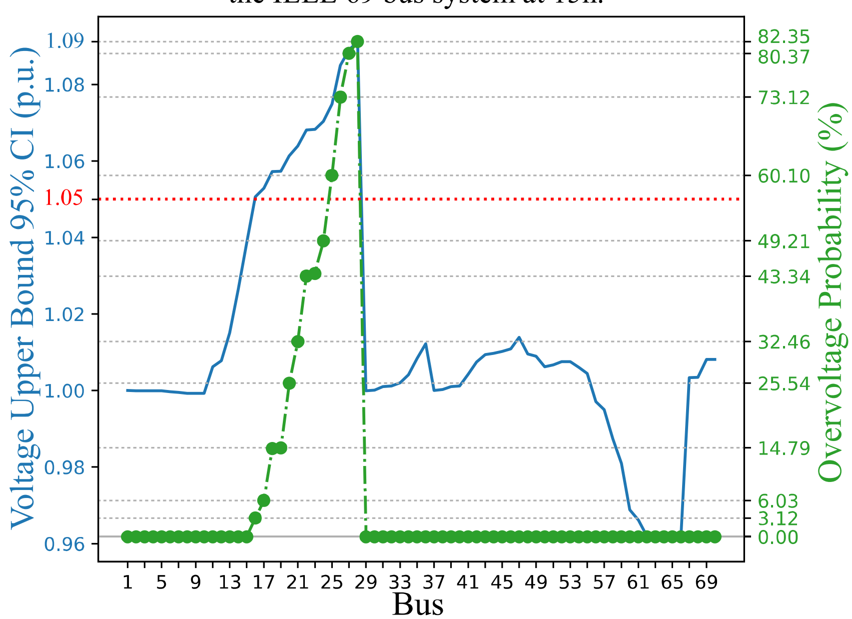

Source: Created by the author.

6.6 OPTIMAL PROBABILISTIC FRAMEWORK APPLIED TO THE IEEE 69 BUS TEST SYSTEM

The IEEE 69 bus system with 8 PV units and 800 EVs, depicted in Fig. 28, is considered for the assessment of the optimal probabilistic framework. The average execution time and iterations of the proposed optimal probabilistic framework to optimize PV generation while reducing overvoltage probability is shown in Table 9. It can be observed that the proposed method based on CM CLT requires only 4.38 seconds to solve the problem, and with a better probability distribution approximation of the CM Edgeworth with 73.48 seconds faster 27.94 and 1.63 times than the MCS of 120.45 seconds, respectively. The proposed method based on *2m+1* PEM CLT takes about 59.50 seconds and with CM Edgeworth takes about 209.41 seconds. One of the advantages of the CM CLT and CM Edgeworth method is their degree of accuracy, few iterations and computational efficiency in regards of MCS and PEM methods.

Table 9. Execution time and iterations of the proposed method for the IEEE 69 bus system.

	Probabilistic Optimization Framework				
	MCS	***2m+1* PEM CLT**	***2m+1* PEM Edgeworth**	**CM CLT**	**CM Edgeworth**
Execution Time (s)	120.45	59.50	209.41	4.38	73.48
Iterations	8	5	10	5	5

Source: Created by the author.

The assessment of the proposed method is carried out using the CM Edgeworth expansion to optimize the PV power injection while satisfying the restriction of overvoltage likelihood with 95% of confidence interval. Fig. 33 describes the voltage optimization with confidence interval of 95% for all voltages that fall within the blue area between the blue line (upper bound) and the green line (lower bound), and the expected voltage with the orange line. The optimization for the voltage confidence interval at bus 28 reached a maximum value of 1.49 p.u. thus maximizing the PV power injection. It is also observed that the voltage variation remains higher at bus 28 despite the optimization and still the neighboring buses keep the effect of higher voltage variation due to the PV generation.

The optimization process is carried out along the day, particularly, during the hour of maximum PV generation from 12 h to 17 h as shown in Fig. 32. The voltage confidence interval of all buses for each hour of analysis fall within the voltage operational limits (blue-area), the maximum voltage upper bound (green line) obtained is about 1.049 p.u. when the PV power injections have its higher solar irradiation. It is also observed that during the peak hours of demand at 20 h, the systems control elevates voltage tap at the substation level to improve the voltage drop due to the high EVs demand.

Fig. 33. Voltage optimization with 95% CI applying the proposed method based CM with Edgeworth expansion for the IEEE 69 bus system.

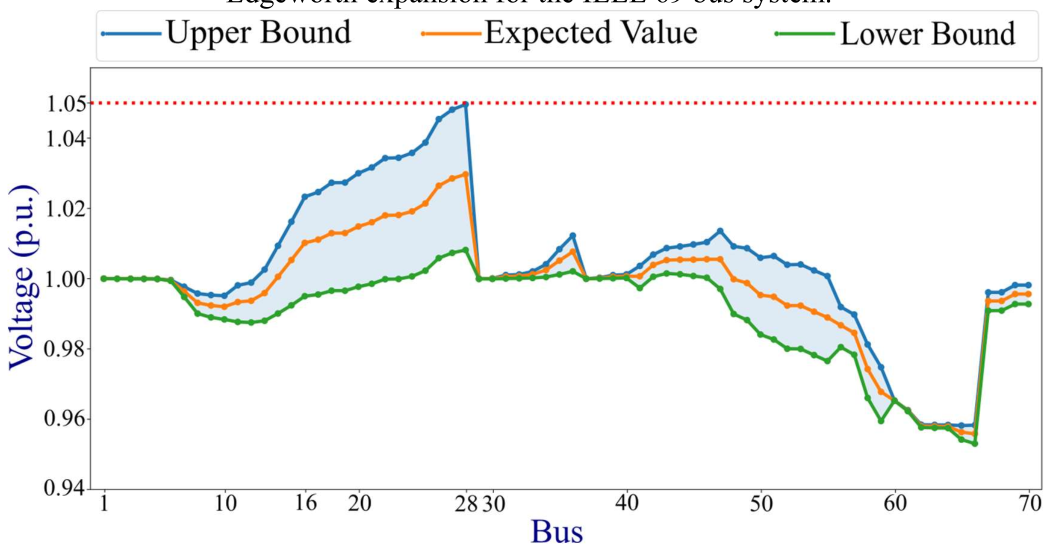

Source: Created by the author.

Fig. 32. Voltage optimization with 95% CI of all bus voltages for a period of 24h based on the CM with Edgeworth expansion for the IEEE 69 bus system.

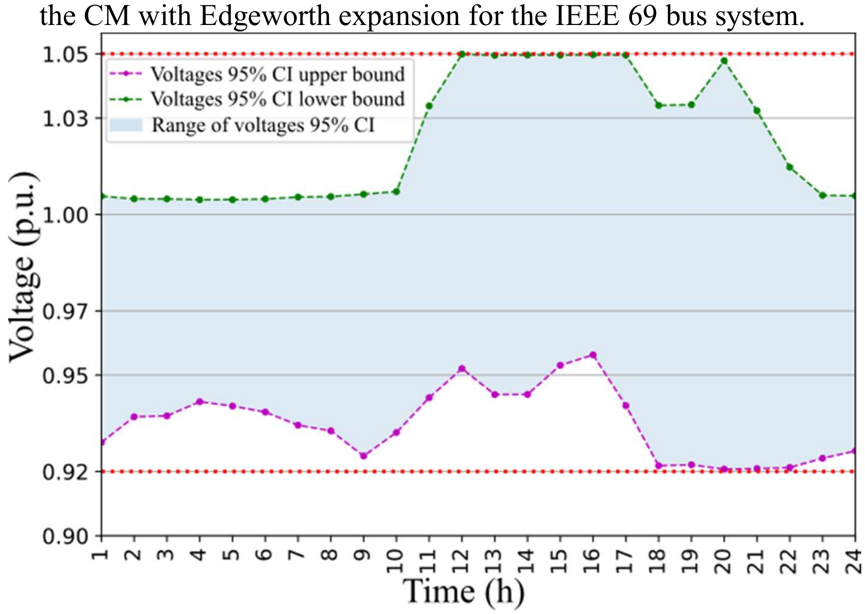

Source: Created by the author.

Regarding the daily evolution of the probabilistically optimal PV generation at bus 28 with 95% of confidence interval is shown in Fig. 34. It can be observed that the optimization of PV generation occurs from 12 h to 17 h with a maximum of 15.84% of PV curtailment about 4.46 MWh at 15has described in Table 10. The total PV energy curtailment is about 3.27 MWh, the probabilistically optimal PV energy is depicted with yellow area with an upper bound of

33.92 MWh and the initial PV energy production with blue are with an upper bound of 37.20 MWh as depicted in Fig. 34.

Fig. 34. Optimal PV Generation bus 28 with 95% CI 24h period for the IEEE 69 bus system.

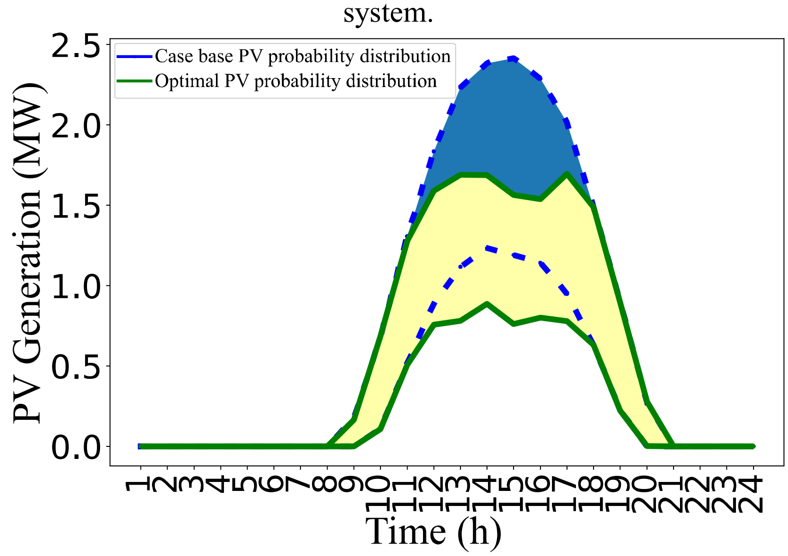

Source: Created by the author.

Table 10. Optimal PV Generation with 95% CI for the PV unit at bus 28 of the IEEE 69 bus system.

	PV Generation with 95% CI (MW)		
Time (h)	**Case base**	**Optimal**	**Curtailment(%)**
12	3.79	3.54	6.49
13	4.75	4.22	11.23
14	5.18	4.51	12.98
15	5.30	4.46	15.84
16	4.89	4.20	14.13
17	4.17	3.88	7.03

Source: Created by the author.

Finally, the optimal probabilistic evolution of power supply from the grid (blue area), PV generation units (gold area), Aggregated EVs charging demand (green area) and load (purple area) with 95% of confidence interval is depicted in Fig. 35. The total optimal energy production is calculated with a 95% of confidence interval for the energy supply with 64.37 ±

Fig. 35. Optimal probabilistic evolution of grid power with 95% CI for the IEEE 69 bus system.

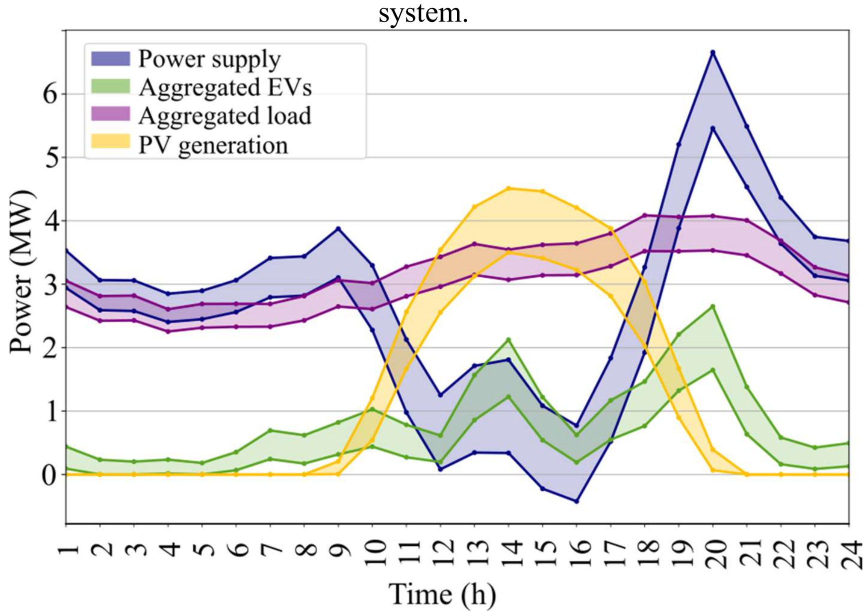

Source: Created by the author.

5.56 MWh, the optimal energy from PV units with 28.89 ± 2.61 MWh, and its energy loss of 3.60 ± 0.45 MWh with an expected reduction about 6.9% respect to the case without optimization.

6.7 PPF EVALUATION OF THE REAL EDS 202 BUS

The application of the PPF based on probabilistic techniques are also applied to a real test electrical distribution system of EDS 202 bus of the city of Guarujá in São Paulo as shown in Fig. 36 with an installation of 6 PV units and 3000 EVs. The installation of a centralized PV unit of 50 MWp and 500 EVs are connected to bus 57, along with five distributed PV systems each of 5 MWp and 500 EVs connected to buses 50, 116, 128, 187, and 194 aiming to support the grid voltage profile. These buses represent the end points of the radial EDS from the feeder location. The major centralized PV unit power injection is 50 MWp at bus 57 with the goal to study the impact of PV generation in terms of likelihood of overvoltage greater than 1.05 p.u., current flow variation and power reverse through lines.

This test system under the analysis of the PPF based on CM with Edgeworth expansion presents the technical challenges of high penetration of PV generation. Specifically, during the hours when the overvoltage probability increases from 12 h to 17 h. In this particular case, the maximum point of irradiation occurs at 15h when overvoltage likelihood becomes notorious at

Fig. 36 Real EDS 202 bus test system with 6 PV units and 3000 EVs.

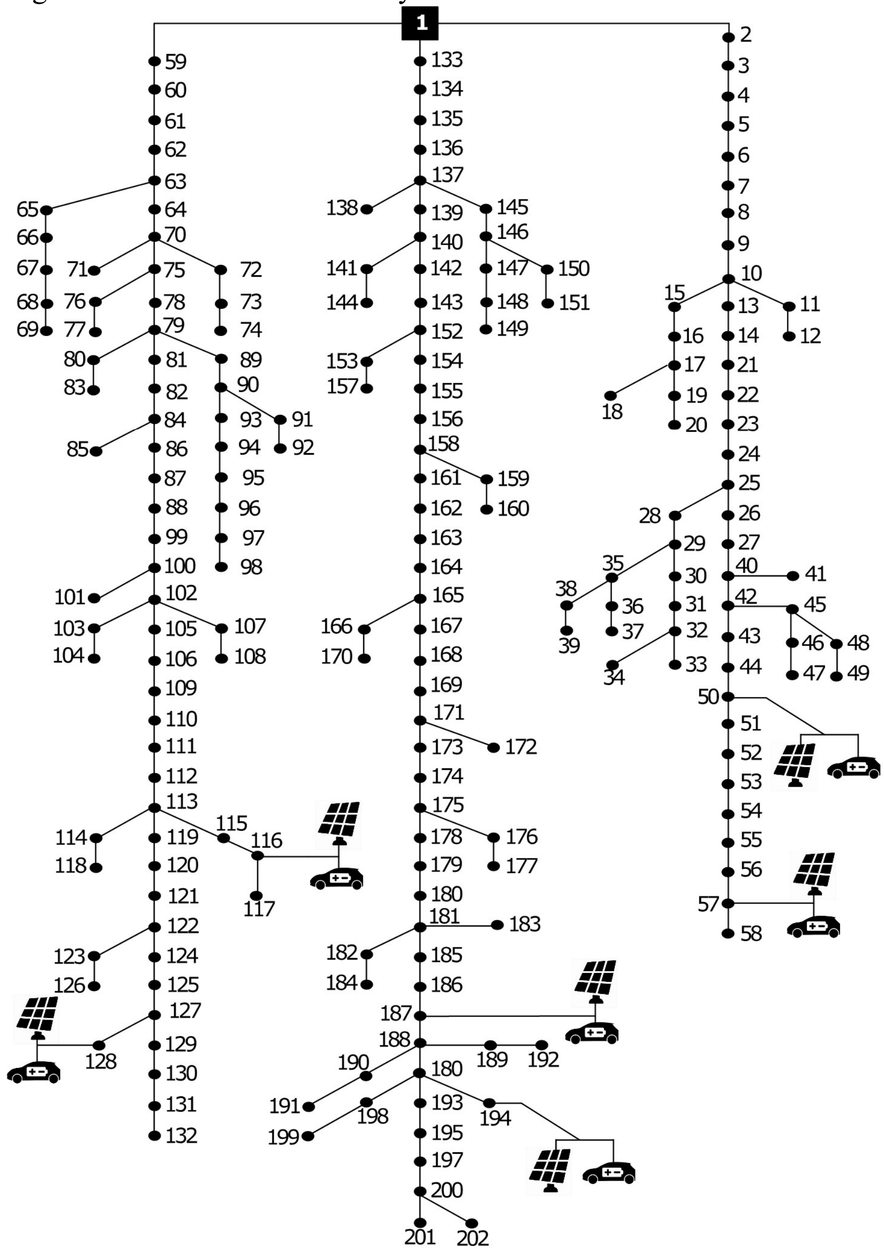

Source: Adapted from (GALLEGO; FRANCO; CORDERO, 2021).

bus 57, increasing line overloading and the effects of power flow reverse through line 56-57 and its neighboring lines.

First, the confidence interval of 95% for all bus voltages at 15 h is depicted in Fig. 37. It is observed that the PV power injection increases the overvoltages likelihood from bus 53 to bus 58 along the radial line connections. This figure also demonstrates that high variation of PV generation at bus 57 that causes high variation of the voltage values thus a higher standard deviation of voltage is observed along buses 22 to 58. It can be observed that the penetration of PV generation from bus 22 52 also causes voltage variation though within their operation limits.

Fig. 37. Confidence Intervals of 95% for all voltages using PPF based CM with Edgeworth expansion applied to the EDS 202 bus system.

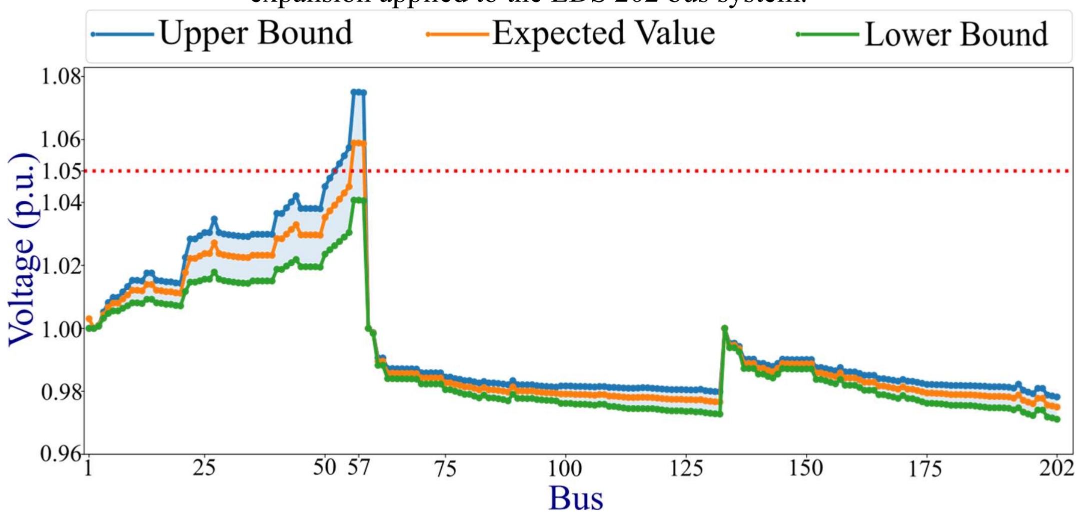

Source: Created by the author.

Fig. 37 also depicts the upper bound of voltages with 95% of confidence in blue-line, the expected value voltages in orange-line and the lower bound of voltages in green-line along the buses. Second, the evaluation of the PPF based on the Edgeworth expansion of the voltage behavior with 95% of confidence interval for all voltages along the day is shown in Fig. 38.

Fig. 38. Confidence interval of 95% for all voltages 24h period of the EDS 202 bus system.

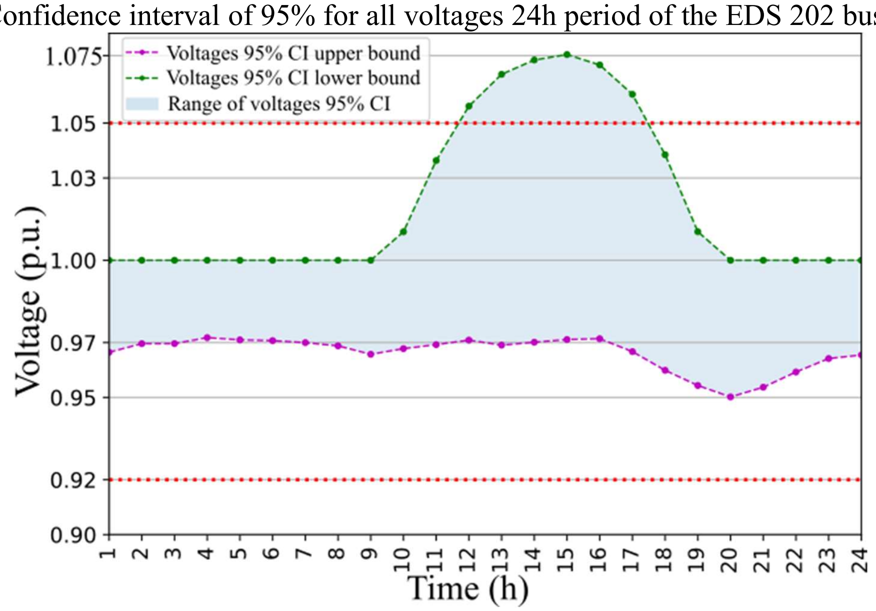

Source: Created by the author.

This statistical voltage analysis points out the higher variation of voltage takes place around 12 h to 17 h with a maximum value of 1.075 p.u. when the overvoltage probability value for voltage limits is greater than 1.05 p.u. (red-dotted line). Despite the fact that EVs is operating during these particular hours, they do not reduce the value of overvoltage likelihood since the major voltage issue happens at bus 57 where only 500 EVs are operating. Another particular features in this figure is the EDS 202 bus system is capable to support the 3000 EVs charging demand at 20 h without compromising voltage drop below the operational limits.

Third, the evaluation of the probability of overvoltage with 95% of confidence interval is computed along the buses as depicted in Fig. 39. This figure shows the overvoltage probability is described in green-line from a minimum value of 2.45% at bus 52 to a maximum value of 83.44% at bus 57. This statistical information is of great importance since the system operator can make decision with a tolerance of PV power injection up to some degree of overvoltage likelihood to maximize the PV generation.

Fig. 39. Voltage upper bound with 95% CI with their respective overvoltage probability of the EDS 202 bus system at 15h.

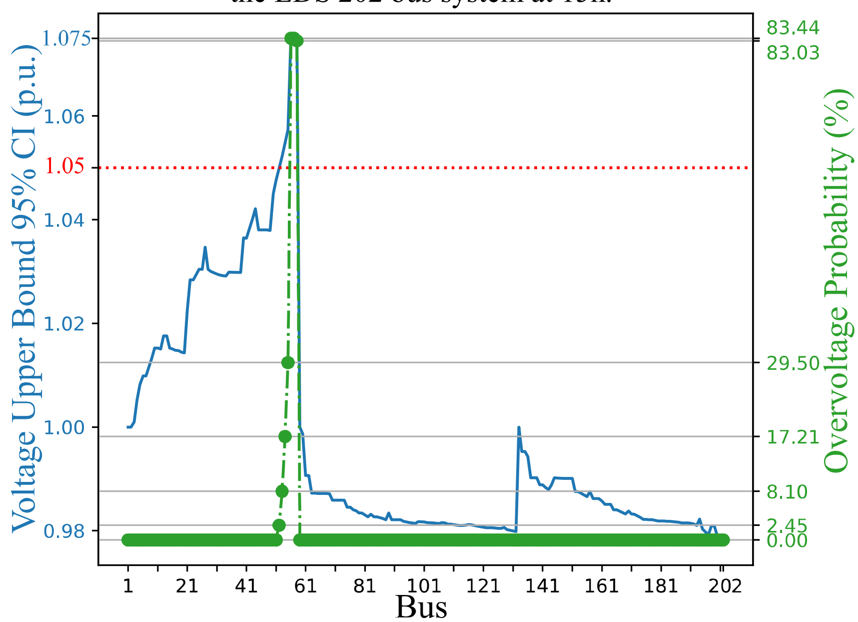

Source: Created by the author.

In this particular case, Fig. 39 points out the PV power injection at bus 57 is creating a high likelihood of overvoltage with almost 6 buses impacted due to the high penetration of PV generation. The next analysis tackles the reduction of overvoltage likelihood to comply voltage operational limits using confidence interval knowledge with the challenge to optimally maximizes the PV power injection of each unit

6.8 OPTIMAL PROBABILISTIC FRAMEWORK ASSESSMENT APPLIED TO THE REAL EDS 202 BUS

The test system of EDS 202 bus with 6 PV units and 3000 EVs depicted in Fig. 36 is considered for the assessment of the optimal probabilistic framework. It can be observed that the proposed method based on CM CLT requires only 12.15 seconds to solve the optimization problem, and the CM Edgeworth with 148.46 seconds faster 20.13 and 1.64 times than the MCS of 244.61 seconds, respectively. The proposed method based on *2m+1* PEM CLT takes about 405.79 seconds and with CM Edgeworth takes about 355.96 seconds. One of the advantages of the CM CLT and CM Edgeworth method is their degree of accuracy, few iterations and computational efficiency in regards of MCS and PEM methods.

Table 11. Execution time and iterations of the proposed method for the EDS 202 bus system.

	Probabilistic Optimization Framework				
	MCS	***2m+1* PEM CLT**	***2m+1* PEM Edgeworth**	**CM CLT**	**CM Edgeworth**
Execution Time (s)	244.61	405.79	366.96	12.15	148.46
Iterations	8	6	4	8	5

Source: Created by the author.

The assessment of the proposed method is carried out using the CM Edgeworth expansion to optimize the PV power injection while satisfying the restriction of overvoltage likelihood with 95% of confidence interval. Fig. 40 describes the voltage optimization with confidence interval of 95% for all voltages that fall within the blue area between the blue line (upper bound) and the green line (lower bound), and the expected voltage with the orange line. The optimization for the voltage confidence interval at bus 56, 57 and 58 reached a maximum value of 1.049 p.u. thus maximizing the PV power injection. It is also observed that the voltage variation remains higher at bus 57 despite the optimization and still the neighboring buses keep the effect of higher voltage variation due to the PV generation.

The optimization process is carried out along the day, particularly, during the hour of maximum PV generation from 12 h to 17 h as shown in Fig. 41. The voltage confidence interval of all buses for each hour of analysis fall within the voltage operational limits (blue-area), the maximum voltage upper bound (green line) obtained is about 1.049 p.u. when the PV power injections have its higher solar irradiation. It is also observed that during the peak hours of demand at 20 h, the systems voltage profile is working within their operational limits.

Fig. 40. Voltage optimization with 95% CI applying the proposed method based CM with Edgeworth expansion for the EDS 202 bus system.

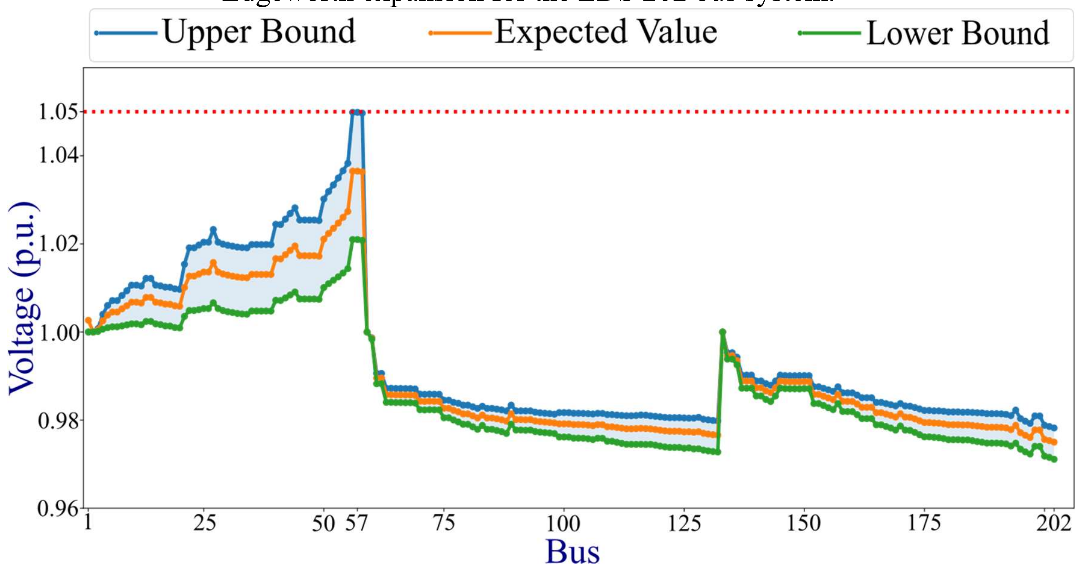

Source: Created by the author.

Fig. 41. Voltage optimization with 95% CI of all bus voltages for a period of 24h based on the CM with Edgeworth expansion for the EDS 202 bus system.

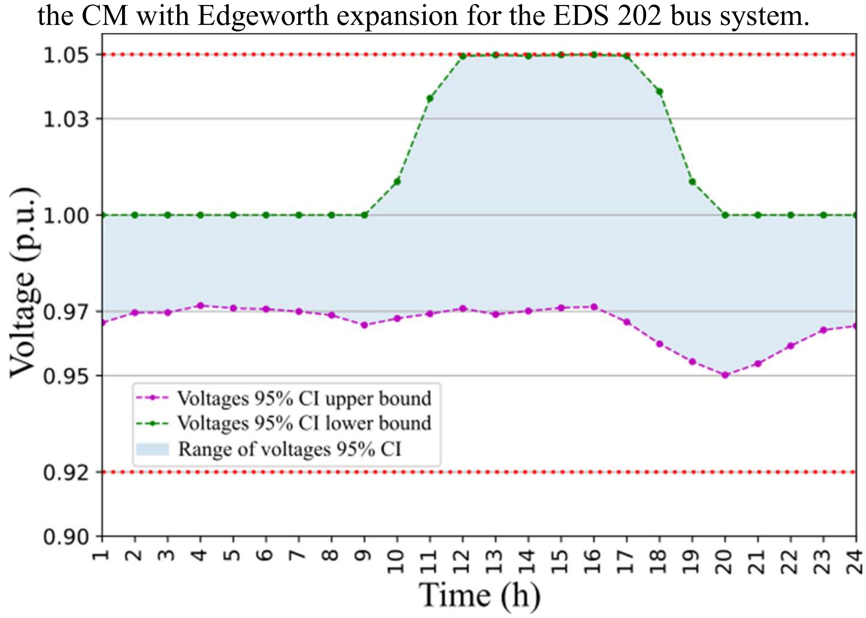

Source: Created by the author.

Now, regarding the daily evolution of the probabilistically optimal PV generation at bus 57 with 95% of confidence interval is shown in Fig. 42. It can be observed that the optimization of PV generation occurs from 12 h to 17 h with a maximum of 34.33% of PV curtailment about 31.72 MWh at 15 h as described in Table 12. The total PV energy curtailment is about 67.72 MWh, the probabilistically optimal PV energy is depicted with yellow area with an upper bound of 292.26 MWh and the initial PV energy production with blue are with an upper bound of 359.98 MWh as depicted in Fig. 42.

Fig. 42. Optimal PV Generation bus 57 with 95% CI 24h period for the EDS 202 bus system.

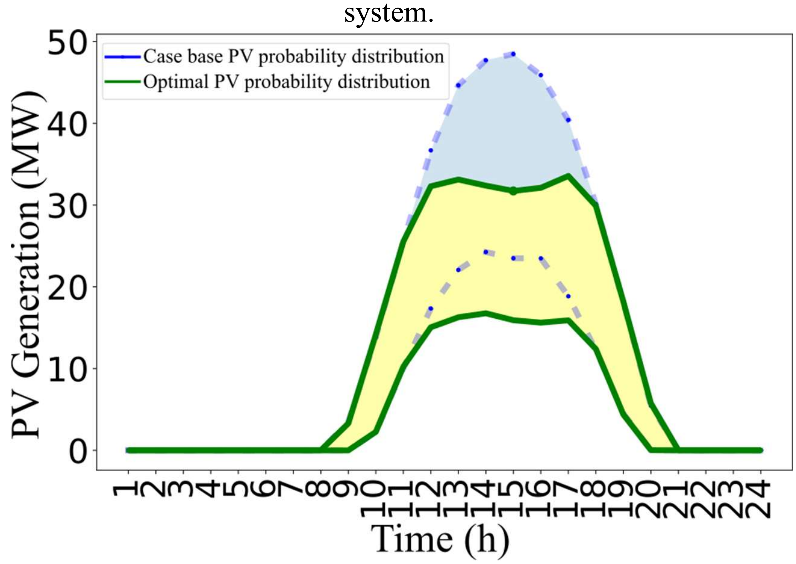

Source: Created by the author.

Table 12. Optimal PV Generation with 95% CI for the PV unit at bus 57 of the EDS 202 bus system.

	PV Generation with 95% CI (MW)		
Time (h)	**Case base**	**Optimal**	**Curtailment(%)**
12	36.59	32.29	11.75
13	44.70	33.12	25.92
14	47.72	32.37	32.17
15	48.30	31.72	34.33
16	45.94	32.11	30.11
17	40.38	33.55	16.91

Source: Created by the author.

Finally, the optimal probabilistic evolution of power supply from the grid (blue area), PV generation units (gold area), Aggregated EVs charging demand (green area) and load (purple area) with 95% of confidence interval is depicted in Fig. 43. The total optimal energy production is calculated with a 95% of confidence interval for the energy supply with 272.82 ±

Fig. 43. Optimal probabilistic evolution of grid power with 95% CI for the EDS 202 bus system.

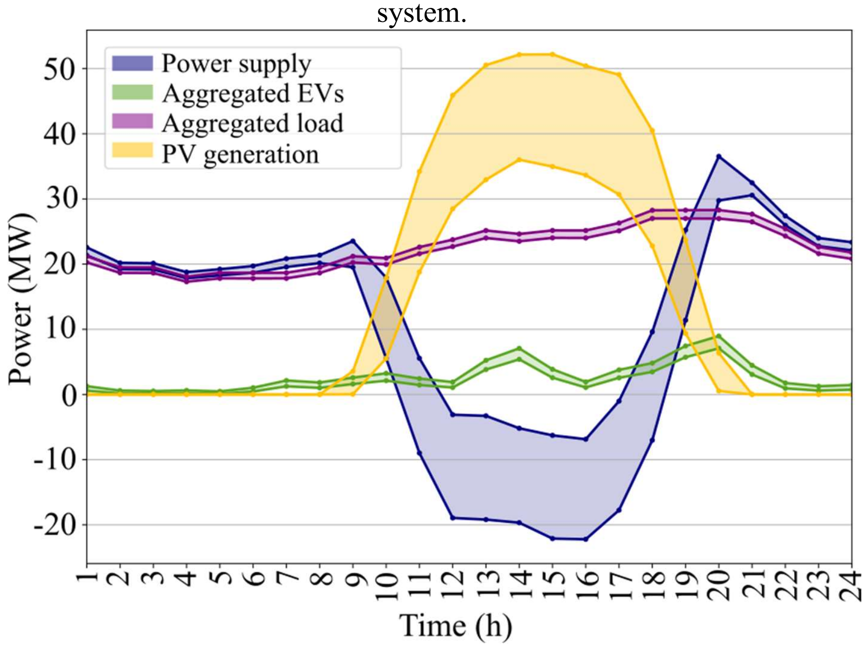

Source: Created by the author.

45.80 MWh, the optimal energy from all PV units with 341.06 ± 45.24 MWh with an expected reduction about 13.53%, 3000 EVs charging demand with 58 ±6 MWh, aggregated load with 538.60 ± 6.31 MWh and its energy loss of 16.72 ± 0.38 MWh with an expected reduction about 30% respect to the case without optimization.

6.9 CHAPTER CONCLUSION

This chapter presented five probabilistic techniques; MCS, *2m+1* PEM CLT, *2m+1* PEM with Edgeworth expansion, CM CLT and CM with Edgeworth expansion; that are implemented for the proposed model of optimal probabilistic framework analysis. The optimal probabilistic framework considered the probability distribution modeling of aggregated demand, PV generation and aggregated EV charging demand, a mathematical model to maximize the PV generation with voltage confidence interval restrictions and data processing for the statistical results with probability distribution of optimal values of the grid operation. The optimization process is implemented within the Python environment that works with the application of AMPL for the mathematical modelling (the solution is obtained using a commercial solver KNITRO) and the evaluation of deterministic power flows obtained using the OpenDSS.

This chapter presented and discussed the characteristics of the probability distribution modeling of aggregated demand, PV generation and aggregated EV charging demand during a specific hour of the day. Then, a boxplot of these uncertain variables variation is developed for a 24-hour period.

A computational performance and a discussion of the PPF analysis based on MCS, *2m+1* PEM with CLT, *2m+1* PEM with Edgeworth expansion, CM with CLT, CW with Edgeworth expansion are examined in terms of their computational effort to solve the PPF for the IEEE 33 bus system, IEEE 69 bus system and EDS 202 bus system with high penetration of PV generation and EVs. The CM with CLT stands out with the fastest computational effort to solve the PPF with 0.63 seconds on average for the three test systems and 70 times faster than the MCS.

Another important characteristic of the CM CLT and CM with Edgeworth expansion is that their relative error percentage of expected value is less than 1%, and for the standard deviation, skews and kurtosis is less than 5 % for voltage, current, active and reactive power flow.

The IEEE 33 bus system, IEEE 69 bus system, and a real EDS 202 bus system with the presence of aggregated EV and PV generation are employed for the proposed model assessment of optimal probabilistic generation of PV units while satisfying voltage confidence interval restrictions.

The installation of 2.5 MWp at bus 18 in the IEEE 33 bus system causes overvoltage challenges in the grid with a total of 4 MWp and 800 EVs. For instance, a 39.29 % of overvoltage likelihood takes place at 15 h and the probabilistic optimization method achieves an optimal value of 1.62 ± 0.27 MW for PV generation at bus 18 at 15 h while the maximum voltage confidence interval of 95 % for all voltages reaching to 1.049 p.u. value. The fastest method is the CM CLT with 4.31 seconds and 5 iterations. The total optimal probabilistic PV energy is 20.27 ± 2.65 MWh with 2.5 % of loss energy reduction along the day.

In a similar fashion, the installation of 2.5 MWp at bus 28 in the IEEE 69 bus system causes overvoltage challenges in the grid with a total of 6 MWp and 800 EVs. For instance, it is observed that the neighbouring voltage buses are highly affected with a range of 3.12 % to 82.35 % of overvoltage likelihood at 15 h. The fastest method to probabilistically optimize the grid is the CM CLT reaching to a maximum confidence interval of 95% for all voltages to 1.049 p.u. with 4.38 seconds and 5 iterations. The probabilistic optimization process yields the optimal curtailment values with a maximum of 15.84 % at 15 h. The optimal PV energy is 28.89 ± 2.61 MWh with 6.9 % of loss energy reduction along the day.

Finally, the installation of a centralized solar power of 50 MWp connected to bus 57 at a real EDS of 202 bus of the city of Guarujá causes overvoltage challenges in the grid with a total of 75 MWp with 3000 EVs. For instance, the maximum overvoltage likelihood was 83.44 % at bus 57 affecting the neighbouring buses with an increased overvoltage probability. The fastest method to probabilistically optimize the grid is the CM CLT reaching to maximum confidence interval of all voltages to 1.049 p.u. with 12.15 seconds and 8 iterations. The probabilistic optimization process yields the optimal curtailment values with a maximum of 34.33 % at 15 h. The optimal PV energy is 341.06 ± 45.24 MWh with 30 % of loss energy reduction along the day.

The results showed that the proposed model probabilistically optimizes the PV generation units complying with the operational voltage restriction of confidence interval level of 95 % for all the presented test systems. The performance evaluation of the proposed model in terms of computational efficiency and accuracy are presented employing the five probabilistic techniques. Among the presented techniques in the proposed model, the CM CLT and CM Edgeworth expansion yield the faster computational burden and accuracy for state variables of voltage, current, power as well as the PV generation probabilistic optimization.

7 CONCLUSION AND FUTURE WORKS

Distributed energy resources (DERs) increasing integration brings new opportunities and challenges for the optimal operation and planning of the electrical distribution system (EDS). Some of its integration benefits come from the independence from fossil fuels, loss reduction, grid and voltage system support. However, the high penetration of these technologies increases variability and uncertainty in the EDS posing technical challenges such as reverse power flow, overvoltage, undervoltage and thermal overloading, overload risk of distribution assets, especially during periods when stochastic generation and variable demand have low coincidence, thus, leading to a more complex analysis of the operation, and planning of the EDS.

In this regard, this chapter presents conclusive remarks on the proposed novel optimal probabilistic framework to probabilistically address the optimal generation of PV units while satisfying confidence levels of overvoltage likelihood in the grid with high penetration of PV generation and EVs. Besides, new lines of research are suggested to continue in the improvement of the probabilistic methods applied to optimal integration of DERs for a secure and safe EDS operation.

7.1 CONCLUSIONS

This work presented a novel optimal probabilistic framework to probabilistically maximize the photovoltaic (PV) power generation while reducing the overvoltage likelihood with a confidence interval restriction in the EDS with high penetration of PV systems and EVs in the EDS

The probability distribution modeling considers a 10000 samples for the aggregated demand using a Normal distribution, the PV generation based on the irradiation model using Beta distribution and the aggregated EVs charging demand is considered as input stochastic variables. An algorithm for the hourly probability distribution of aggregated EVs charging demand is developed based on their stochastic charging behavior, power charge types, distance travel, hourly probability of charge and EVs characteristics of minimum SOC and battery type.

This thesis implements and leverages the potential of different probabilistic techniques such as Point Estimate method (PEM) and Cumulant method (CM), and the theory of probability distribution function reconstruction such as the Central Limit Theorem (CLT) and Edgeworth expansion to the problem of the probabilistic power flow (PPF). This thesis also develops a novel algorithm for the optimal probabilistic framework with the goal to be computational efficient and accurate when compared to the benchmark model of Monte Carlo simulation (MCS). The implementation of the PPF based on MCS, *2m+1* PEM with CLT, *2m+1* PEM with Edgeworth expansion, CM with CLT, and CM with Edgeworth expansion were tested and compared to the PPF based on MCS using the IEEE 33 bus system, IEEE 69 bus system and real EDS 202 bus system with high penetration of PV power generation and EVs.

These tests proved satisfactory results of the proposed method to probabilistically assess and optimize the PV generation with high degree of accuracy and computational efficiency. Among the probabilistic techniques, the CM with CLT and the CM with Edgeworth expansion is that their relative error percentage of expected value is less than 1%, and for the standard deviation, skews and kurtosis is less than 5 % for voltage, current, active and reactive power flow.

The computational efficiency of the PPF based on CM with CLT and CM with Edgeworth expansion is basically equal to one deterministic power flow calculation plus the variables cumulants computations, thus, its execution time is about 2.5 to 70 times faster when compared to MCS. On the other hand, the *2m+1* PEM with CLT and *2m+1* PEM with Edgeworth expansion presents 1.3 times faster than the MCS, it is worth to note that its efficacy decreases when the number of uncertain variables increases in the analysis of the EDS.

Now, regarding the proposed method of the novel optimal probabilistic framework, this works considered a mathematical formulation of the EDS operation to maximize PV generation while satisfying the criteria of voltage confidence interval restriction of 95 %. There is also developed an algorithm that employs the statistical information of the probability distribution of all voltages, the expected values of aggregated demand, PV generation and aggregated EVs charging demand obtained from PPF within the optimization process. Then, the probabilistic optimization is tested in the three electrical distribution system with high penetration of PV generation and EVs causing overvoltage challenges. The proposed method is assessed in terms of its computational effort and iteration to solve the problem, its degree of accuracy of the statistical information and probability distribution reconstruction to maximize PV generation, optimize the voltage confidence interval with 95 % meeting the operational probabilistic restriction for all voltages.

The proposed method based on the CM with CLT proved its high computational efficiency to solve the optimization process with an average of 0.63 seconds for the PPF, and 7 seconds for the probabilistic optimization framework. Now regarding the CM with Edgeworth expansion computational efficiency reaches an average of 18.13 seconds for the PPF and

88.7 seconds for the probabilistic optimization framework though it yields more accurate optimal probability distribution of PV power generation in all test cases. It is worth mentining that the Edgeworth expansion is a powerful function to reconstruct the true behavior of uncertain variables showing that it well estimates the contours and shapes of voltages, currents, PV power generation, and power flow through lines. On the other hand, the assumption of Normal distribution for the uncertain variables output with the application of the Central Limit Theorem (CLT) to the proposed method based on $2m+1$ PEM CLT and CM CLT showed that it fails to reconstruct the true distribution.

Now, the application of the proposed method in the test cases yield the following results for PV energy and energy loss. First, the probabilistic optimal approach for the case of the IEEE 33 bus system yield a total optimal probabilistic PV energy of 20.27 ± 2.65 MWh with 2.5 % of loss energy reduction along the day. Second, for the IEEE 69 bus system, it is obtained a total optimal probabilistic PV energy of 28.89 ± 2.61 MWh with 6.9 % of loss energy reduction along the day. Third, for the real EDS 202 bus system, the optimal probabilistic PV energy is 341.06 ± 45.24 MWh with 30 % of loss energy reduction along the day.

Although this study has some limitations associated with the stochastic variable's correlation and a more detailed probabilistic modeling of different load profiles, more variety of EVs type charging data, and other uncertainties present in the EDS, the proposed novel probabilistic optimization framework of this research brings crucially and potentially statistical information to be used for an efficient and sustainable grid operation and assist the operators and planners to make informed-decision at what point is needed an intervention of generation curtailment, and to accept some degree of risk tolerance of PV generation with the levels of confidence intervals while guaranteeing overvoltage likelihood restrictions.

The proposed method is a potential optimal probabilistic tool for practical applications in electrical distribution systems with high penetration of PV generation and EVs yielding high degree of accuracy, a more realistic analysis of stochastic grid, to provide a wide range of statistical information such as expected values, standard deviation, confidence intervals, probability distribution of the state variables with an efficiency computation effort.

7.2 FUTURE WORKS

The proposed novel probabilistic optimal approach considered within their mathematical formulation a balanced electrical distribution representation though this formulation can also be applied to an unbalanced three-phase EDS. Moreover, the proposed method can be extended to consider other objective functions such as loss minimization, cost operation minimization, and cost of carbon emission reduction and probability constraints for current, power flow reverse, and line congestion for a suitable and sustainable grid operation and planning. This potential improvement represents the next challenge regarding the development of a more complex suitable probabilistic tools for the increasing deployment of new carbon technologies and DERs into the grid.

Further studies can be undertaken to combine the potential of the probabilistic techniques along the process of optimization to improve computation efficiency and robustness of the solution in terms of their statistical information and probability distribution of the grid state variables (e.g., PPF based on combined CM with Edgeworth expansion and MCS).

Finally, future works may consider different load profiles, wind power, different EV types of data and probability charging behaviors, the introduction of other sources of uncertainties like battery, demand response, microgrids as well as grid configuration. Moreover, the proposed method can be further explored using the potential of combined metaheuristics to propose a probabilistic approach for PV hosting capacity, grid resilience studies, and grid reconfigurations in the presence of high penetration of DERs.

REFERENCES

ANEEL. **Electric Vehicles**. 2021. Available in https://www.gov.br/aneel/pt-br/assuntos/veiculos-eletricos.

ANEEL. **Power installed Capacity in Brazil**. 2023. Available in: https://www.gov.br/aneel/pt-br/centrais-de-conteudos/relatorios-e-indicadores/geracao.

CORDERO, L. G.; FRANCO, J. F.. Probabilistic Power Flow Analysis Based on Point-Estimate Method for High Penetration of Photovoltaic Generation in Electrical Distribution Systems. In: ANAIS DO CONGRESSO BRASILEIRO DE AUTOMÁTICA 2020 2020, **Anais**...: sbabra, dec. 2020. Available in: https://www.sba.org.br/open_journal_systems/index.php/sba/article/view/1078.

BARAN, M. E.; WU, F. F. Network reconfiguration in distribution systems for loss reduction and load balancing. **IEEE Transactions on Power Delivery**, [*s. l.*], v. 4, n. 2, p. 1401–1407, apr. 1989.

CORDERO, L. G.; SOARES, J.; FRANCO, J. F.; VALE, Z. Probabilistic Algorithm based on 2m+1 Point Estimate Method Edgeworth considering Voltage Confidence Intervals for Optimal PV Generation. In: 2022 17TH INTERNATIONAL CONFERENCE ON PROBABILISTIC METHODS APPLIED TO POWER SYSTEMS (PMAPS) 2022, **Anais**... : IEEE, JUN. 2022. Available in: https://ieeexplore.ieee.org/document/9810644/.

BLINNIKOV, S.; MOESSNER, R. Expansions for nearly Gaussian distributions. **Astronomy and Astrophysics Supplement Series**, [*s. l.*], v. 130, n. 1, p. 193–205, may. 1998.

BRANDAO, F.; PÉREZ, J. M.; VALENTE, C.; BALLARIN, E.; TAKASHINA, Y. ampl/amplpy: [*s. l.*], NOV. 2021.

BRAZIL FI GROUP. Rota 30 Plan. [*s. l.*], 2018 Available in: https://rota30.com.br.

BYRD, R. H.; NOCEDAL, J.; WALTZ, R. A. Knitro: An integrated package for nonlinear optimization. *In*: **Large-Scale Nonlinear Optimization**. New York: Springer-Verlag, 2006. p. 35–59.

CARSTENS, D. D. D. S.; DA CUNHA, S. K. Solar energy growth in Brazil: Essential dimensions for the technological transition. **International Journal of Energy Economics and Policy**, [*s. l.*], v. 8, n. 4, p. 293–302, 2018.

CONSTANTE-FLORES, G. E.; ILLINDALA, M. S. Data-Driven Probabilistic Power Flow Analysis for a Distribution System With Renewable Energy Sources Using Monte Carlo Simulation. **IEEE Transactions on Industry Applications**, [*s. l.*], v. 55, n. 1, p. 174–181, jan. 2019.

CORDERO, L. G.; SOARES, J.; FRANCO, J. F.; VALE, Z. Probabilistic Algorithm based on 2m+1 Point Estimate Method Edgeworth considering Voltage Confidence Intervals for Optimal PV Generation. In: 2022 17TH INTERNATIONAL CONFERENCE ON PROBABILISTIC METHODS APPLIED TO POWER SYSTEMS (PMAPS) 2022, **Anais**... : IEEE,jun. 2022. Avaliable in: https://ieeexplore.ieee.org/document/9810644/.

DE LIMA, T. D.; FRANCO, J. F.; LEZAMA, F.; SOARES, J. A Specialized long-term distribution system expansion planning method with the integration of distributed energy resources. **IEEE Access**, [*s. l.*], v. 10, p. 19133–19148, 2022.

DILEEP, G. A survey on smart grid technologies and applications. **Renewable Energy**, [*s. l.*], v. 146, p. 2589–2625, fev. 2020.

DUGAN, R. C.; MCDERMOTT, T. E. An open source platform for collaborating on smart grid research. In: 2011 IEEE POWER AND ENERGY SOCIETY GENERAL MEETING 2011, **Anais** [...] : IEEE,jul. 2011. Available in: https://ieeexplore.ieee.org/document/6039829/.

FAN, M.; VITTAL, V.; HEYDT, G. T.; AYYANAR, R. Probabilistic power flow studies for transmission systems with photovoltaic generation using cumulants. **IEEE Transactions on Power Systems**, [*s. l.*], v. 27, n. 4, p. 2251–2261, nov. 2012.

FERNANDES, A. T.; N. LOURENCO, L. F.; MONARO, R. M.; CARDOSO, J. R. Statistical modeling of solar irradiance for northeast Brazil. *In*: INTERNATIONAL CONFERENCE ON RENEWABLE ENERGY RESEARCH AND APPLICATIONS (ICRERA), 8., 2019. **Anais** [...] : IEEE, nov. 2019. Available in: https://ieeexplore.ieee.org/document/8996714/

FOURER, R.; GAY, D. M.; KERNIGHAN, B. W. AMPL - A Modeling Language for Mathematical Programming: Second Edition. [*s. l.*], p. 519–554, 2003.

GALLEGO, L. A.; FRANCO, J. F.; CORDERO, L. G. A fast-specialized point estimate method for the probabilistic optimal power flow in distribution systems with renewable distributed generation. **International Journal of Electrical Power & Energy Systems**, [*s. l.*], v. 131, n. February, p. 107049, out. 2021.

GIRALDO, J. S.; LOPEZ, J. C.; CASTRILLON, J. A.; RIDER, M. J.; CASTRO, C. A. Probabilistic OPF Model for Unbalanced Three-Phase Electrical Distribution Systems Considering Robust Constraints. **IEEE Transactions on Power Systems**, [*s. l.*], v. 34, n. 5, p. 3443–3454, set. 2019.

HASHEMI, S.; ØSTERGAARD, J. Methods and strategies for overvoltage prevention in low voltage distribution systems with PV. **IET Renewable Power Generation**, [*s. l.*], v. 11, n. 2, p. 205–214, fev. 2017.

IEA. Global EV Outlook 2022 - Securing supplies for an electric future. **Global EV Outlook 2022**, [*s. l.*], p. 221, 2022.

IRENA, M. T. **RENEWABLE GENERATION COSTS IN 2022**. [*s.l: s.n.*]. Available in: https://www.irena.org/Publications/2023/Aug/Renewable-Power-Generation-Costs-in-2022.

CORDERO, L. G. **Online Data**. 2023. Available in: https://github.com/luidis2020/PhD_thesis_data.

NAVARRO-ESPINOSA, A.; OCHOA, L. F. Probabilistic impact assessment of low carbon technologies in LV distribution systems. **IEEE Transactions on Power Systems**, [*s. l.*], v.

31, n. 3, p. 2192–2203, 2016.

NEOCHARGE. **Electric Vehicles Market Evolution**. 2023. Available in: https://www.neocharge.com.br/carros-eletricos-brasil.

NOR, N. M.; ALI, A.; IBRAHIM, T.; ROMLIE, M. F. Battery Storage for the Utility-Scale Distributed Photovoltaic Generations. **IEEE Access**, [*s. l.*], v. 6, p. 1137–1154, 2018.

PRUSTY, B. R.; JENA, D. A critical review on probabilistic load flow studies in uncertainty constrained power systems with photovoltaic generation and a new approach. **Renewable and Sustainable Energy Reviews**, [*s. l.*], v. 69, n. November 2016, p. 1286–1302, mar. 2017.

RAMADHANI, U. H.; SHEPERO, M.; MUNKHAMMAR, J.; WIDÉN, J.; ETHERDEN, N. Review of probabilistic load flow approaches for power distribution systems with photovoltaic generation and electric vehicle charging. **International Journal of Electrical Power & Energy Systems**, [*s. l.*], v. 120, n. December 2019, p. 106003, set. 2020.

SABILLON ANTUNEZ, C.; FRANCO, J. F.; RIDER, M. J.; ROMERO, R. A new methodology for the optimal charging coordination of electric vehicles considering vehicle-to-grid technology. **IEEE Transactions on Sustainable Energy**, [*s. l.*], v. 7, n. 2, p. 596–607, apr. 2016.

STREZOSKI, L.; PADULLAPARTI, H.; DING, F.; BAGGU, M. Integration of Utility Distributed Energy Resource Management System and Aggregators for Evolving Distribution System Operators. **Journal of Modern Power Systems and Clean Energy**, [*s. l.*], v. 10, n. 2, p. 277–285, 2022.

SUN, K.; XIAO, H.; LIU, S.; YOU, S.; YANG, F.; DONG, Y.; WANG, W.; LIU, Y. A review of clean electricity policies—From countries to utilities. **Sustainability**, [s. l.], v. 12, n. 19, p. 7946, set. 2020.

ULLAH, Z.; WANG, S.; WU, G.; HASANIEN, H. M.; JABBAR, M. W.; QAZI, H. S.; TOSTADO-VÉLIZ, M.; TURKY, R. A.; ELKADEEM, M. R. Advanced studies for probabilistic optimal power flow in active distribution networks: A scientometric review. **IET Generation, Transmission & Distribution**, [*s. l.*], v. 16, n. 18, p. 3579–3604, set. 2022.

VAN ROSSUM, G.; DRAKE, F. L. Python Tutorial. **Python Software Foundation**, [*s. l.*], p. 1–136, 2012.

VERBIC, G.; CANIZARES, C. A. Probabilistic optimal power flow in electricity markets based on a two-point estimate method. **IEEE Transactions on Power Systems**, [*s. l.*], v. 21, n. 4, p. 1883–1893, nov. 2006.

XIE, Z. Q.; JI, T. Y.; LI, M. S.; WU, Q. H. Quasi-monte carlo based probabilistic optimal power flow considering the correlation of wind speeds using copula function. **IEEE Transactions on Power Systems**, [*s. l.*], v. 33, n. 2, p. 2239–2247, mar. 2018.

YANG, X.; GU, C.; YAN, X.; LI, F. Reliability-based probabilistic network pricing with demand uncertainty. **IEEE Transactions on Power Systems**, [*s. l.*], v. 8950, n. c, p. 1–1, 2020.

ZHANG, P.; LEE, S. T. Probabilistic Load Flow Computation Using the Method of Combined Cumulants and Gram-Charlier Expansion. **IEEE Transactions on Power Systems**, [*s. l.*], v. 19, n. 1, p. 676–682, fev. 2004.

ZHOU, Z.; TANG, F.; LIU, D.; WANG, C.; GAO, X. Probabilistic assessment of distribution network with high penetration of distributed generators. **Sustainability**, [*s. l.*], v. 12, n. 5, p. 1709, fev. 2020.

APPENDIX A – PUBLISHED WORKS

International Journals

1) L. A. Gallego, J. F. Franco, and L. G. Cordero, "A fast-specialized point estimate method for the probabilistic optimal power flow in distribution systems with renewable distributed generation," Int. J. Electr. Power Energy Syst., vol. 131, no. February, p. 107049, Oct. 2021. DOI: 10.1016/j.ijepes.2021.107049

Conference Papers

1) L. G. Cordero and J. F. Franco, "Probabilistic Power Flow Analysis Based on Point-Estimate Method for High Penetration of Photovoltaic Generation in Electrical Distribution Systems," in Anais do Congresso Brasileiro de Automática 2020, 2020. DOI: 10.48011/asba.v2i1.1078
2) L. G. Cordero, J. Soares, J. F. Franco, and Z. Vale, "Probabilistic Algorithm based on 2m+1 Point Estimate Method Edgeworth considering Voltage Confidence Intervals for Optimal PV Generation," in 2022 17th International Conference on Probabilistic Methods Applied to Power Systems (PMAPS), 2022, no. 313047, pp. 1–6. DOI: 10.1109/PMAPS53380.2022.9810644
3) L. G. Cordero, J. Soares, and J. F. Franco, "Otimização Probabilística de Reconfiguração de Redes de Distribuição com Penetração de Geração Fotovoltaica, " no. Mc, pp. 1–6, 2022. CLAGTEE 2022, Rio de Janeiro. DOI: 10.29327/547386
4) Luis G. Cordero, Brian Jaramillo-Leon, Jonatas B. Leite, John F. Franco, José Almeida, Fernando Lezama, Joao Soares, "Probabilistic-based Optimization for PV Hosting Capacity with Confidence Interval Restrictions," in Proceedings of the Companion Conference on Genetic and Evolutionary Computation, 2023, pp. 1933–1940. GECCO 2023. DOI: 10.1145/3583133.3596351

APPENDIX B – DATA IEEE 33 BUS

		Demand	
Bus name	Type	(kW)	(kVAr)
1	Slack	0	0
2	PQ	100	60
3	PQ	90	40
4	PQ	120	80
5	PQ	60	30
6	PQ	60	20
7	PQ	200	100
8	PQ	200	100
9	PQ	60	20
10	PQ	60	20
11	PQ	45	30
12	PQ	60	35
13	PQ	60	35
14	PQ	120	80
15	PQ	60	10
16	PQ	60	20
17	PQ	60	20
18	PQ	90	40
19	PQ	90	40
20	PQ	90	40
21	PQ	90	40
22	PQ	90	40
23	PQ	90	50
24	PQ	420	200
25	PQ	420	200
26	PQ	60	25
27	PQ	60	25
28	PQ	60	20
29	PQ	120	70
30	PQ	200	600
31	PQ	150	70
32	PQ	210	100
33	PQ	60	40

Line		Impedance (p.u.)	
From	To	R	X
1	2	0.0922	0.047
2	3	0.493	0.2511
3	4	0.366	0.1864
4	5	0.3811	0.1941
5	6	0.819	0.707
6	7	-0.1872	0.6188
7	8	0.7114	0.2351
8	9	1.03	0.74
9	10	1.044	0.74
10	11	0.1966	0.065
11	12	0.3744	0.1238
12	13	1.468	1.155
13	14	0.5416	0.7129
14	15	0.591	0.526
15	16	0.7463	0.545
16	17	1.289	1.721
17	18	0.732	0.574
2	19	0.164	0.1565
19	20	1.5042	1.3554
20	21	0.4095	0.4784
21	22	0.7089	0.9373
3	23	0.4512	0.3083
23	24	0.898	0.7091
24	25	0.896	0.7011
6	26	0.203	0.1034
26	27	0.2842	0.1447
27	28	1.059	0.9337
28	29	0.8042	0.7006
29	30	0.5075	0.2585
30	31	0.9744	0.963
31	32	0.3105	0.3619
32	33	0.341	0.5302

Source: Adapted from (BARAN; WU, 1989).

APPENDIX C – DATA IEEE 69 BUS

Bus name	Type	Demand (kW)	Demand (kVAr)
1	Slack	0	0
2	PQ	0	0
3	PQ	0	0
4	PQ	0	0
5	PQ	0	0
6	PQ	0	0
7	PQ	2.6	2.2
8	PQ	40.4	30
9	PQ	75	54
10	PQ	30	22
11	PQ	28	19
12	PQ	145	104
13	PQ	145	104
14	PQ	8	5.5
15	PQ	8	5.5
16	PQ	0	0
17	PQ	45.5	30
18	PQ	60	35
19	PQ	60	35
20	PQ	0	0
21	PQ	1	0.6
22	PQ	114	81
23	PQ	5.3	3.5
24	PQ	0	0
25	PQ	28	20
26	PQ	0	0
27	PQ	14	10
28	PQ	14	10
29	PQ	26	18.6
30	PQ	26	18.6
31	PQ	0	0
32	PQ	0	0
33	PQ	0	0
34	PQ	14	10
35	PQ	19.5	14
36	PQ	6	4
37	PQ	0	0

Line From	Line To	Impedance (p.u.) R	Impedance (p.u.) X
1	2	0.0005	0.0012
2	3	0.0005	0.0012
3	4	0.0001	0.0001
4	5	0.0015	0.0036
5	6	0.0251	0.0294
6	7	0.3660	0.1864
7	8	0.3811	0.1941
8	9	0.0922	0.0470
9	10	0.0493	0.0251
10	11	0.8190	0.2707
11	12	0.1872	0.0619
12	13	0.7114	0.2351
13	14	1.0300	0.3400
14	15	1.0440	0.3450
15	16	1.0580	0.3496
16	17	0.1966	0.0650
17	18	0.3744	0.1238
18	19	0.0047	0.0016
19	20	0.3276	0.1083
20	21	0.2106	0.0696
21	22	0.3416	0.1129
22	23	0.0140	0.0046
23	24	0.1591	0.0526
24	25	0.3463	0.1145
25	26	0.7488	0.2475
26	27	0.3089	0.1021
27	28	0.1732	0.5720
3	29	0.0044	0.0108
29	30	0.0640	0.1565
30	31	0.3978	0.1315
31	32	0.0702	0.0232
32	33	0.3510	0.1160
33	34	0.8390	0.2816
34	35	1.7080	0.5646
35	36	1.4740	0.4873
4	60	0.0044	0.0108
60	61	0.0640	0.1565

38	PQ	79	56.4
39	PQ	385	274.5
40	PQ	385	274.5
41	PQ	40.5	28.3
42	PQ	3.6	2.7
43	PQ	4.35	3.5
44	PQ	26.4	19
45	PQ	24	17.2
46	PQ	0	0
47	PQ	0	0
48	PQ	0	0
49	PQ	100	72
50	PQ	0	0
51	PQ	1244	888
52	PQ	32	23
53	PQ	0	0
54	PQ	227	162
55	PQ	59	42
56	PQ	18	13
57	PQ	18	13
58	PQ	28	20
59	PQ	28	20
60	PQ	26	18.55
61	PQ	26	18.55
62	PQ	0	0
63	PQ	24	17
64	PQ	24	17
65	PQ	1.2	1
66	PQ	0	0
67	PQ	6	4.3
68	PQ	0	0
69	PQ	39.2	26.3
70	PQ	39.2	26.3

61	62	0.1053	0.1230
62	63	0.0304	0.0355
63	64	0.0018	0.0021
64	65	0.7283	0.8509
65	66	0.3100	0.3623
66	67	0.0410	0.0478
67	68	0.0092	0.0116
68	69	0.1089	0.1373
69	70	0.0009	0.0012
5	37	0.0034	0.0084
37	38	0.0851	0.2083
38	39	0.2898	0.7091
39	40	0.0822	0.2011
9	41	0.0928	0.0473
41	42	0.3319	0.1114
10	43	0.1740	0.0886
43	44	0.2030	0.1034
44	45	0.2842	0.1447
45	46	0.2813	0.1433
46	47	1.5900	0.5337
47	48	0.7837	0.2630
48	49	0.3042	0.1006
49	50	0.3861	0.1172
50	51	0.5075	0.2585
51	52	0.0974	0.0496
52	53	0.1450	0.0738
53	54	0.7105	0.3619
54	55	1.0410	0.5302
12	56	0.2012	0.0611
56	57	0.0047	0.0014
13	58	0.7394	0.2444
58	59	0.0047	0.0016

Source: Adapted from (GALLEGO; FRANCO; CORDERO, 2021).

APPENDIX D – DATA EDS 202 BUS

		Demand	
Bus name	Type	(kW)	(kVAr)
1	Slack	0.000	0.000
2	PQ	0.000	0.000
3	PQ	38.250	23.700
4	PQ	0.000	0.000
5	PQ	63.750	39.500
6	PQ	0.000	0.000
7	PQ	0.000	0.000
8	PQ	38.250	23.700
9	PQ	95.200	58.990
10	PQ	63.750	39.500
11	PQ	0.000	0.000
12	PQ	510.000	316.020
13	PQ	0.000	0.000
14	PQ	0.000	0.000
15	PQ	0.000	0.000
16	PQ	63.750	39.500
17	PQ	127.500	79.010
18	PQ	63.750	39.500
19	PQ	63.750	39.500
20	PQ	255.000	158.010
21	PQ	0.000	0.000
22	PQ	0.000	0.000
23	PQ	255.000	158.010
24	PQ	255.000	158.010
25	PQ	382.500	237.020
26	PQ	0.000	0.000
27	PQ	191.250	118.510
28	PQ	0.000	0.000
29	PQ	51.000	31.600
30	PQ	95.630	59.250
31	PQ	95.630	59.250
32	PQ	0.000	0.000
33	PQ	350.630	217.260
34	PQ	350.630	217.260
35	PQ	0.000	0.000
36	PQ	0.000	0.000
37	PQ	63.750	39.500

Line		Impedance (p.u.)	
From	To	R	X
1	2	0.00001	0.00001
2	3	0.01883	0.04232
3	4	0.065905	0.14812
4	5	0.03766	0.08464
5	6	0.01883	0.04232
6	7	0.00001	0.00001
7	8	0.01883	0.04232
8	9	0.016947	0.038088
9	10	0.01883	0.04232
10	11	0.00001	0.00001
11	12	0.05935	0.04654
10	13	0.01883	0.04232
13	14	0.00001	0.00001
10	15	0.00001	0.00001
15	16	0.046705	0.02445
16	17	0.09341	0.0489
17	18	0.074728	0.03912
17	19	0.18682	0.0978
19	20	0.074728	0.03912
14	21	0.03766	0.08464
21	22	0.041426	0.093104
22	23	0.00001	0.00001
23	24	0.00659	0.014812
24	25	0.00659	0.014812
25	26	0.00001	0.00001
26	27	0.024479	0.055016
25	28	0.00001	0.00001
28	29	0.065387	0.03423
29	30	0.046705	0.02445
30	31	0.046705	0.02445
31	32	0.046705	0.02445
32	33	0.059416	0.02026
32	34	0.089124	0.03039
29	35	0.09341	0.0489
35	36	0.00001	0.00001
36	37	0.037364	0.01956
35	38	0.00001	0.00001

38	PQ	0.000	0.000	38	39	0.037364	0.01956
39	PQ	95.630	59.250	27	40	0.009415	0.02116
40	PQ	0.000	0.000	40	41	0.037135	0.0126625
41	PQ	255.000	158.010	40	42	0.009415	0.02116
42	PQ	0.000	0.000	42	43	0.009415	0.02116
43	PQ	191.250	118.510	43	44	0.009415	0.02116
44	PQ	95.630	59.250	42	45	0.059416	0.02026
45	PQ	0.000	0.000	45	46	0.00001	0.00001
46	PQ	0.000	0.000	46	47	0.037135	0.0126625
47	PQ	63.750	39.500	45	48	0.00001	0.00001
48	PQ	0.000	0.000	48	49	0.037135	0.0126625
49	PQ	605.630	375.270	44	50	0.014122	0.03174
50	PQ	573.750	355.520	50	51	0.013181	0.029624
51	PQ	191.250	118.510	51	52	0.011298	0.025392
52	PQ	255.000	158.010	52	53	0.011298	0.025392
53	PQ	765.000	474.030	53	54	0.011298	0.025392
54	PQ	255.000	158.010	54	55	0.011298	0.025392
55	PQ	0.000	0.000	55	56	0.07427	0.025325
56	PQ	0.000	0.000	56	57	0.00001	0.00001
57	PQ	318.750	197.510	57	58	0.103978	0.035455
58	PQ	318.750	197.510	1	59	0.0000001	0.0000001
59	PQ	0.000	0.000	59	60	0.01597	0.04095
60	PQ	25.500	15.800	60	61	0.099014	0.25389
61	PQ	0.000	0.000	61	62	0.00001	0.00001
62	PQ	0.000	0.000	62	63	0.041522	0.10647
63	PQ	0.000	0.000	63	64	0.00001	0.00001
64	PQ	0.000	0.000	63	65	0.019164	0.04914
65	PQ	95.630	59.250	65	66	0.00001	0.00001
66	PQ	0.000	0.000	66	67	0.01597	0.04095
67	PQ	38.250	23.700	67	68	0.00001	0.00001
68	PQ	0.000	0.000	68	69	0.133686	0.045585
69	PQ	102.000	63.200	64	70	0.01883	0.04232
70	PQ	0.000	0.000	70	71	0.111405	0.0379875
71	PQ	89.250	55.300	70	72	0.00001	0.00001
72	PQ	0.000	0.000	72	73	0.133686	0.045585
73	PQ	0.000	0.000	73	74	0.081697	0.0278575
74	PQ	38.250	23.700	70	75	0.020713	0.046552
75	PQ	0.000	0.000	75	76	0.00001	0.00001
76	PQ	0.000	0.000	76	77	0.163394	0.055715
77	PQ	510.000	316.020	75	78	0.011298	0.025392
78	PQ	595.000	368.690	78	79	0.007532	0.016928
79	PQ	0.000	0.000	79	80	0.00001	0.00001
80	PQ	0.000	0.000	79	81	0.009415	0.02116
81	PQ	382.500	237.020	81	82	0.011298	0.025392

82	PQ	0.000	0.000	80	83	0.126259	0.0430525
83	PQ	350.630	217.260	82	84	0.00001	0.00001
84	PQ	0.000	0.000	84	85	0.013181	0.029624
85	PQ	38.250	23.700	84	86	0.004707	0.01058
86	PQ	255.000	158.010	86	87	0.005649	0.012696
87	PQ	446.250	276.520	87	88	0.009415	0.02116
88	PQ	382.500	237.020	79	89	0.00001	0.00001
89	PQ	0.000	0.000	89	90	0.178248	0.06078
90	PQ	0.000	0.000	90	91	0.0000001	0.0000001
91	PQ	0.000	0.000	91	92	0.111405	0.037987
92	PQ	95.630	59.250	90	93	0.00001	0.00001
93	PQ	191.250	118.510	93	94	0.056046	0.027924
94	PQ	216.750	134.310	94	95	0.028023	0.013962
95	PQ	95.630	59.250	95	96	0.028023	0.013962
96	PQ	191.250	118.510	96	97	0.028023	0.013962
97	PQ	63.750	39.500	97	98	0.051375	0.025597
98	PQ	382.500	237.020	88	99	0.020713	0.046552
99	PQ	0.000	0.000	99	100	0.00001	0.00001
100	PQ	0.000	0.000	100	101	0.014122	0.03174
101	PQ	63.750	39.500	100	102	0.005649	0.012696
102	PQ	0.000	0.000	102	103	0.00001	0.00001
103	PQ	0.000	0.000	103	104	0.07427	0.025325
104	PQ	63.750	39.500	102	105	0.004707	0.01058
105	PQ	127.500	79.010	105	106	0.005649	0.012696
106	PQ	95.630	59.250	102	107	0.00659	0.014812
107	PQ	106.250	65.840	107	108	0.010356	0.023276
108	PQ	127.500	79.010	106	109	0.011298	0.025392
109	PQ	95.630	59.250	109	110	0.00001	0.00001
110	PQ	0.000	0.000	110	111	0.007532	0.016928
111	PQ	127.500	79.010	111	112	0.007532	0.016928
112	PQ	127.500	79.010	112	113	0.007532	0.016928
113	PQ	0.000	0.000	113	114	0.00001	0.00001
114	PQ	0.000	0.000	113	115	0.005649	0.012696
115	PQ	318.750	197.510	115	116	0.007532	0.016928
116	PQ	350.630	217.260	116	117	0.009415	0.02116
117	PQ	446.250	276.520	114	118	0.051989	0.017727
118	PQ	63.750	39.500	113	119	0.007532	0.016928
119	PQ	127.500	79.010	119	120	0.007532	0.016928
120	PQ	63.750	39.500	120	121	0.00659	0.014812
121	PQ	382.500	237.020	121	122	0.005649	0.012696
122	PQ	0.000	0.000	122	123	0.00001	0.00001
123	PQ	76.500	47.400	122	124	0.00001	0.00001
124	PQ	255.000	158.010	124	125	0.015064	0.033856
125	PQ	191.250	118.510	123	126	0.065387	0.03003

126	PQ	255.000	158.010	125	127	0.009415	0.02116
127	PQ	233.750	144.840	127	128	0.009415	0.02116
128	PQ	573.750	355.520	127	129	0.015064	0.033856
129	PQ	276.250	171.180	129	130	0.013181	0.029624
130	PQ	255.000	158.010	130	131	0.013181	0.029624
131	PQ	393.130	243.600	131	132	0.016947	0.038088
132	PQ	510.000	316.020	1	133	0.00001	0.00001
133	PQ	0.000	0.000	133	134	0.069671	0.156584
134	PQ	0.000	0.000	134	135	0.00001	0.00001
135	PQ	0.000	0.000	135	136	0.015064	0.033856
136	PQ	0.000	0.000	136	137	0.060256	0.135424
137	PQ	0.000	0.000	137	138	0.009415	0.02116
138	PQ	0.000	0.000	137	139	0.00001	0.00001
139	PQ	63.750	39.500	139	140	0.020713	0.046552
140	PQ	0.000	0.000	140	141	0.00001	0.00001
141	PQ	0.000	0.000	140	142	0.009415	0.02116
142	PQ	38.250	23.700	142	143	0.005649	0.012696
143	PQ	38.250	23.700	141	144	0.028023	0.01467
144	PQ	63.750	39.500	137	145	0.00001	0.00001
145	PQ	0.000	0.000	145	146	0.074728	0.03912
146	PQ	63.750	39.500	146	147	0.056046	0.02934
147	PQ	0.000	0.000	147	148	0.00001	0.00001
148	PQ	0.000	0.000	148	149	0.037364	0.01956
149	PQ	95.630	59.250	146	150	0.00001	0.00001
150	PQ	0.000	0.000	150	151	0.046705	0.02445
151	PQ	63.750	39.500	143	152	0.005649	0.012696
152	PQ	0.000	0.000	152	153	0.00001	0.00001
153	PQ	0.000	0.000	152	154	0.005649	0.012696
154	PQ	63.750	39.500	154	155	0.005649	0.012696
155	PQ	212.500	131.680	155	156	0.005649	0.012696
156	PQ	63.750	39.500	153	157	0.037364	0.01956
157	PQ	63.750	39.500	156	158	0.005649	0.012696
158	PQ	0.000	0.000	158	159	0.028023	0.01467
159	PQ	63.750	39.500	159	160	0.046705	0.02445
160	PQ	38.250	23.700	158	161	0.009415	0.02116
161	PQ	63.750	39.500	161	162	0.011298	0.025392
162	PQ	0.000	0.000	162	163	0.00001	0.00001
163	PQ	0.000	0.000	163	164	0.00001	0.00001
164	PQ	95.630	59.250	164	165	0.01883	0.04232
165	PQ	0.000	0.000	165	166	0.00001	0.00001
166	PQ	0.000	0.000	165	167	0.005649	0.012696
167	PQ	446.250	276.520	167	168	0.005649	0.012696
168	PQ	191.250	118.510	168	169	0.007532	0.016928
169	PQ	255.000	158.010	166	170	0.065387	0.03423

170	PQ	605.630	375.270
171	PQ	63.750	39.500
172	PQ	127.500	79.010
173	PQ	63.750	39.500
174	PQ	191.250	118.510
175	PQ	0.000	0.000
176	PQ	0.000	0.000
177	PQ	208.250	129.040
178	PQ	191.250	118.510
179	PQ	127.500	79.010
180	PQ	127.500	79.010
181	PQ	0.000	0.000
182	PQ	0.000	0.000
183	PQ	255.000	158.010
184	PQ	127.500	79.010
185	PQ	850.000	526.700
186	PQ	127.500	79.010
187	PQ	510.000	316.020
188	PQ	0.000	0.000
189	PQ	0.000	0.000
190	PQ	0.000	0.000
191	PQ	191.250	118.510
192	PQ	448.380	277.830
193	PQ	255.000	158.010
194	PQ	510.000	316.020
195	PQ	382.500	237.020
196	PQ	255.000	158.010
197	PQ	191.250	118.510
198	PQ	446.250	276.520
199	PQ	133.880	82.960
200	PQ	95.630	59.250
201	PQ	382.500	237.020
202	PQ	1030.200	638.360

169	171	0.00001	0.00001
171	172	0.07122	0.055848
171	173	0.009415	0.02116
173	174	0.009415	0.02116
174	175	0.009415	0.02116
175	176	0.00001	0.00001
176	177	0.074728	0.03912
175	178	0.003766	0.008464
178	179	0.003766	0.008464
179	180	0.005649	0.012696
180	181	0.0000001	0.0000001
181	182	0.00001	0.00001
181	183	0.046705	0.02445
182	184	0.0607165	0.031785
181	185	0.005649	0.012696
185	186	0.005649	0.012696
186	187	0.005649	0.012696
187	188	0.005649	0.012696
188	189	0.00001	0.00001
188	190	0.00001	0.00001
190	191	0.0385775	0.030251
189	192	0.0504475	0.039559
188	193	0.022596	0.050784
193	194	0.065387	0.03423
193	195	0.046705	0.02445
195	196	0.046705	0.02445
196	197	0.046705	0.02445
193	198	0.009415	0.02116
198	199	0.009415	0.02116
197	200	0.046705	0.02445
200	201	0.112092	0.05868
200	202	0.09341	0.0489

Source: Adapted from (GALLEGO; FRANCO; CORDERO, 2021).